NASA/TM—2004-213289

Results From a Parametric Acoustic Liner Experiment Using P&W GEN1 HSR Mixer/Ejector Model

K.C. Boyd and J.D. Wolter
Glenn Research Center, Cleveland, Ohio

October 2004

The NASA STI Program Office . . . in Profile

Since its founding, NASA has been dedicated to the advancement of aeronautics and space science. The NASA Scientific and Technical Information (STI) Program Office plays a key part in helping NASA maintain this important role.

The NASA STI Program Office is operated by Langley Research Center, the Lead Center for NASA's scientific and technical information. The NASA STI Program Office provides access to the NASA STI Database, the largest collection of aeronautical and space science STI in the world. The Program Office is also NASA's institutional mechanism for disseminating the results of its research and development activities. These results are published by NASA in the NASA STI Report Series, which includes the following report types:

- TECHNICAL PUBLICATION. Reports of completed research or a major significant phase of research that present the results of NASA programs and include extensive data or theoretical analysis. Includes compilations of significant scientific and technical data and information deemed to be of continuing reference value. NASA's counterpart of peer-reviewed formal professional papers but has less stringent limitations on manuscript length and extent of graphic presentations.

- TECHNICAL MEMORANDUM. Scientific and technical findings that are preliminary or of specialized interest, e.g., quick release reports, working papers, and bibliographies that contain minimal annotation. Does not contain extensive analysis.

- CONTRACTOR REPORT. Scientific and technical findings by NASA-sponsored contractors and grantees.

- CONFERENCE PUBLICATION. Collected papers from scientific and technical conferences, symposia, seminars, or other meetings sponsored or cosponsored by NASA.

- SPECIAL PUBLICATION. Scientific, technical, or historical information from NASA programs, projects, and missions, often concerned with subjects having substantial public interest.

- TECHNICAL TRANSLATION. English-language translations of foreign scientific and technical material pertinent to NASA's mission.

Specialized services that complement the STI Program Office's diverse offerings include creating custom thesauri, building customized databases, organizing and publishing research results . . . even providing videos.

For more information about the NASA STI Program Office, see the following:

- Access the NASA STI Program Home Page at ***http://www.sti.nasa.gov***

- E-mail your question via the Internet to help@sti.nasa.gov

- Fax your question to the NASA Access Help Desk at 301–621–0134

- Telephone the NASA Access Help Desk at 301–621–0390

- Write to:
  NASA Access Help Desk
  NASA Center for AeroSpace Information
  7121 Standard Drive
  Hanover, MD 21076

NASA/TM—2004-213289

Results From a Parametric Acoustic Liner Experiment Using P&W GEN1 HSR Mixer/Ejector Model

K.C. Boyd and J.D. Wolter
Glenn Research Center, Cleveland, Ohio

National Aeronautics and
Space Administration

Glenn Research Center

October 2004

Document History

This research was originally published internally as HSR054 in August 1997.

Note that at the time of research, the NASA Lewis Research Center was undergoing a name change to the NASA John H. Glenn Research Center at Lewis Field. Both names may appear in this report.

Available from

NASA Center for Aerospace Information
7121 Standard Drive
Hanover, MD 21076

National Technical Information Service
5285 Port Royal Road
Springfield, VA 22100

Available electronically at http://gltrs.grc.nasa.gov

Results From a Parametric Acoustic Liner Experiment Using P&W GEN1 HSR Mixer/Ejector Model

Kathleen C. Boyd and John D. Wolter
National Aeronautics and Space Administration
Glenn Research Center
Cleveland, Ohio 44135

Abstract

This report documents the results of an acoustic liner test performed using a Gen 1 HSR mixer/ejector model installed on the Jet Exit Rig in the Nozzle Acoustic Test Rig in the Aeroacoustic Propulsion Lab of NASA Lewis Research Center. Acoustic liner effectiveness and single-component thrust performance results are discussed. Results from 26 different types of single-degree-of-freedom and bulk material liners are compared with each other and against a hardwall baseline. Design parameters involving all aspects of the facesheet, the backing cavity, and the type of bulk material were varied in order to study the effects of these design features on the acoustic impedance, acoustic effectiveness and on nozzle thrust performance. Overall, the bulk absorber liners are more effective at reducing the jet noise than the single-degree-of-freedom liners. Many of the design parameters had little effect on acoustic effectiveness, such as facesheet hole diameter and honeycomb cell size. A relatively large variation in the impedance of the bulk absorber in a bulk liner is required to have a significant impact on the noise reduction. The thrust results exhibit a number of consistent trends, supporting the validity of this new addition to the facility. In general, the thrust results indicate that thrust performance benefits from increased facesheet thickness and decreased facesheet porosity.

Introduction

The development of the next generation High Speed Civil Transport (HSCT) is highly dependent upon environmental and economic constraints. Low noise exhaust nozzle technology has significant impact on both issues. It is essential that the exhaust system design meet acoustic requirements while providing adequate thrust and still maintaining an acceptable weight. Acoustic liners are required for HSCT mixer/ejector nozzles to attenuate the internal broad band, high-frequency mixing noise and shock associated noise generated within the ejector and meet FAR 36 Stage 3 noise goals.

The general objective for this test was to acquire far-field acoustic data and single-component thrust for a hardwall baseline and various acoustic liners that line the ejector shroud and sidewalls of a mixer/ejector model. The purpose was to demonstrate the acoustic effectiveness of various liner concepts that have been tested in the laboratory. Several parameters of the liner design were varied in order to study the effect of these design parameters and the effect of acoustic impedance on the acoustic attenuation and nozzle performance. This report will attempt to summarize the results of the test in order to gain insight and understanding into the effects caused by acoustic liners in an exhaust nozzle environment.

Facility

This experiment was done using the Jet Exit Rig (JER) in the Nozzle Acoustic Test Rig (NATR) of the Aeroacoustic Propulsion Lab (APL) at NASA Lewis Research Center in Cleveland, Ohio. The JER is an exhaust nozzle high temperature test rig that is fed by 450 lb/s compressed air which is heated by a hydrogen ignition system. The NATR is a free-jet facility that provides flight simulation up to speeds of Mach 0.3. It is 53 inches in diameter at the exit and is fed by a combination of 120 lb/s compressed air and an ejector system. The APL is an anechoic dome designed for both far-field acoustic testing and the reduction of community noise caused by exhaust nozzle testing.

Far-field acoustic data acquisition is acquired in this facility using a 25 microphone array arranged at a 48 foot constant radius from 45° to 165° at 5° increments measured from the model inlet. The microphones are B&K 1/4" and are arranged on stands that are 10 feet high, level with the model centerline. Data is acquired, stored and processed on NASA LeRC's Digital Acoustic Data System which runs on a UNIX-based Concurrent computer system.

Hardware

The model used in this test was the Pratt & Whitney sub scale (approximately 1/10 scale) High Speed Research (HSR) model of a mixer/ejector exhaust system. It was developed for the Gen 1 HSR program and was chosen for this experiment, in part, because of the high amount of internal mixing noise that is present within the ejector exhaust nozzle. A high amount of internal noise is preferred for determining the differences in acoustic attenuation produced by each liner.

The model was tested with the vortical mixer and the long ejector walls. The hardware geometry stayed constant with a SAR of 4.9 and a MAR of 0.97. Previous tests have shown that only liners on the aft half of the ejector are adequately effective. It has also been shown that if all four sides of the ejector are lined there is approximately twice the attenuation than if two of the sides are lined. Therefore, in order to achieve maximum liner effectiveness with minimum hardware, only the aft half of all four sides of the ejector was lined. Figure 1 shows the model installed in the NATR during this experiment.

A total of 26 liner configurations were tested along with a hardwall baseline configuration. The liners can be separated into 2 types, single degree of freedom and bulk. Both of these types of designs are being considered for the full scale model.

Several parameters in the design of each type of liner were varied in order to determine the effect they have on the acoustic attenuation of the far-field noise generated by the model. The variation of each parameter also has an effect on the normal impedance of the liner. Expected conclusions are drawn based on variances in impedance and can be compared with the measured results to determine the effect of normal impedance on attenuation in a mixed-flow environment.

A single degree of freedom acoustic liner has the basic construction of a honeycomb core sandwiched between a perforated plate and a solid backing plate. Noise reduction is achieved when sound enters the honeycomb through the perforate and resonates inside the cell, losing energy in the process. Ten configurations of this type were tested, shown in table 1.

Table 1 - SDOF perforated facesheet/honeycomb

Config #	Facesheet porosity (%)	Facesheet hole dia (in)	Facesheet thickness (in)	Honeycomb depth (in)	Honeycomb cell size (in)
1	7	0.04	0.025	0.375	0.375
2	10	0.04	0.025	0.375	0.375
3	15	0.04	0.025	0.375	0.375
4	10	0.02	0.025	0.375	0.375
5	10	0.06	0.025	0.375	0.375
6	10	0.04	0.025	0.375	0.75
7	10	0.04	0.044	0.375	0.375
8	10	0.04	0.063	0.375	0.375
9	10	0.04	0.025	0.25	0.375
10	10	0.04	0.025	0.5	0.375

The main attenuation in a bulk liner is produced from the sound entering an acoustically absorbing material and being attenuated by the material before it has a chance to reflect back. A facesheet is placed over the bulk to protect it from the harsh environment inside the ejector. Sixteen variations of bulk liners were tested, shown in table 2.

Table 2 – Bulk Liners

Config #	Bulk Material	Bulk Material Thickness (in)	Facesheet Porosity	Facesheet Thickness (in)
14	Ultramet SiC 200 ppi	0.375	0.37	0.025
15	Ultramet SiC 400 ppi	0.375	0.37	0.025
16	Ultramet SiC 200 ppi	0.375	0.20	0.025
17	Ultramet SiC 400 ppi	0.375	0.20	0.025
19	Lockheed HTP 4.6 lbs/ft^3	0.375	0.37	0.025
20	Lockheed HTP 4.9 lbs/ft^3	0.375	0.37	0.025
21	Lockheed HTP 3.3 lbs/ft^3	0.375	0.37	0.025
22	Lockheed HTP 4.6 lbs/ft^3	0.375	0.20	0.025
24	HTP 4.6 lbs/ft^3 in honeycomb	0.375	0.37	0.025
25	Lockheed HTP 4.6 lbs/ft^3	0.25	0.37	0.025
26	Americom SiC 100 ppi	0.375	0.37	0.025
27	Americom SiC 100 ppi	0.375	0.20	0.025
28	Lockheed HTP 16 lbs/ft^3	0.375	0.37	0.025
29	Lockheed HTP 4.6 lbs/ft^3	0.375	0.37	0.010
30	GTRI microspheres	0.375	0.37	0.025
36	Ultramet SiC 200 ppi	0.375	0.37	0.010

Test Conditions

The matrix of power conditions in the Table 3 below was run for almost half of the liner configurations. The conditions that are shaded were run for all 26 liner configurations. In this report, comparisons will be made at power conditions 1, 3, and 6 at free-jet Mach numbers of 0.0 and 0.3, unless otherwise noted.

Table 3 – Power Conditions

Condition	Free-Jet Mach	Nozzle Pressure Ratio	Temp (R)
1	0	**1.99**	**1139**
2	0	2.37	1238
3	0	**2.48**	**1291**
4	0	2.96	1416
5	0	3.25	1482
6	0	**3.43**	**1551**
7	0	3.4	1590
1	0.3	**1.99**	**1139**
2	0.3	2.37	1238
3	0.3	**2.48**	**1291**
4	0.3	2.96	1416
5	0.3	3.25	1482
6	0.3	**3.43**	**1551**
7	0.3	3.4	1590
1	0.1	1.99	1139
3	0.1	2.48	1291
6	0.1	3.43	1551

Acoustic Impedance Predictions

SDOF

A simplistic attempt at predicting the normal impedance of these single-degree-of-freedom liners was done during the design phase in order to systematically vary the normal impedance from the 'optimum' impedance that had been predetermined. This optimum impedance range was:

Normalized Resistance R/ρc: 1.5 to 2.0 ρc
Normalized Reactance X/ρc: -1.0 to 0.0 ρc

The predictions were for normal impedance with grazing flow of M=0.65 at a temperature of 500°F. These conditions were estimated from previous tests with this model and the temperature was verified in this test to be fairly accurate. Thermal paints used in this test showed that the temperature within the liners varied from 400° to 500°F. The equations used for normal resistance and reactance were:

$$R/\rho c = 0.3\ M / \sigma$$
$$X/\rho c = X_m/\rho c + X_c/\rho c$$

$$X_c/\rho c = -\cot(kh)$$
$$X_m/\rho c = k(t+\varepsilon d) / \sigma$$
$$\varepsilon = 0.85(1 - 0.7\sqrt{\sigma}) / (1 + 305\ M^3)$$

where

$R/\rho c$	facesheet resistance
$X/\rho c$	facesheet reactance
$X_m/\rho c$	facesheet mass reactance
$X_c/\rho c$	cavity reactance
h	cavity depth
k	wave number, ω/c
t	facesheet thickness
d	facesheet hole diameter
ε	dimensionless end correction
σ	facesheet porosity
M	grazing flow Mach number

Actual impedance measurements were not performed on these SDOF liner, so only the impedance predictions are shown here and will be addressed when each comparison is discussed. It is obvious from the equation for resistance that the only parameter that affects the prediction of this part of the impedance is the facesheet porosity, independent of frequency. For that reason, the only resistance prediction shown is for the variation of facesheet porosity. All the other configurations have a resistance equal to the 10% open area case, which is 1.95.

Bulk Liners

During the design phase, the impedance of the bulk liners was designed to systematically vary from the optimum impedance based on the normal impedance of the bulk material alone. The facesheet effects were not added to the predictions because one facesheet should generally have the same effect no matter what material is behind it. The bulk material impedance was predicted using a semi-empirical method known as Delany-Bazley [1] which is mainly based on the flow resistance of the material. Normal impedance and flow resistance measurements were done at GEAE to verify that the predictions were on target. Delany-Bazley generally compares well with measured normal impedance and serves as an adequate means of predicting impedance when the flow resistance is known. Since the purpose of this report is not to validate acoustic bulk liner prediction methods, impedance values for the bulk liners included in this report show the measured values.

Acoustic Results

All configurations were tested, at least, at power conditions 1, 3 and 6 at static and flight free jet conditions as shown previously in Table 3. These three conditions are used to compare the effect of the variation of liner design parameters on the acoustic impedance and liner effectiveness for reducing the jet noise. The mixer/ejector model that

was used was chosen because of the high amount internal noise that is generated within the ejector and the ease of liner design and model changes. It is best to view these results as comparisons from liner to liner instead of an overall effectiveness of each liner on this particular model. In some figures, the hardwall case is used as a reference to show the significance of the relative changes in noise suppression.

Figures 2a-2f show third-octave spectra over a range of operating conditions at static and flight free jet conditions. A comparison between the hardwall configuration matched up with one typical SDOF liner and one typical bulk liner is used to show the general liner effectiveness for this model. Configuration 2 is a single degree-of-freedom liner with facesheet porosity of 10%, facesheet thickness 0.025 inches, facesheet hole diameter of 0.04 inches and 0.375 inch honeycomb depth and cell size. Configuration 19 is 0.375 inch deep with Lockheed HTP 4.6 lbs/ft^3 with a 37% open facesheet, 0.025 inch thick and 0.07 inch hole diameter. The effect of the liners begins to appear at just above 1 kHz, implying the point at which internal mixing noise is generated inside the ejector. The bulk liner provides more attenuation than the SDOF liner, which is more evident above 7-8 kHz. This was generally the case for all the liners tested.

Figures 3a-3h provide a look at changes in spectra with directivity at the low power condition at the static and flight cases. Liner effectiveness appeared similar over all angles. Peak noise generally occurred at 115° off jet axis. This angle was chosen for all subsequent spectra comparisons.

Figure 4 shows the EPNL for the above comparison. EPNL was calculated at full scale, 1500 foot sideline for a free jet Mach number of 0.3. The SDOF liner configuration resulted in 3.4 to 5.2 EPNdB of attenuation while the bulk liner gave 5.7 to 8.3 EPNdB attenuation at power conditions 1, 3, and 6 shown in Table 3.

SDOF Liners

Figures 5a-5f show the impedance predictions for all of the SDOF liners. The purpose of these comparisons was to attempt to systematically vary one part of the impedance by different methods while keeping the other part essentially constant. By varying facesheet porosity, the resistance part of the impedance was systematically changed, although the reactance is changed slightly in the higher frequency range. Some of the other facesheet parameters had some affect on the reactance. It is also important to determine how parameters other than impedance affect the liner effectiveness. Honeycomb and backing variations are also studied to determine their effect on liner effectiveness.

Figures 6a-6f show the attenuation differences when the porosity of the facesheet on a SDOF liner is varied. They show that increased open area improves liner attenuation, even above 10%, up to the 15% open facesheet. This was evident over all ranges of power conditions, but slightly more prominent at the highest power condition. These results do not agree with the expected result based on the impedance prediction. For this model, predictions showed that a 10% open perforate would be closer to the target impedance, specifically the resistance. It is possible that the Mach number used in the prediction is actually higher than 0.65, making the resistance for the 15% facesheet in the optimum range and the 10% higher than optimum. It is also possible that either the target impedance or the impedance prediction is not accurate.

Figure 7 shows the EPNL values for the above comparison of facesheet porosity on SDOF liners. The EPNL for the 7% open facesheet was nominally 1 EPNdB higher that the 10% and 15% open configurations, which had very close EPNL curves.

Figures 8a-8f show the third-octave spectra for the SDOF facesheet hole diameter comparison. Based on the impedance prediction (Figure 5c), hole diameter has almost no effect on the predicted impedance in grazing. The spectra also show very little difference between the 3 variations of hole diameter. The only noticeable difference in the acoustic attenuation when the hole diameter was varied from 0.02 inches to 0.06 inches is seen in Figure 9a, the lowest power condition at Mfj=0.0. This trend shows that attenuation increases with decreasing hole size over all affected frequencies.

Figure 9 shows that the EPNL curves agree with the overall conclusion that hole diameter does not greatly impact liner effectiveness.

Figures 10a-10f show the effect of a variation in facesheet thickness on the spectra. This design feature has a distinct impact on the facesheet mass reactance, causing the liner reactance to increase with increasing thickness, as shown in the impedance predictions. The spectra in Figure 0 show a crossing point near 5 kHz. From 2 - 5 kHz, the thickest facesheet, 0.063 inch, has a lower spectra. But above 5 kHz, the thinnest facesheet, 0.025 inch produces the lowest spectra.

Figure 11 shows the effect of facesheet thickness on EPNL. Spectral differences above 5 kHz have a more significant effect on EPNL, since the thinner facesheet was about 1 EPNdB lower over all power conditions

Figures 12a-12f show the spectra for 2 different honeycomb cell sizes with the same facesheet. This parameter relates to the diameter of each of the honeycomb cells. It had no apparent effect on the impedance (Figure 5e). It also had negligible effect on acoustic attenuation in this test. This may prove to be useful information when scaling issues are approached for a full scale liner.

Figures 13a-13f show changes in spectra when honeycomb depth is varied. Cavity depth affects the cavity reactance of a liner, which can be seen in Figure 5f. Varying this parameter is also known as 'tuning' the liner, where the depth should equal one-quarter of the wavelength of sound that the liner is being designed to suppress. For these test conditions, the tuning frequencies of a 0.25 inch, a 0.375 inch, and a 0.5 inch deep cavity are approximately 18000 Hz, 12500 Hz, and 9000 Hz respectively. The attenuation achieved from the deeper liner is the best of the three at frequencies between 1 and 6 kHz. The trend then shifts with increasing frequency so that the best liner between 6 and 20 kHz is the 0.25 inch deep liner, and above that the attenuation was about the same.

Figure 14 shows the EPNL for the variation in honeycomb depth. Surprisingly, the tuning frequency had virtually no effect on EPNL.

Bulk Liners

Figures 15a-15b show the measured normal impedance at ambient conditions for the 4 densities of Lockheed HTP. The lower three densities were chosen because their impedance values were to be above, below, and very near the optimum impedance. HTP 16 was chosen because the impedance of bulk materials appears to converge at higher frequencies, above 10 kHz, regardless of their flow resistance. HTP 16 was included in this test to attempt to confirm the theory that is takes a large variation in the flow resistance of a bulk liner to have a significant impact on the noise suppression.

Figures 16a-16f show 4 different densities of Lockheed's HTP material versus the hardwall case. The lowest three densities show very little difference in attenuation. The highest density (16 lbs/ft^3) was noticeably less effective in the lower frequency range of 2-10 kHz, but the differences converged at higher frequencies. This comparison tends to confirm the impedance predictions using Delany-Bazley which shows that for varying flow resistance, the impedance tends to converge together at higher frequencies (above 10-20 kHz). This would suggest that they would also produce a similar amount of attenuation at the higher frequencies, shown by the results of this comparison.

Figure 17 shows the EPNL curves for the HTP material. EPNL values for the 3 lowest densities are essentially the same, while HTP16 was about 1 EPNdB higher.

Figures 18a-18b show the measured normal impedance for 3 porosities of silicon carbide with no facesheet. Amercom manufactured the 100 pores per inch (ppi) sample. The 200 ppi and 400 ppi SiC was made by Ultramet. Impedance increases with increasing porosity.

Figures 19a-19b show the measured normal impedance for 3 porosities of silicon carbide with a 37% open facesheet. The relative differences in the impedance with a facesheet look identical to Figure 18, where there was no facesheet.

Figures 20a-20f show the difference in attenuation between the 3 silicon carbide liners with a 37% open facesheet. The spectra show slightly more attenuation with lower porosity at the high power condition. The lower power condition shows very small differences between the 3 liners.

Figure 21 shows that the EPNL values for all silicon carbide liners with a 37% open facesheet are within about 0.5 EPNdB.

Figures 22a-22b show the measured normal impedance for 400 ppi SiC with a 37% open facesheet and with a 20% open facesheet. The less open facesheet increases both the resistance and the reactance part of the impedance.

Figures 23a-23f show comparisons when the facesheet was 37% open versus 20% open for several bulk materials. They all produced the same effect, which is the expected result. The 20% open facesheet produces less attenuation than the 37% open facesheet.

Figures 24a-24b show the EPNL curves for the above comparison with HTP 4.6 and SiC 400 ppi. For both bulk materials, the EPNL was generally about 1.7 EPNdB higher with the 20% open facesheet.

Figures 25a-25b show the measured normal impedance for SiC 200 ppi with 0.025" thick facesheet and 0.010" thick facesheet, both 37% open. With grazing flow, facesheet reactance increases with increasing thickness, as shown in the single-degree-of-freedom comparisons. Therefore, a thicker facesheet over a bulk material would have a higher resistance than a thinner facesheet with the same bulk. However, the normal impedance is unaffected by a change in facesheet thickness.

Figures 26a-26d show the spectral comparison when facesheet thickness is varied. Two variations of bulk liners were tested in which the facesheet thickness was changed, while the porosity (37%) and the hole diameter (0.07 inches) were held constant. HTP 4.6 lbs/ft3 and SiC 200 ppi both showed some acoustic benefit with the thinner facesheet (0.01 inches versus 0.024 inches) at the static case, and even less benefit in the flight case.

Figures 27a-27b show the EPNL curves for a variation in facesheet thickness. Because there was little benefit in the flight case, there was little difference between the two facesheets in EPNL. This type of information will help when compromising between mechanical design parameters and acoustic design parameters if a bulk liner is used.

Figures 28a-28b show the measured normal impedance for HTP 4.6 with no facesheet for 0.375 and 0.25 inches thick. The thinner liner has a much lower resistance and reactance over most of the frequency range.

Figures 29a-29b shows the effect on the third octave spectra of HTP 4.6 lbs/ft3 with two different thicknesses. When the thickness of the bulk material was reduced from 0.375 to 0.25 inch, the amount of attenuation was reduced in the lower frequency range, from 2 - 5 kHz, by as much as 2 dB (model scale, 1/3 octave spl, 1 ft lossless). The attenuation at the higher frequencies, above 5 kHz, was the same for both liners

Figure 30 shows that there were no noticeable differences in the EPNL for these two configurations where bulk thickness is varied.

Figures 31a-31b show the difference in the spectra between a bulk liner with HTP 4.6 installed in honeycomb against the same bulk material without a honeycomb core. Both liners had the same facesheet and backing depth. The purpose of the honeycomb core was to force the bulk to become a locally reacting material. This did not have a notable effect on the attenuation caused by the liner. This information will prove useful if the design warrants more structural strength from the acoustic liner panels.

Single Component Force Balance

Axial force on the nozzle was measured using a single component loadcell balance located in the body of the Jet Exit Rig upstream of the combustor. The metric/non-metric break in the force balance is achieved using a dual bellows arrangement designed to cancel pressure forces for each gas flowtube. Two of these flowtubes provide air for the model and one provides hydrogen fuel. Forces are measured in the force balance using a Sensotec miniature loadcell.

This test program was the first use of the single component force balance (SCFB). Typically when a force system is used in an aerodynamic test, the force system is calibrated in situ using a reference nozzle, such as an ASME standard nozzle, whose thrust characteristics are well known. Additionally, a drag tare calibration is usually performed to separate nozzle internal thrust, external drag, and rig drag. Due to time constraints in the test program, no such calibrations were performed. Therefore, the reader is cautioned to treat the reported force data with caution, as no check on the absolute thrust levels has been made.

The calibration used for this experiment is based on a static "deadweight" calibration performed at NASA LeRC. A known axial load was applied to the force balance to determine the primary sensitivity coefficient. This calibration was repeated with the balance flowtubes pressurized to determine the sensitivity of the balance to internal pressure loads. Due to the design of the flowtubes, this pressure correction was small. An ASME calibration, if performed, would have been used to correct for the transfer of axial momentum across the metric/non-metric break of the force balance. Since the flowtubes were designed to eliminate axial momentum transfer, it is expected that this correction would also be small.

SCFB Equations

Nozzle Pressure Ratio (NPR) was defined as:

$$NPR = \frac{P_{T7}}{P_0}$$

where P_{T7} is the total pressure of the primary nozzle, and P_0 is the static pressure of the freejet flow.

The ideal primary nozzle exit velocity (V_{id}) was defined as:

$$Vid = \sqrt{\frac{2\gamma R T_{T7}}{\gamma - 1}\left(1 - NPR^{\frac{\gamma-1}{\gamma}}\right)}$$

The ideal thrust based on actual mass flow ($F_{id,act}$) was defined as:

$$F_{id,act} = w_p V_{id}$$

where w_p is the measured mass flow through the primary nozzle.

Velocity coefficient (C_v) was defined as:

$$Cv = \frac{F_m}{F_{id,act}}$$

where F_m is the measured force on the nozzle.

SCFB Results

To ensure repeatability of the data, four liner configurations were repeated on separate test runs. These repeats provide a consistency check of the force data. Figure 32 shows the results of these repeat runs. Shown is C_v plotted against NPR. As with all of the force data, two bands of data appear on each plot. The upper band of data was recorded at static conditions. The lower band of data was recorded at a freejet Mach number of 0.3. The results shown in Figure 32d represent the worst case in terms of consistency of the data. The data recorded on the first and second runs of June 24 exhibit a three percent discrepancy in velocity coefficient. It is believed that inconsistent testing procedures are responsible for this large discrepancy. In general, figure 32 indicates about a 1-1_ percent variability in the velocity coefficient data. It is important to note that many of the "relationships" described in the following paragraphs are based on differences in velocity coefficients that are within this error band. Therefore, these results should be viewed with caution.

Figures 33-43 show the results of parametric variations of liner characteristics. Shown is C_v plotted against NPR. On each plot, the results of hardwall testing are plotted for reference.

Figure 33 shows the effect of liner porosity on thrust performance for the SDOF liners. The results indicate a decrease in performance with increasing porosity.

Figure 34 shows the effect of facesheet hole diameter on thrust performance for the SDOF liners. The plot suggests a possible decrease in performance with increasing hole size. However the effect, if any, is small.

Figure 35 shows the effect of honeycomb cell size on thrust performance for the SDOF liners. The results of this test are inconsistent. For a freejet Mach number of 0.3 indicate a performance increase with increasing cell size. The static results indicate a slight performance decrease with increasing cell size.

Figure 36 shows the effect of facesheet material thickness on thrust performance for the SDOF liners. The results indicate an increase in performance with increasing facesheet thickness.

Figure 37 shows the effect of honeycomb depth on thrust performance for the SDOF liners. The results do not indicate a monotonic relationship. In general the thickest and thinnest honeycombs produced the highest thrust at about the same levels, with the medium thickness honeycomb producing a lower thrust.

Figure 38 shows the effect of facesheet characteristics on thrust performance for the Ultramet SiC bulk liners. There are two plots in this figure: a) for the 200 ppi material, and b) for the 400 ppi material. Both plots show a decrease in thrust performance with increasing facesheet porosity, although in figure 38b, the effect is not as strong. This finding is consistent with the results from the SDOF liners, shown in figure 33. Figure 38a also depicts the effect of facesheet thickness on thrust performance. The results indicate increased performance with increasing facesheet thickness. This trend is consistent with the results from the SDOF liners, shown in figure 36.

Figure 39 shows the effect of bulk material pores per inch on thrust performance for the Ultramet SiC bulk liners. There are two plots in the figure: a) for a 0.37 porosity facesheet, and b) for a 0.20 porosity facesheet. On both plots, the 200 ppi material has better thrust performance than the 400 ppi material.

Figure 40 shows the effect of material density on thrust performance for the Rohr/Lockheed HTP bulk liners. The highest density material, which was significantly denser than the others tested, appears to have the highest thrust performance. For the other three materials, however, there is no clear correlation between material density and performance.

Figure 41 shows the effect of facesheet characteristics on thrust performance for the Rohr/Lockheed HTP 1 bulk liners. No clear correlation can be seen between facesheet porosity and performance. This result is inconsistent with the results from the SDOF and Ultramet SiC liners. The results also indicate an increase in thrust performance with increasing facesheet thickness. This result is consistent with the results from the SDOF and Ultramet SiC liners.

Figure 42 shows the effect of bulk material geometry for the Rohr/Lockheed HTP 1 bulk liners. The performance of the 0.375 x 0.375 honeycomb material is greater than the 0.375 thick bulk material. There is no clear correlation between bulk material thickness and thrust performance. This result is similar to that seen for the SDOF liners in figure 37.

Figure 43 shows the effect of facesheet porosity on thrust performance for the Amercom SiC material. The result is not definitive, the thicker facesheet producing better performance at low NPRs and the thinner facesheet producing better performance at high NPRs for the static condition. This result appears to be similar to that for the Rohr/Lockheed HTP 1 bulk liners, shown in figure 41. There is no data for the thinner facesheet for a freejet Mach number of 0.3.

The thrust results presented above exhibit a number of consistent trends, which support the validity of the thrust data despite the lack of calibration. In general, the results indicate that thrust performance benefits from increased facesheet thickness and decreased facesheet porosity.

References

1. "Aeroacoustics of Flight Vehicles: Theory and Practice, Volume 2: Noise Control", NASA Reference Publication 1258, Vol. 2, August 1991.

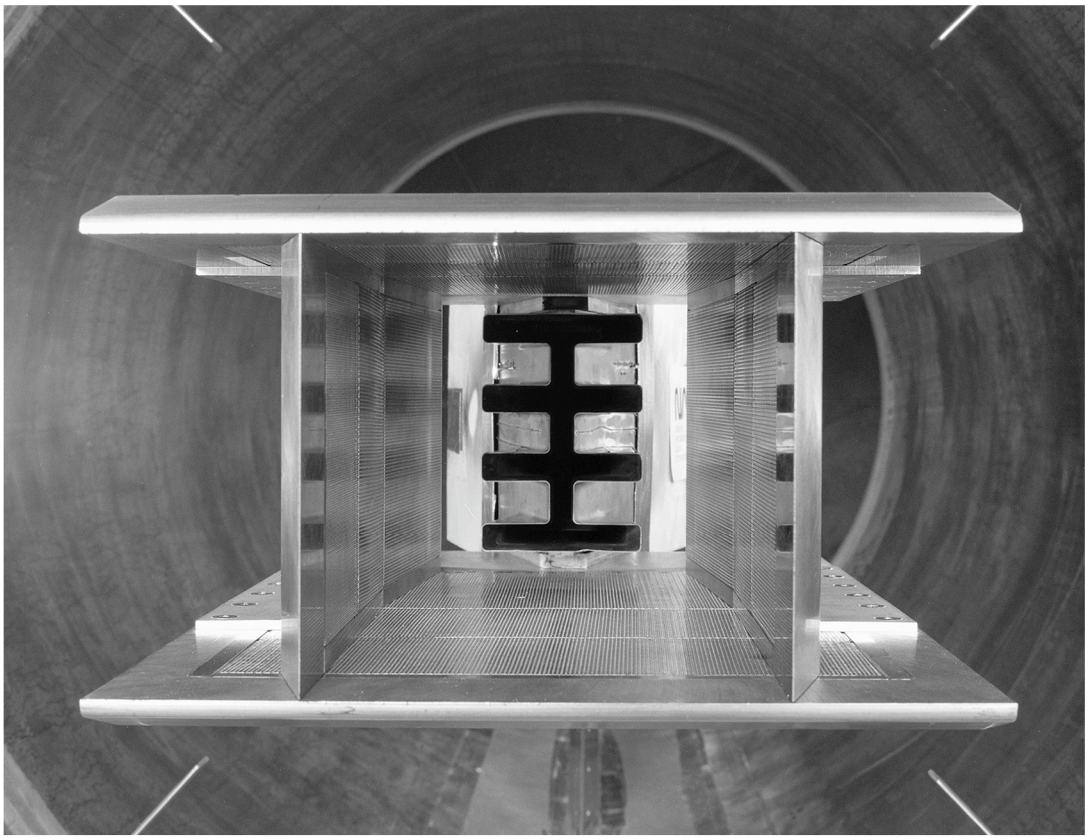

Figure 1.—Pratt & Whitney Generation 1 (GEN1) Model in the Nozzle Acoustic Test Rig (NATR).

Hardwall vs. SDOF vs. Bulk
NPR=1.99 T = 1139 R
1 Ft Radius, Lossless, Model Scale, 115°

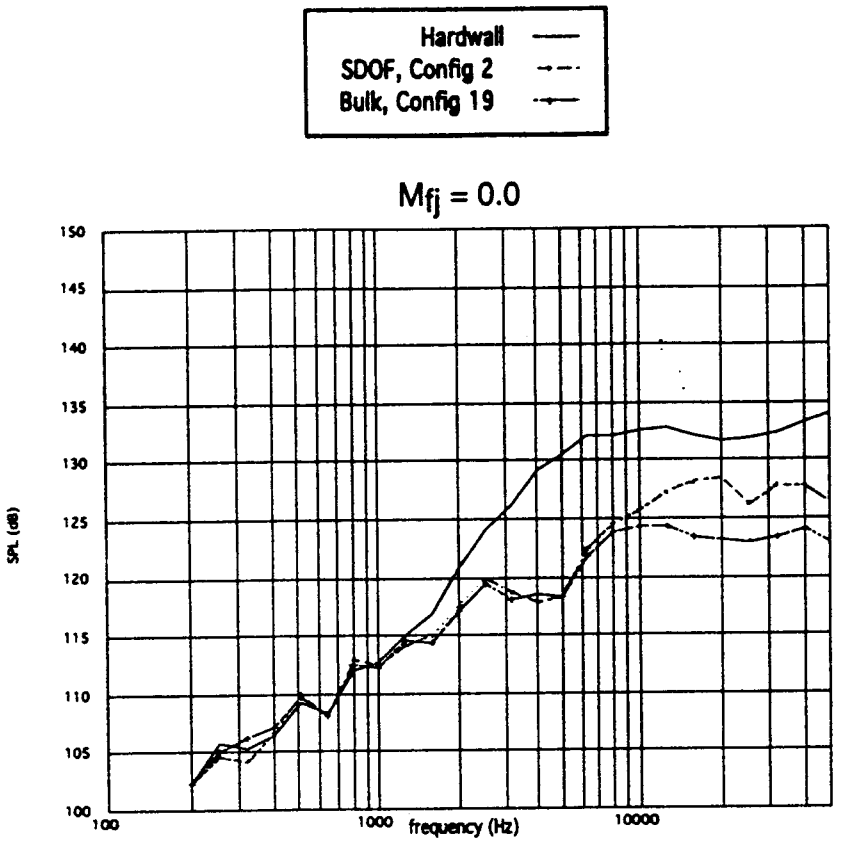

Figure 2

Hardwall vs. SDOF vs. Bulk
NPR=2.48 T = 1291 R
1 Ft Radius, Lossless, Model Scale, 115°

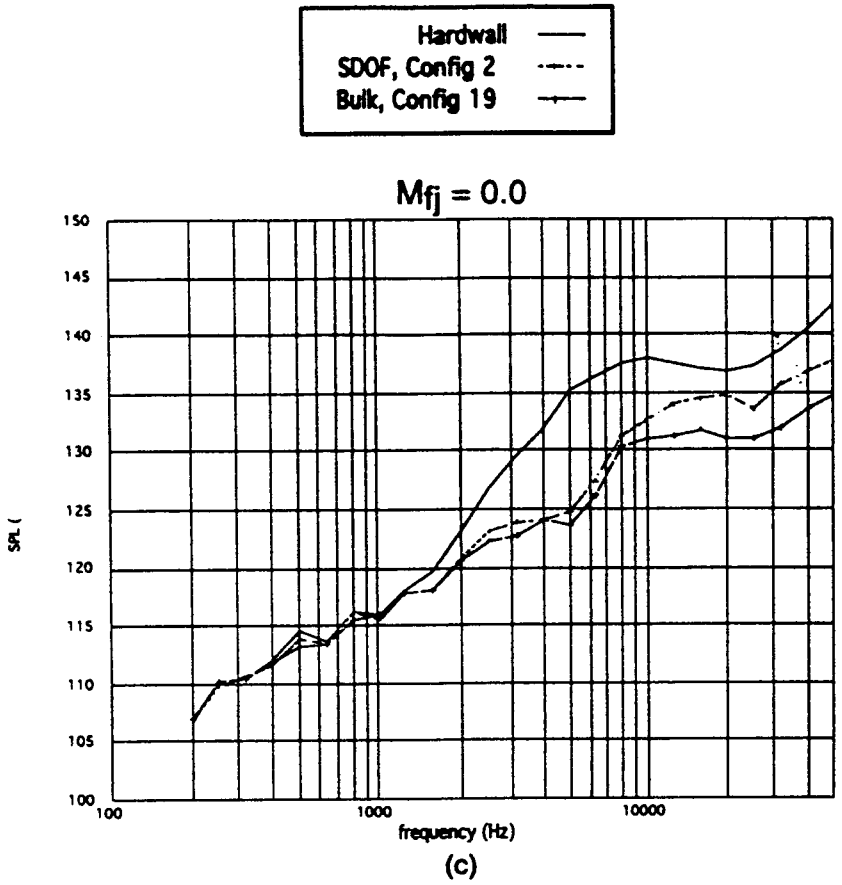

Figure 2 (continued)

Hardwall vs. SDOF vs. Bulk
NPR=3.43 T = 1551 R
1 Ft Radius, Lossless, Model Scale, 115°

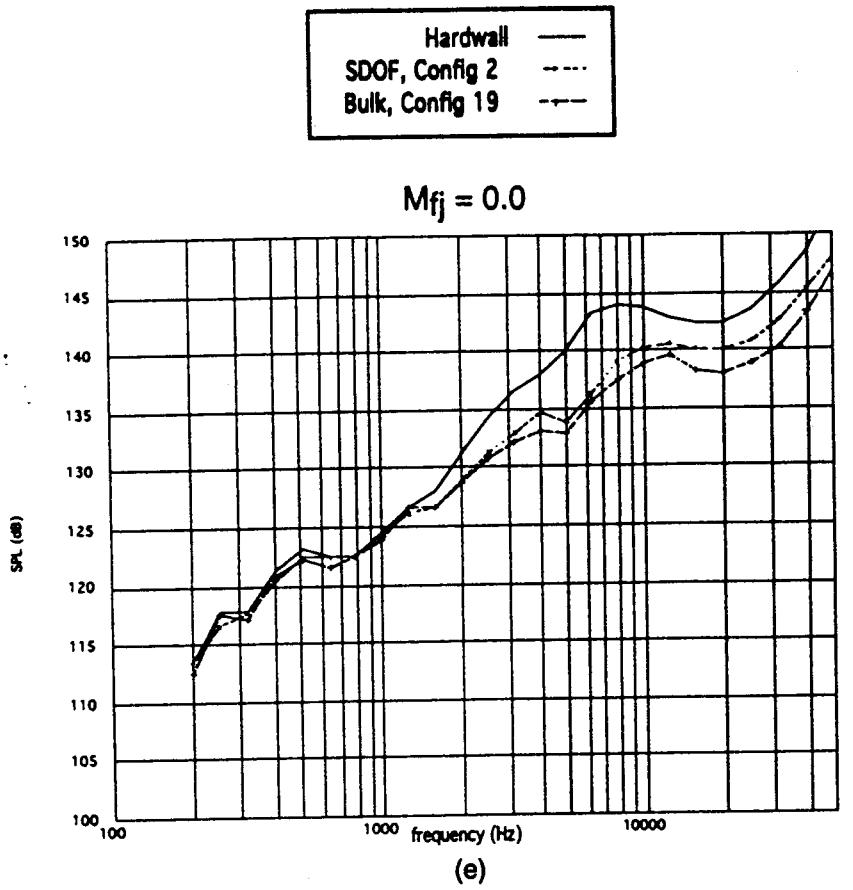

Figure 2 (continued)

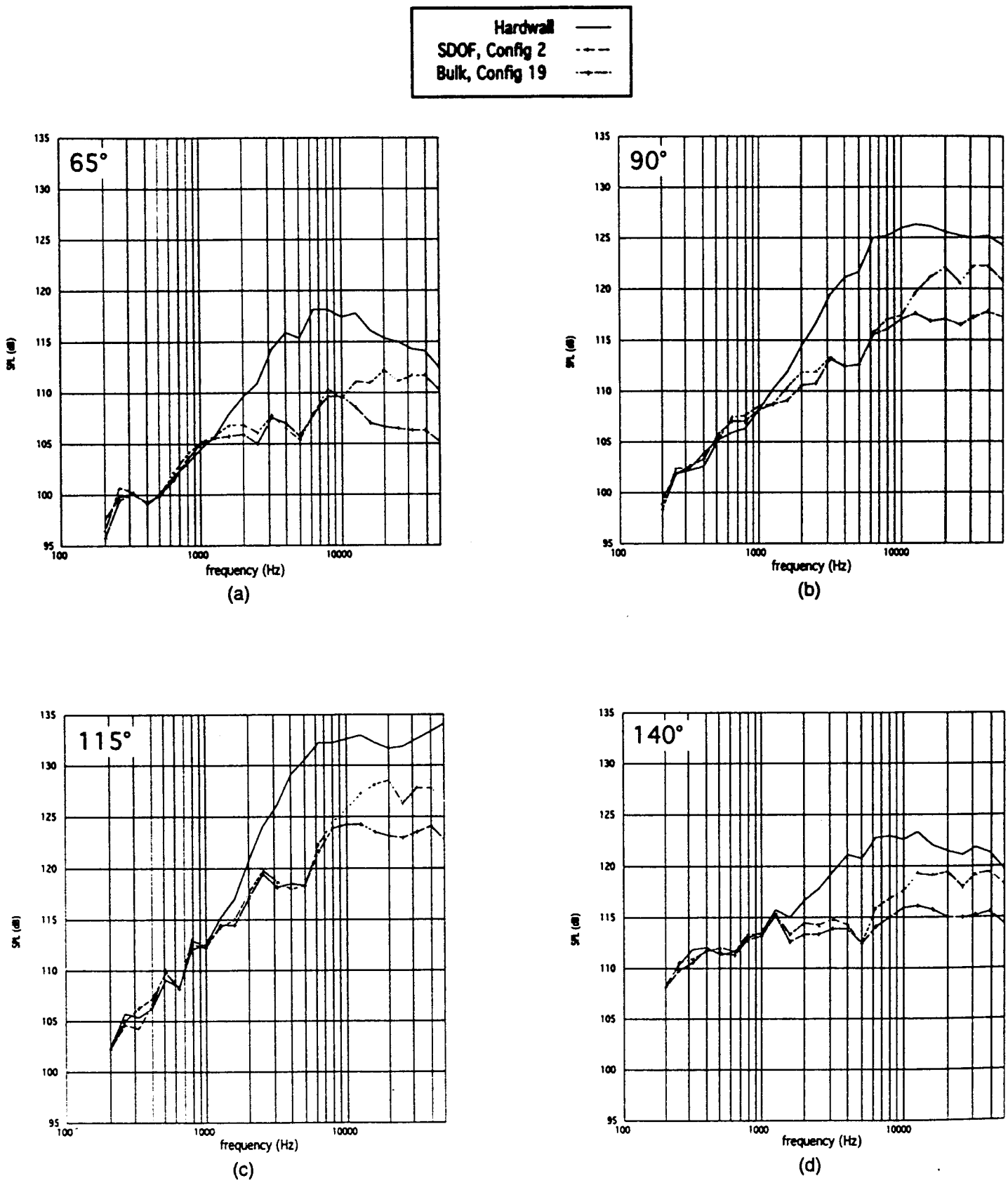
Hardwall vs. SDOF vs. Bulk
NPR=1.99 T = 1139 R, Mfj = 0.0
1 Ft Radius, Lossless, Model Scale
Hardwall
SDOF, Config 2
Bulk, Config 19
65°
90°
115°
140°
SPL (dB)
frequency (Hz)
(a)
(b)
(c)
(d)

Figure 3

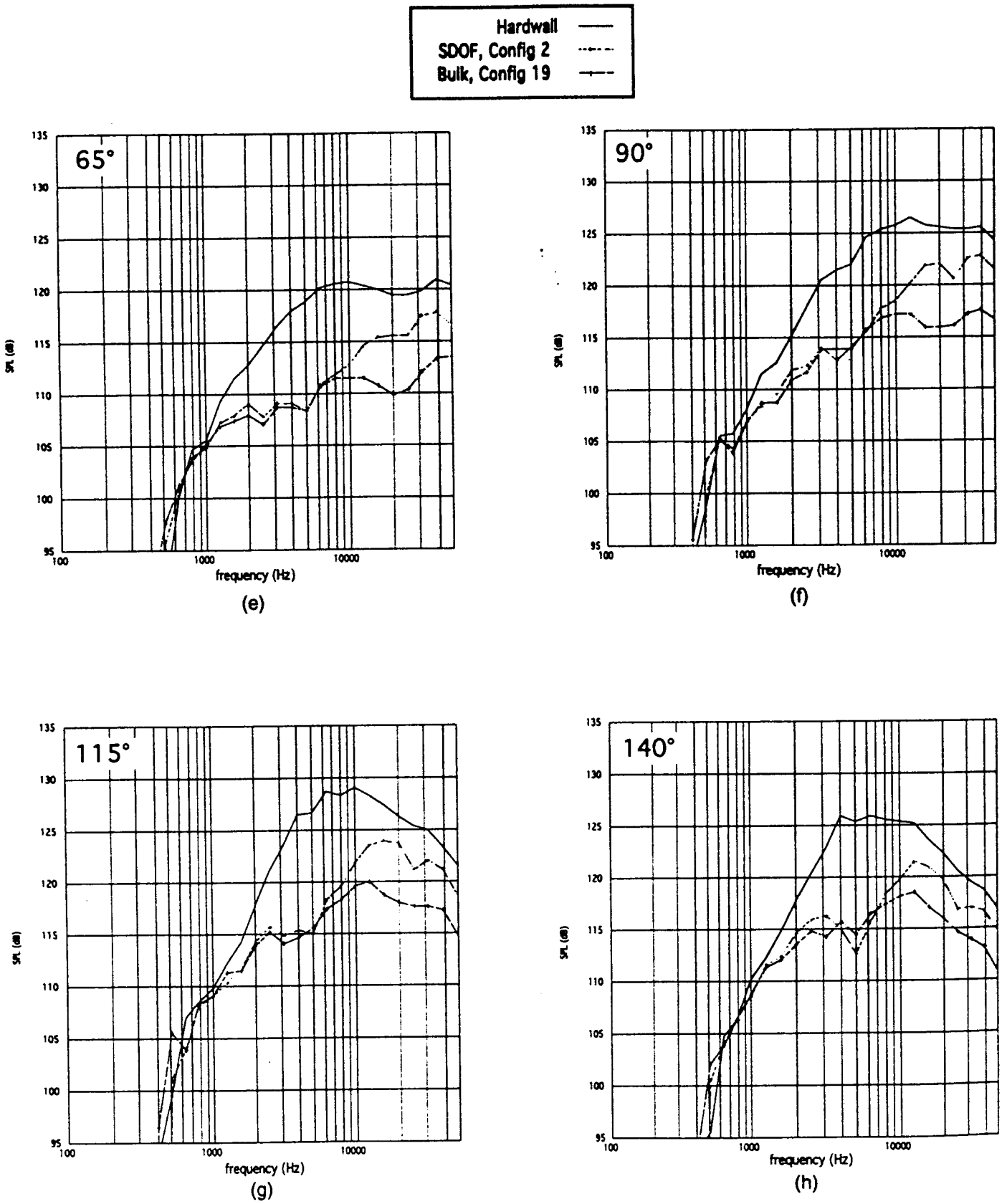

Figure 3 (continued)

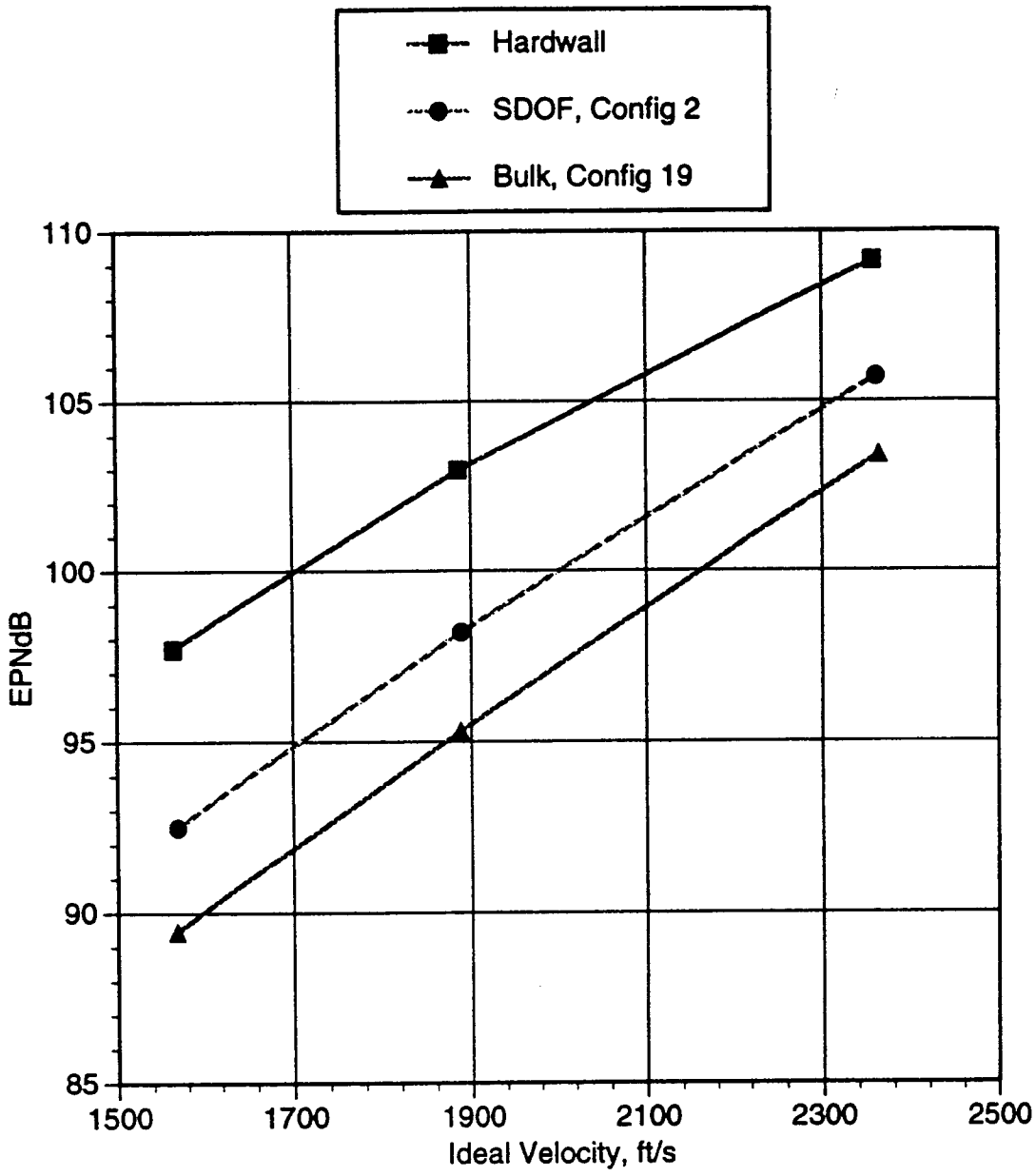
Harwall vs. SDOF vs. Bulk
EPNL, Full Scale, Mfj=0.3
Hardwall
SDOF, Config 2
Bulk, Config 19
EPNdB
110
105
100
95
90
85
1500
1700
1900
2100
2300
2500
Ideal Velocity, ft/s

Figure 4

Predicted Normal Acoustic Impedance
SDOF Liners

Fig 5a: Facesheet Porosity

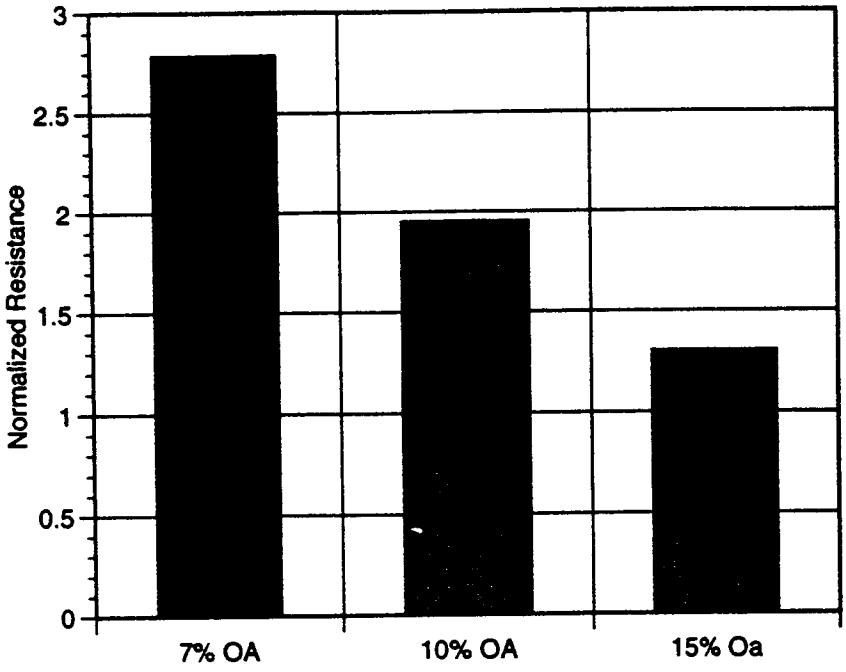

Fig 5b: Facesheet Porosity

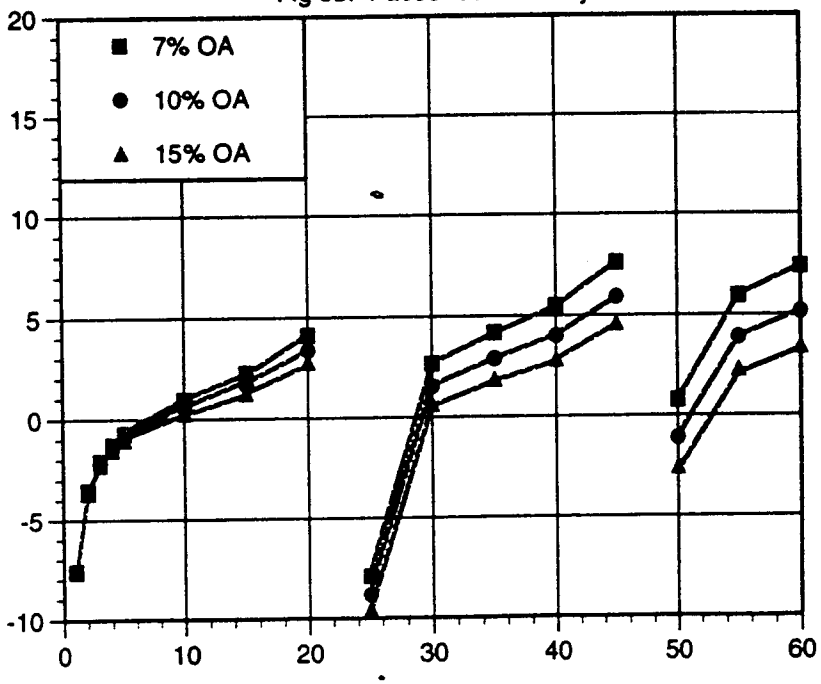

Figure 5

Fig 5c: Facesheet Hole Diameter

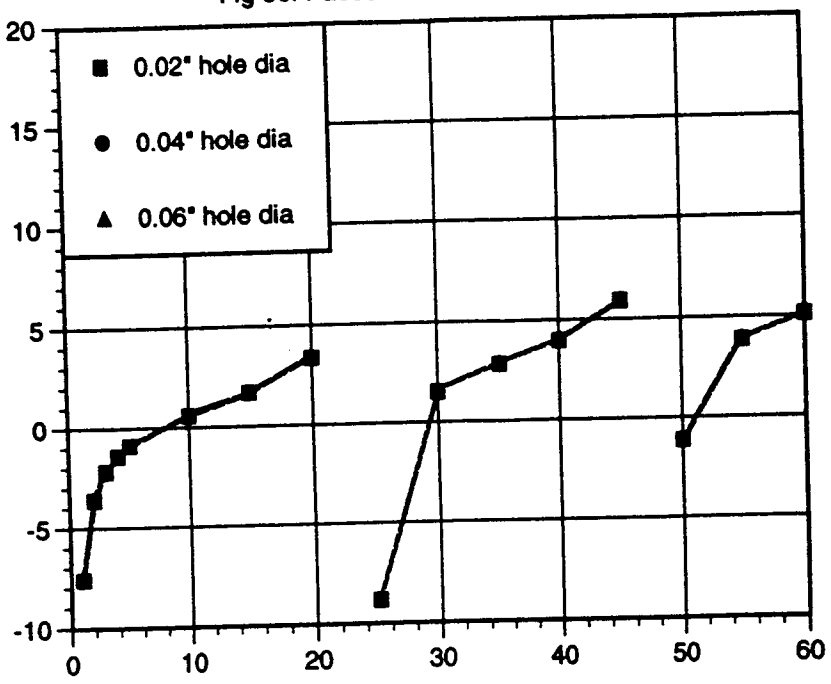

Fig 5d: Facesheet Thickness

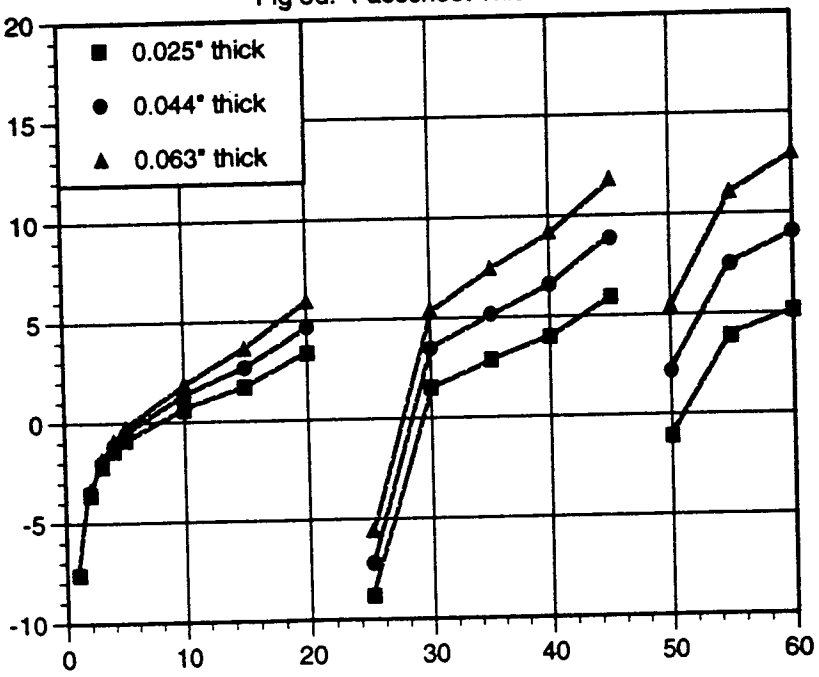

Figure 5 (continued)

Fig 5e: Honeycomb Cell Size

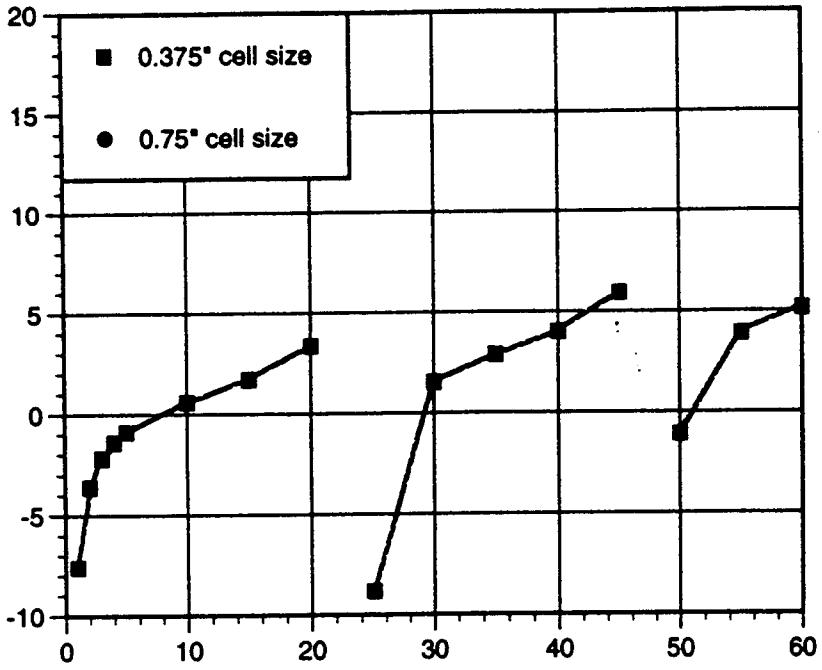

Fig 5f: Honeycomb Depth

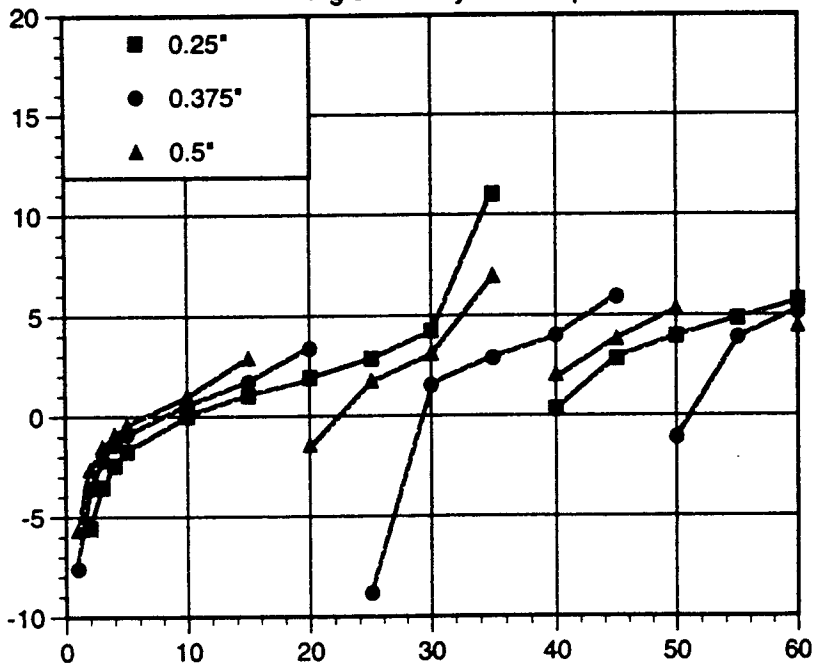

Figure 5 (continued)

Facesheet Porosity Effects
SDOF, 0.375" Deep 0.375" Cell Honeycomb
1 Ft Radius, Lossless, Model Scale, 115°

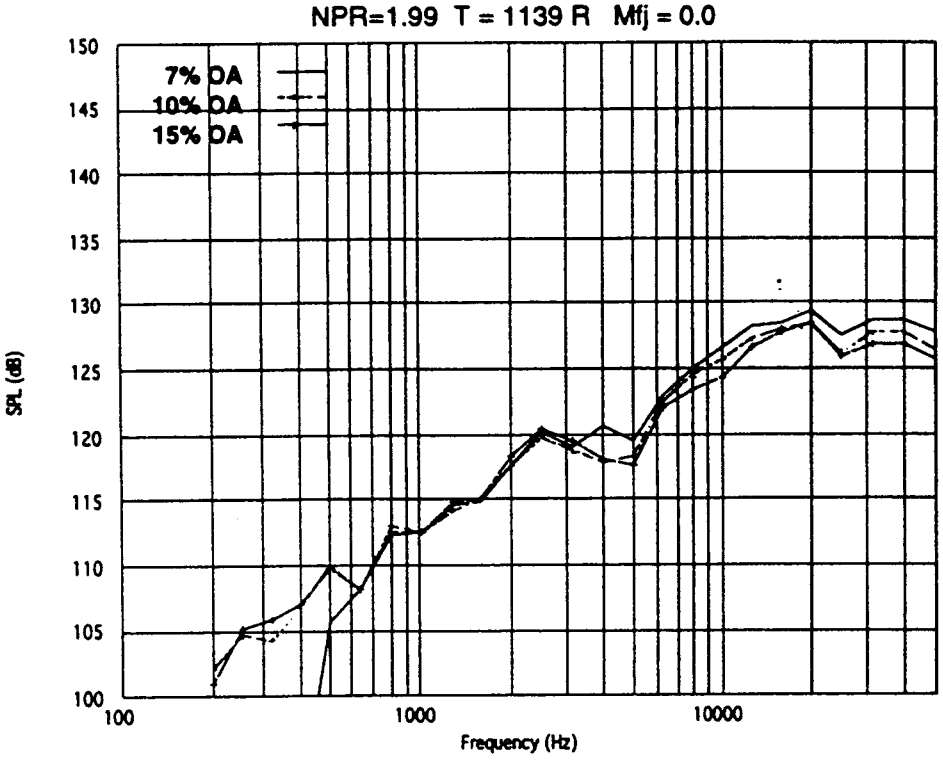

(a)

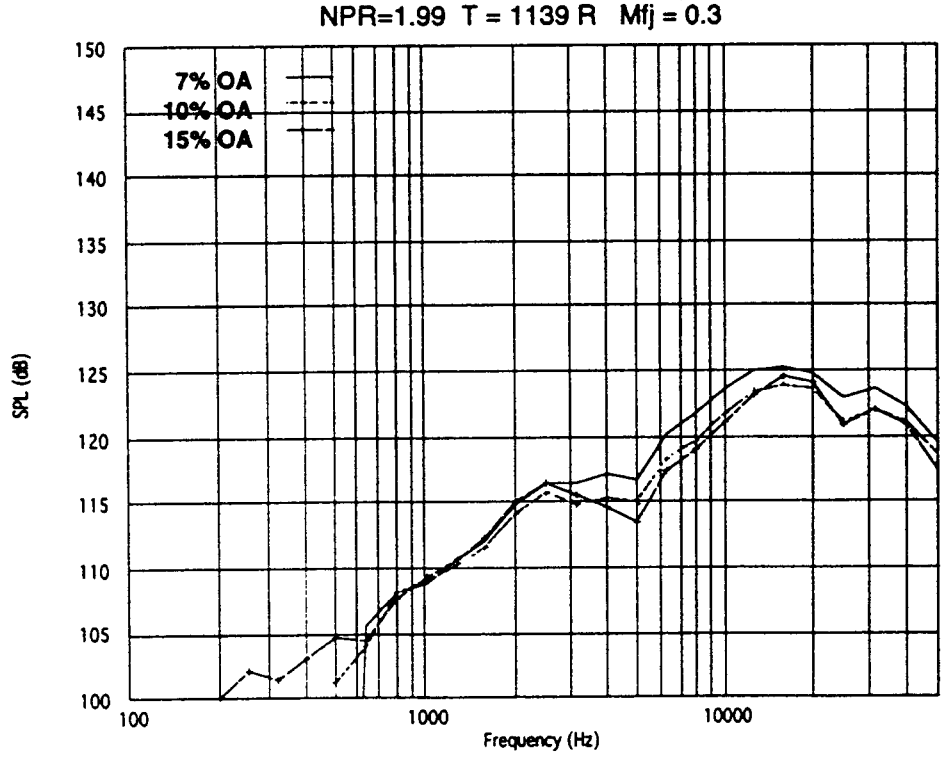

(b)

Figure 6

Facesheet Porosity Effects
SDOF, 0.375" Deep 0.375" Cell Honeycomb
1 Ft Radius, Lossless, Model Scale, 115°

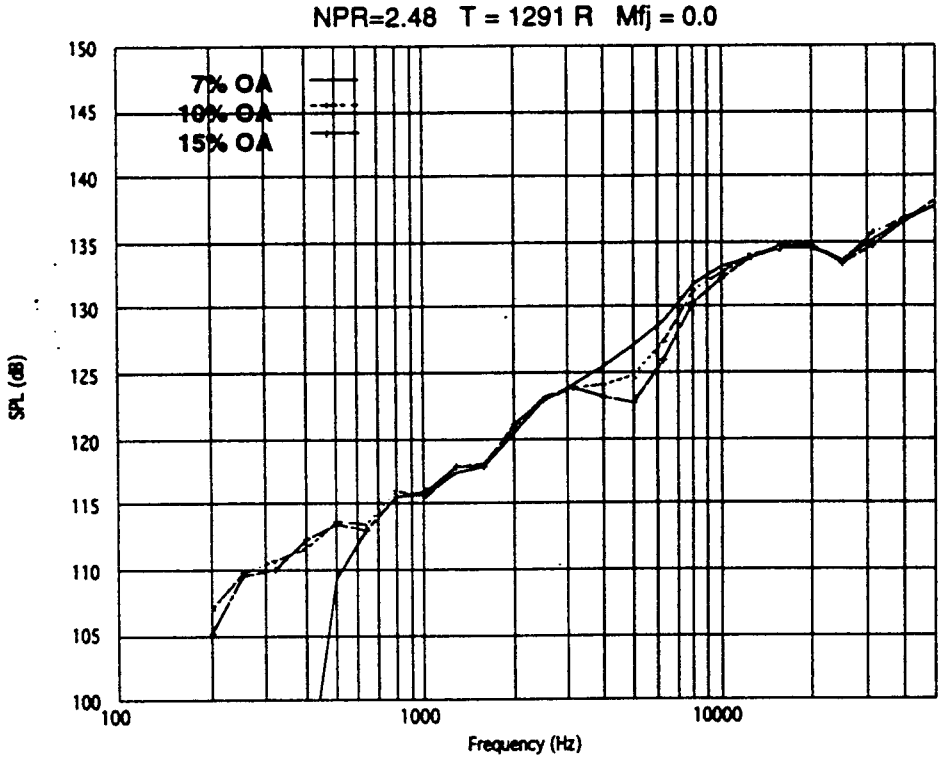

(c)

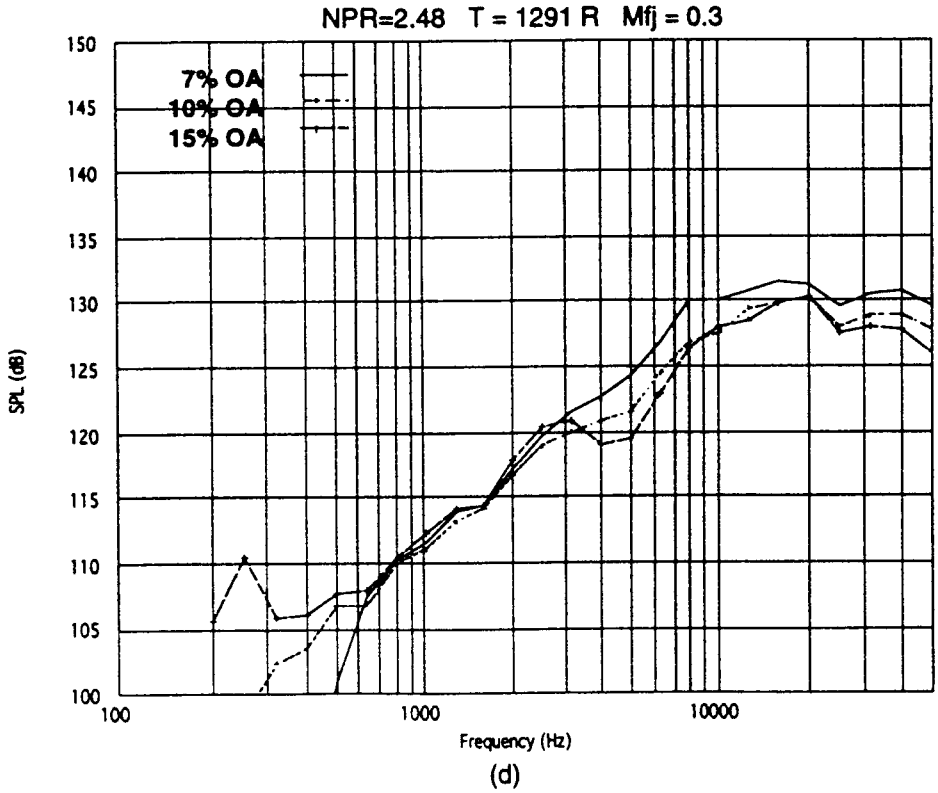

(d)

Figure 6 (continued)

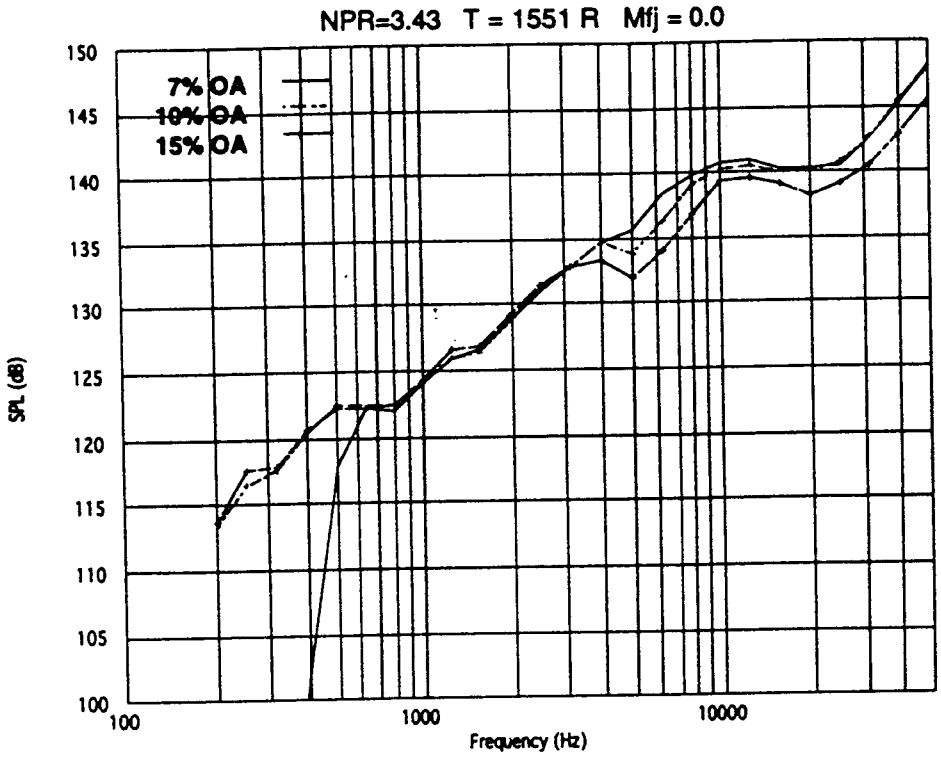

(e)

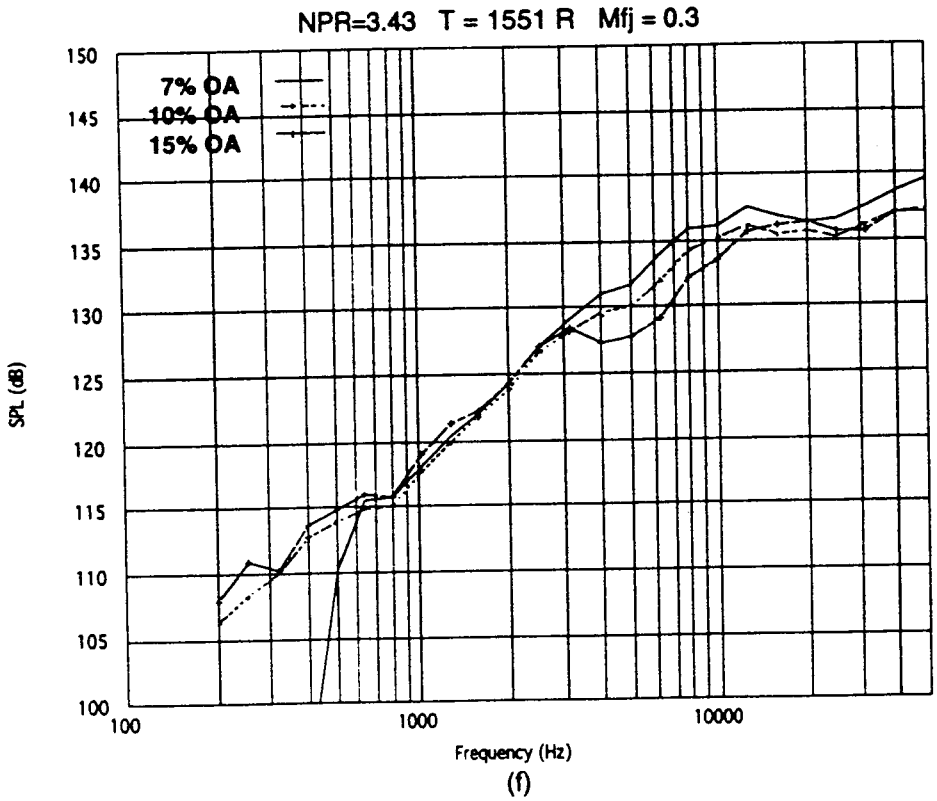

(f)

Figure 6 (continued)

Facesheet Porosity Effects
EPNL, Full Scale, Mfj=0.3

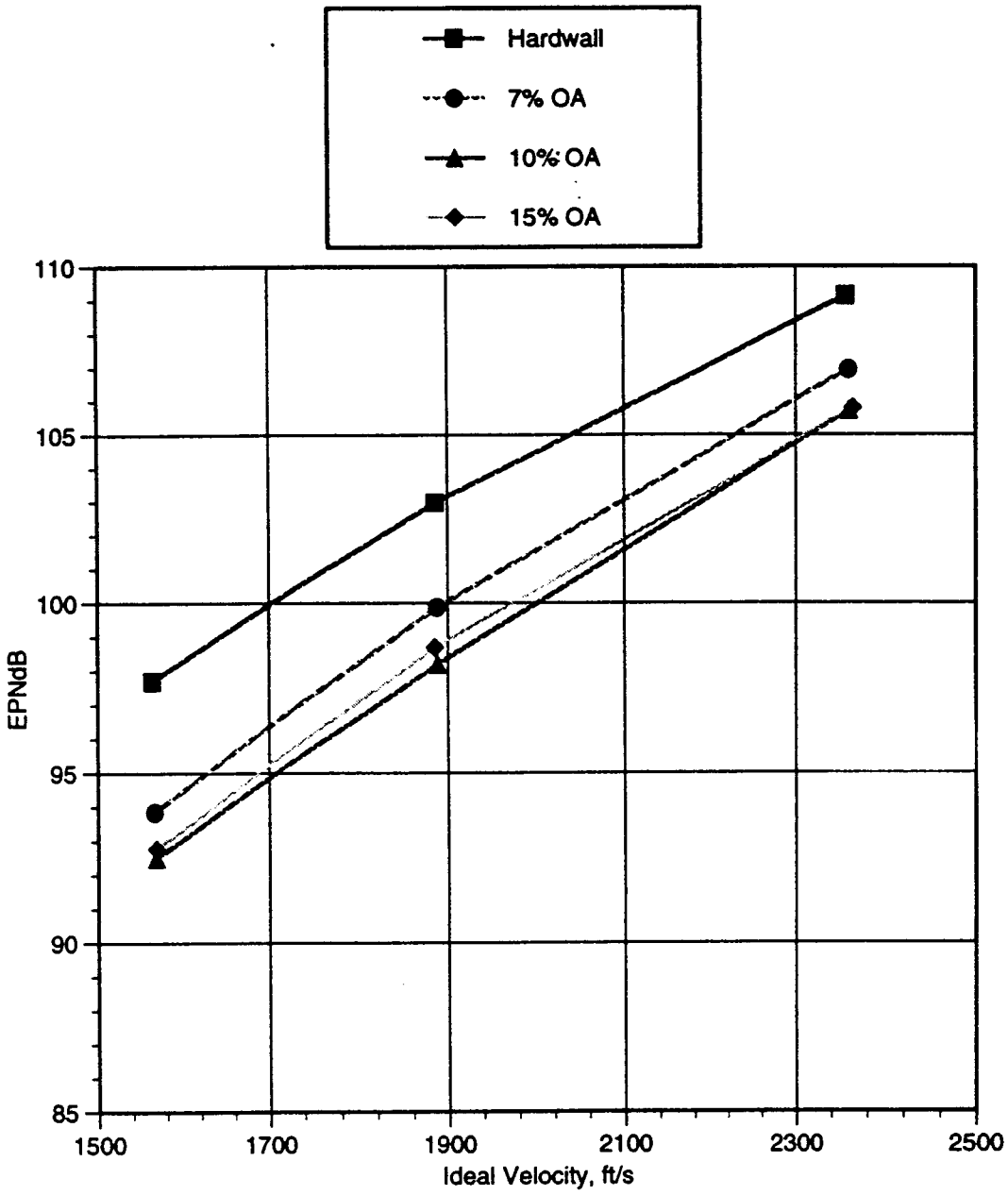

Figure 7

Facesheet Hole Diameter Effects
SDOF, 0.375" Deep 0.375" Cell Honeycomb
1 Ft Radius, Lossless, Model Scale, 115°

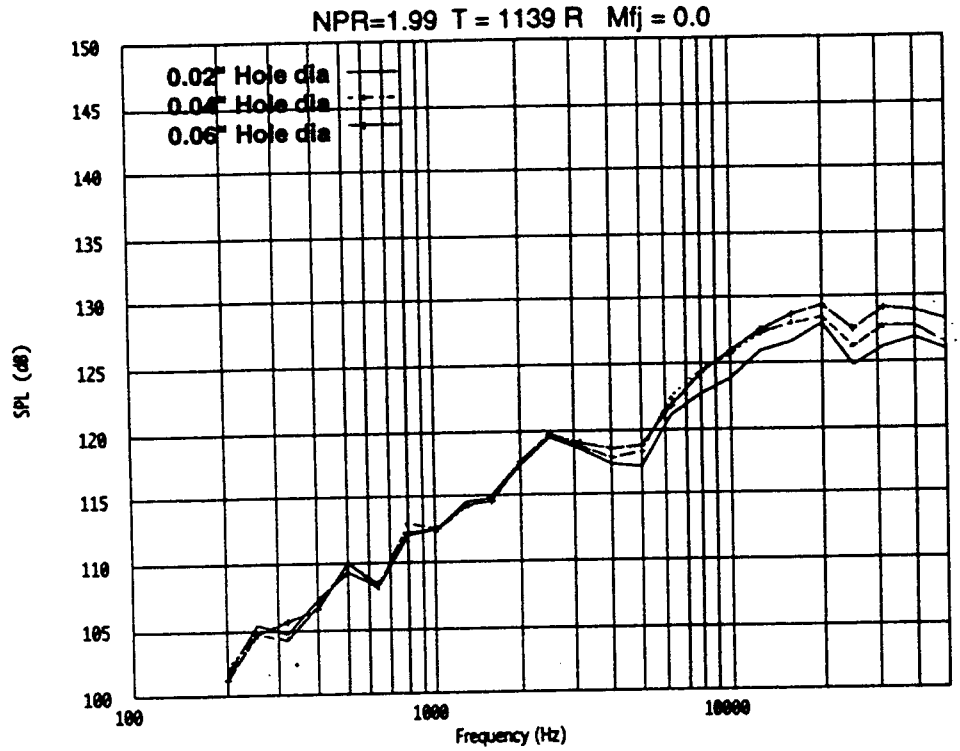

(a)

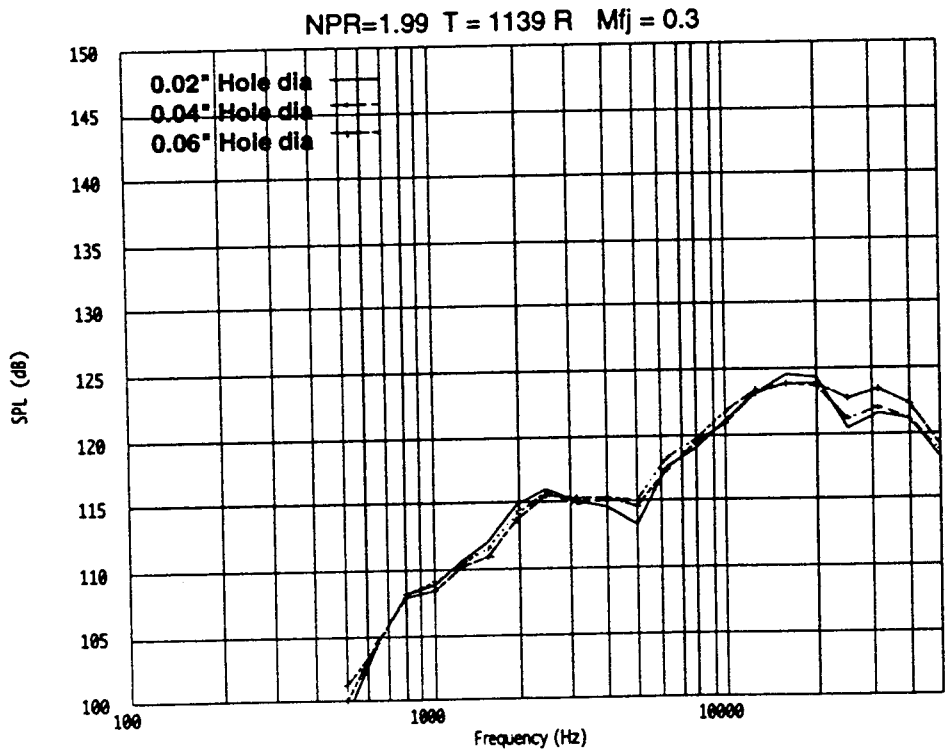

(b)

Figure 8

Facesheet Hole Diameter Effects
SDOF, 0.375" Deep 0.375" Cell Honeycomb
1 Ft Radius, Lossless, Model Scale, 115°

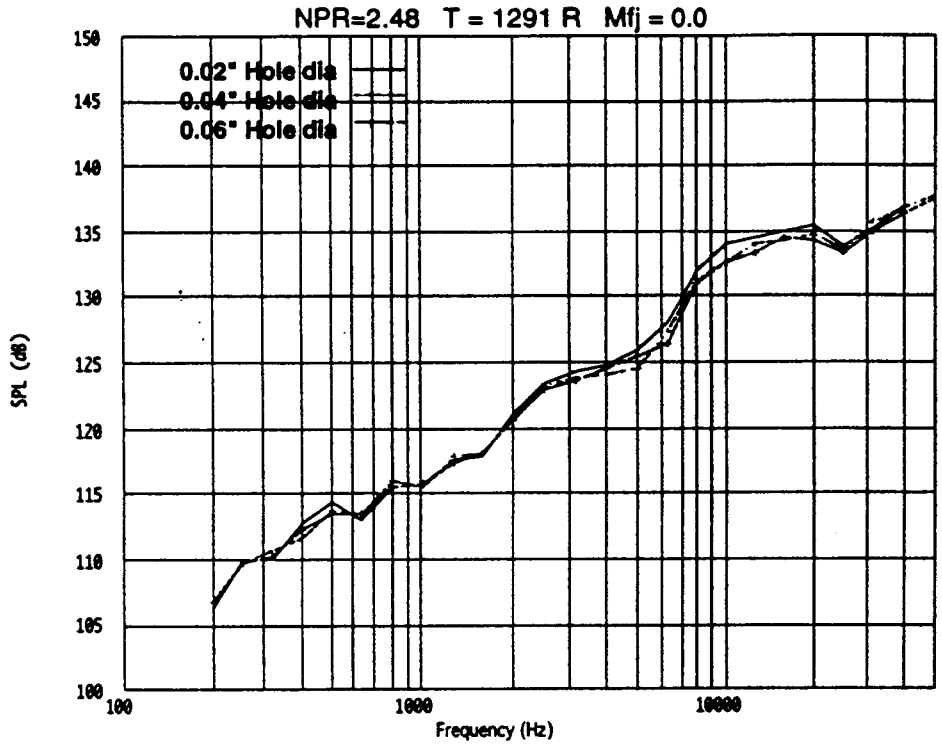

(c)

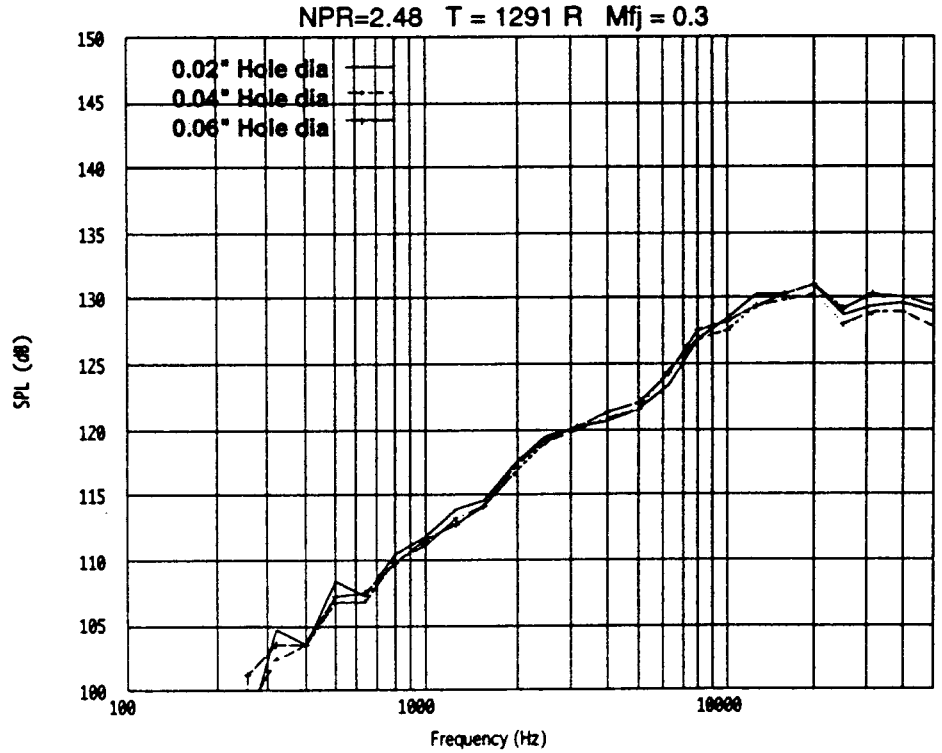

(d)

Figure 8 (continued)

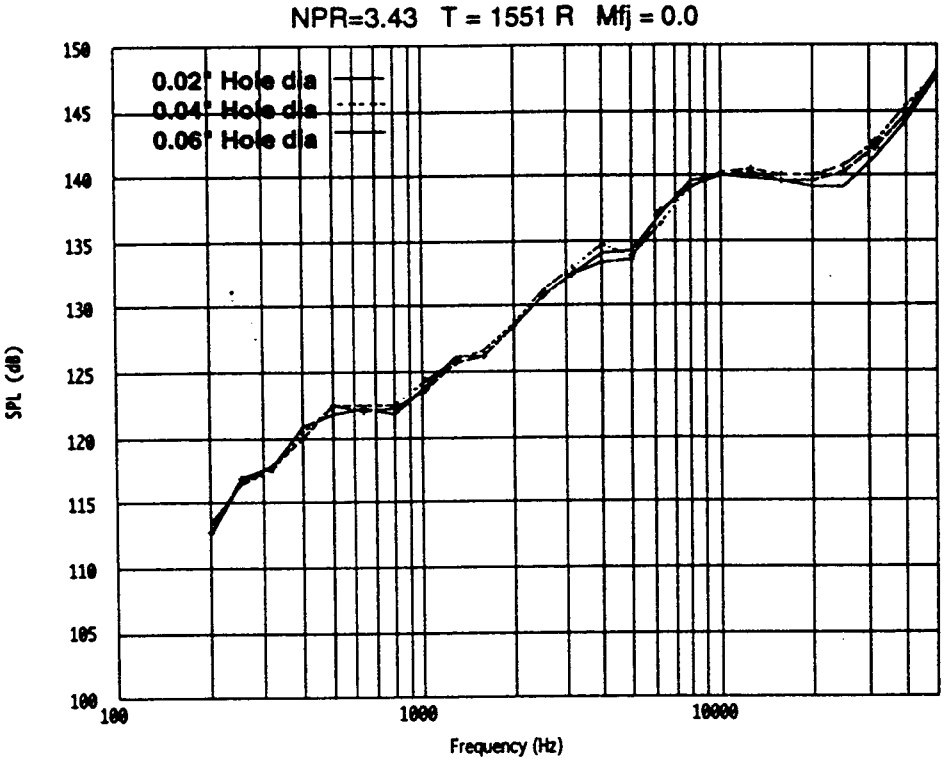

(e)

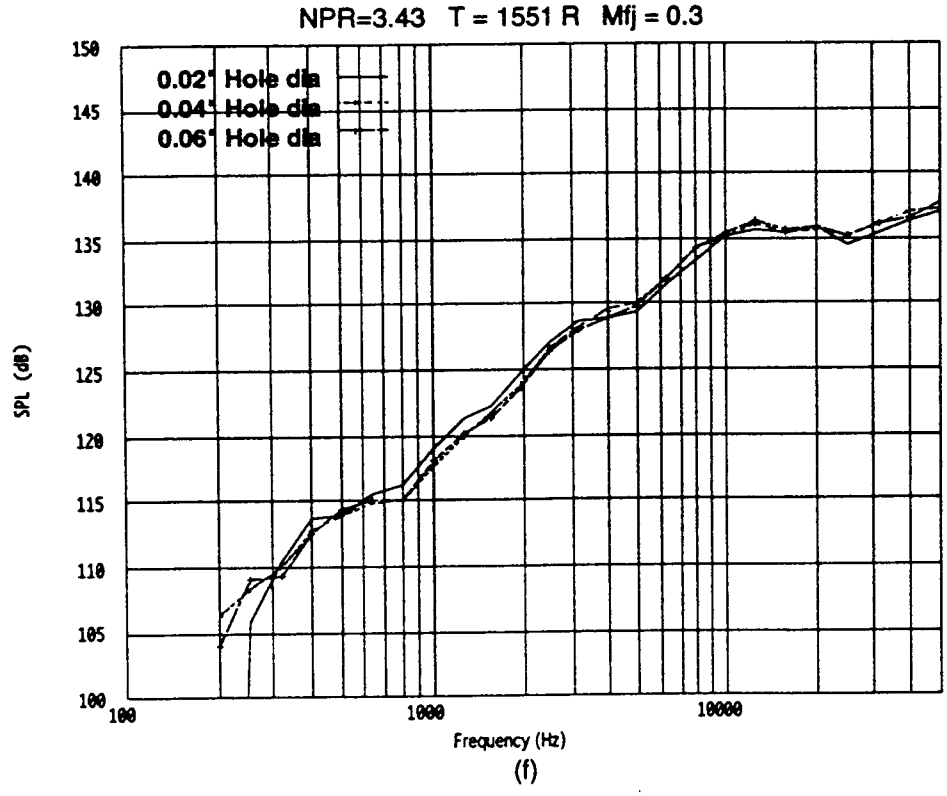

(f)

Figure 8 (continued)

Facesheet Hole Diameter Effects
EPNL, Full Scale, Mfj=0.3

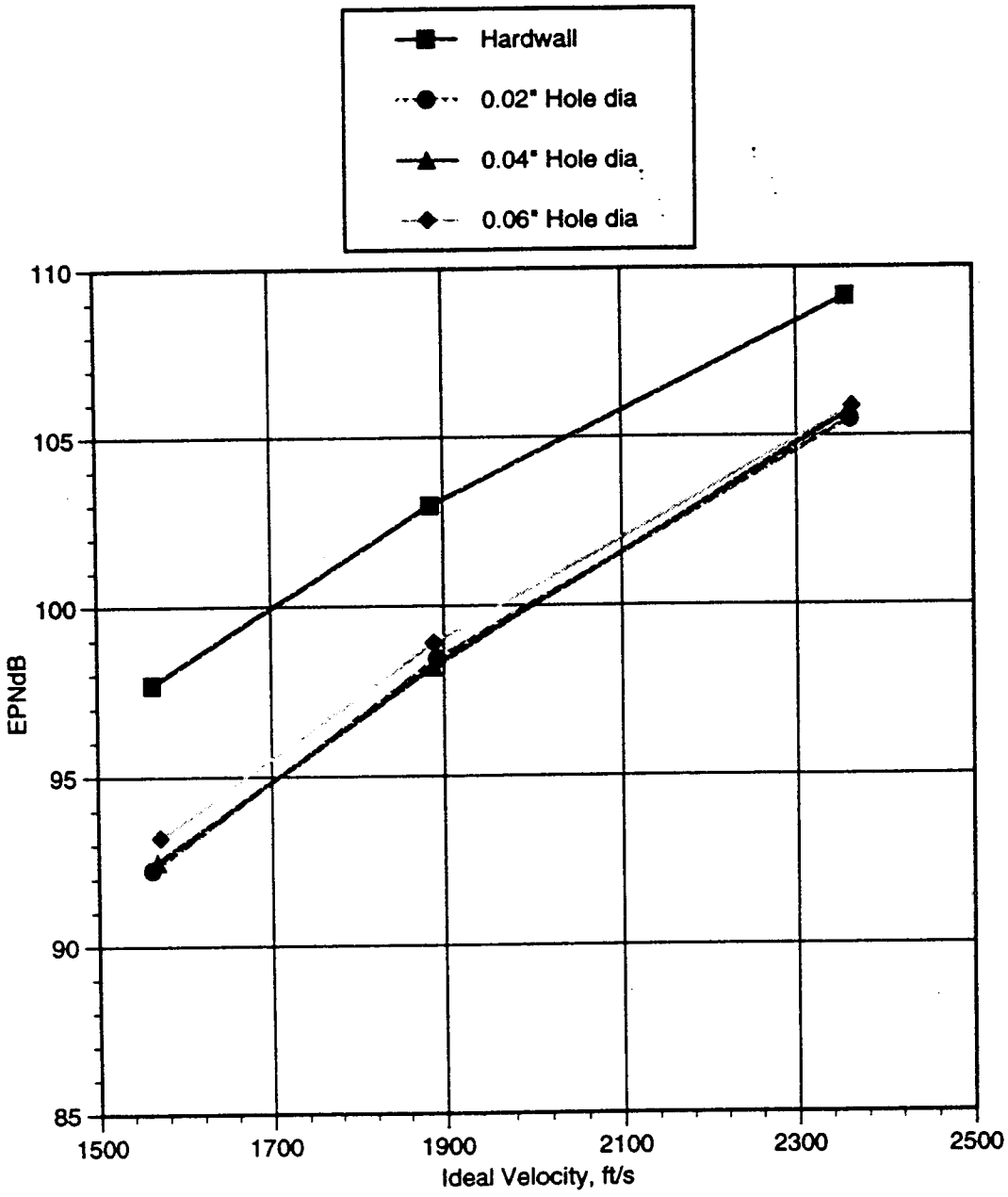

Figure 9

Facesheet Thickness Effects
SDOF, 0.375 Deep 0.375 Cell Honeycomb
1 Ft Radius, Lossless, Model Scale, 115°

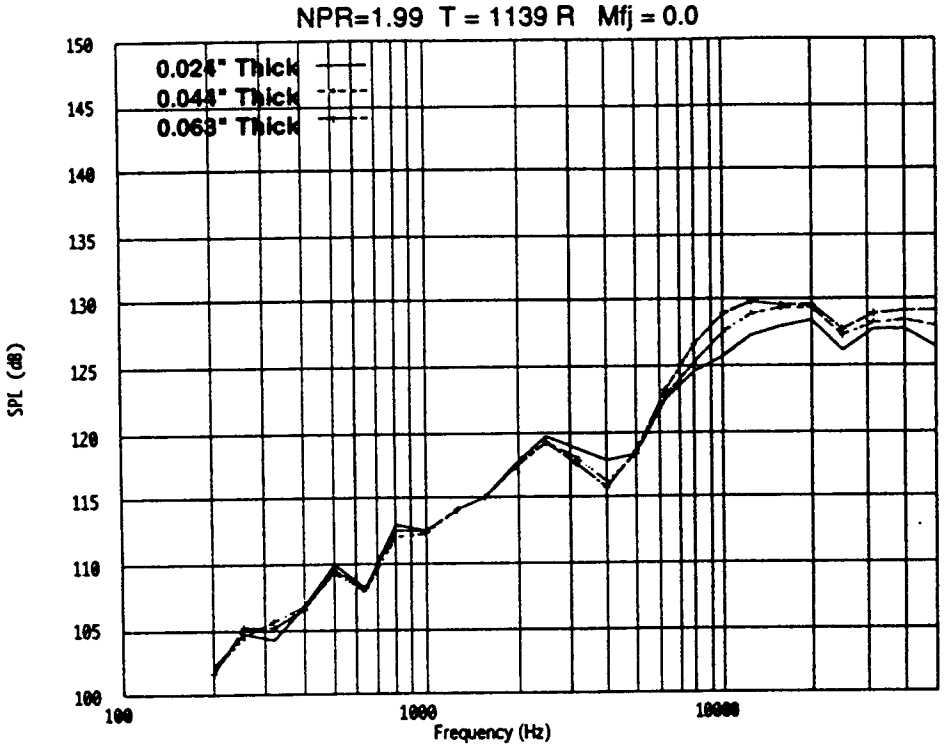

(a)

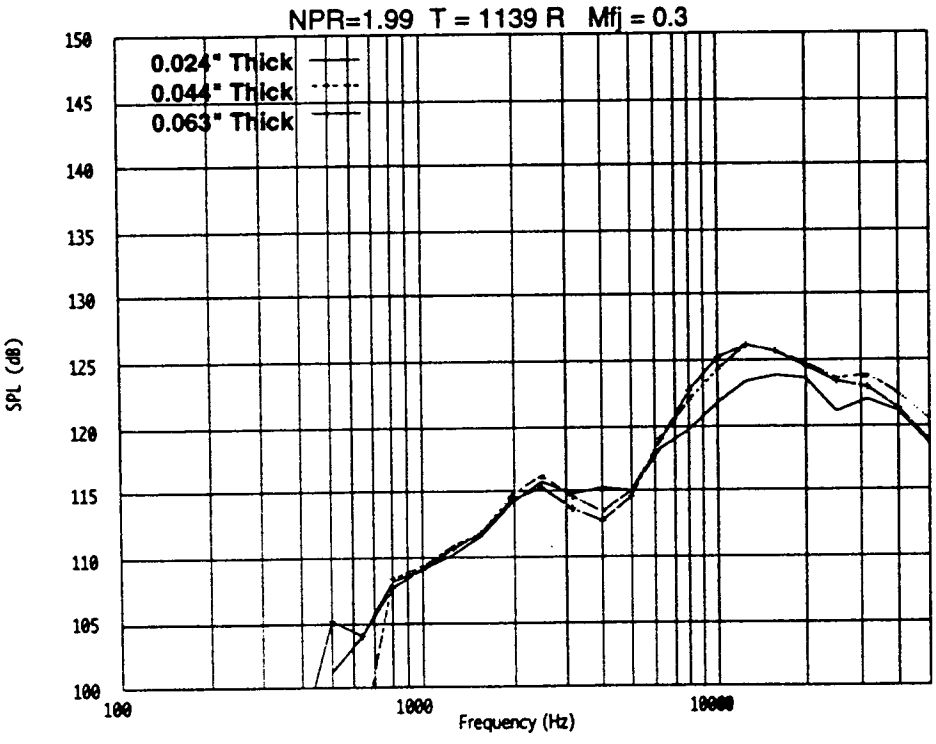

(b)

Facesheet Thickness Effects
SDOF, 0.375 Deep 0.375 Cell Honeycomb
1 Ft Radius, Lossless, Model Scale, 115°

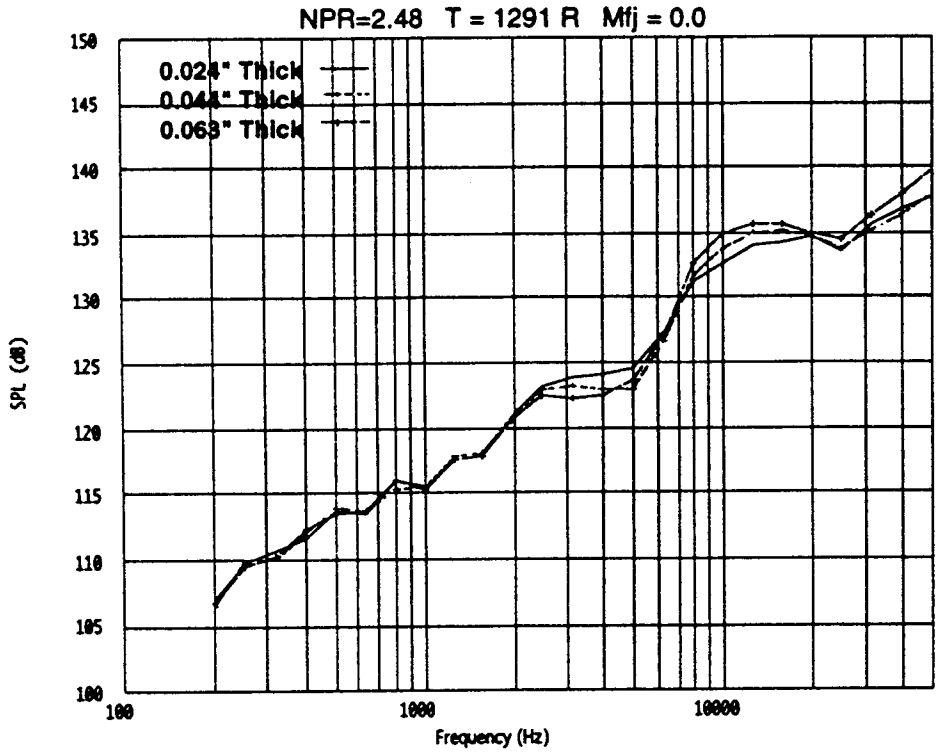

(c)

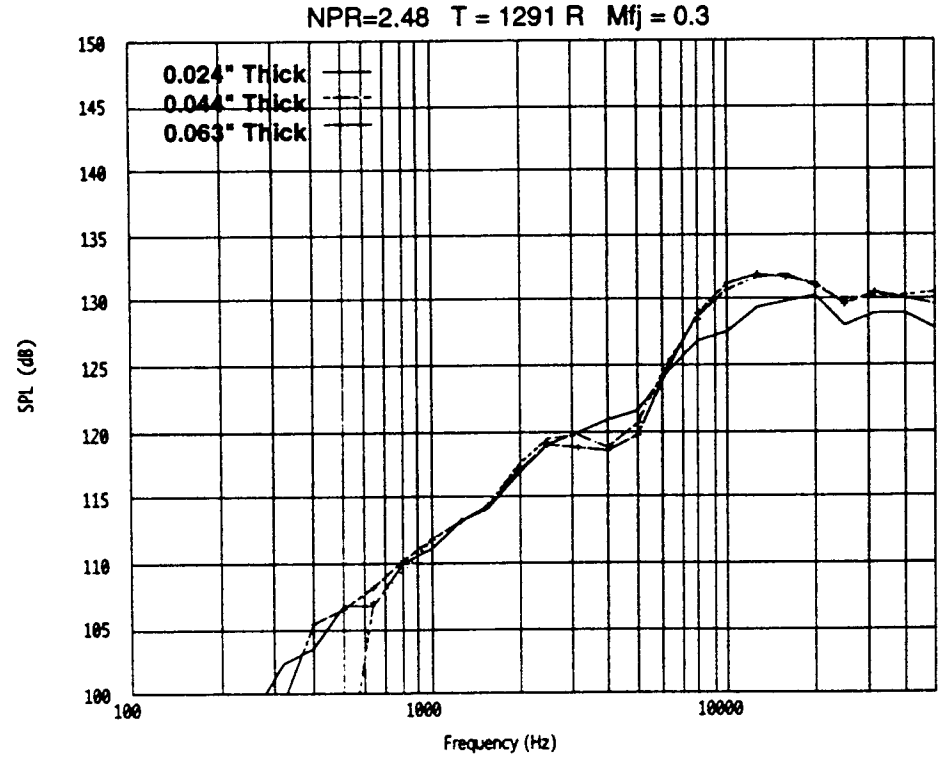

(d)

Figure 10 (continued)

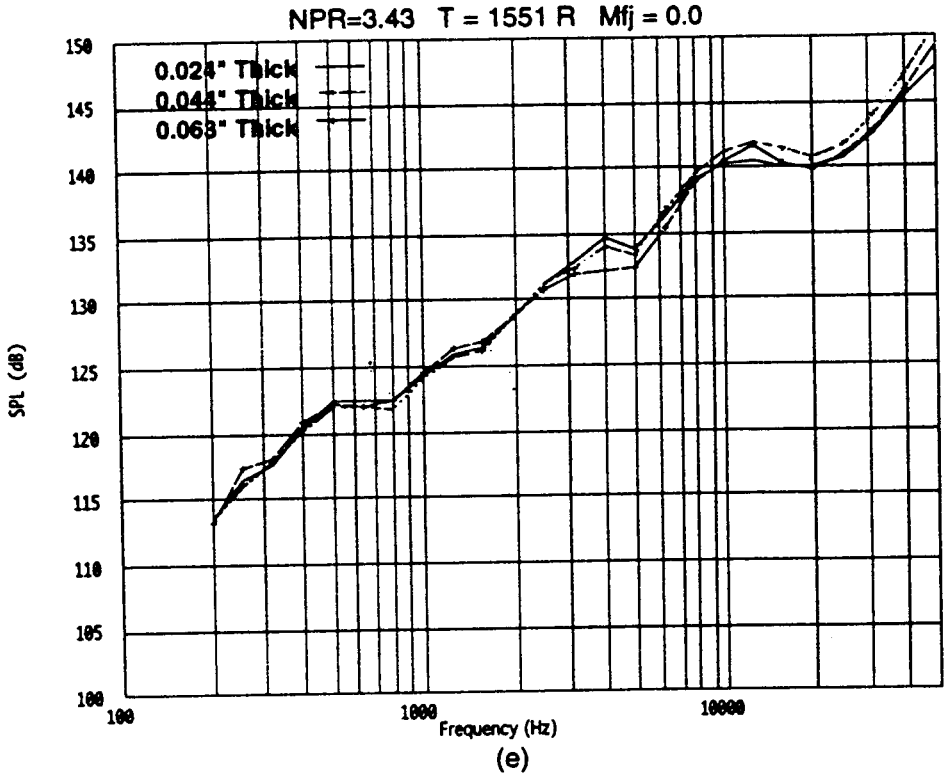

(e)

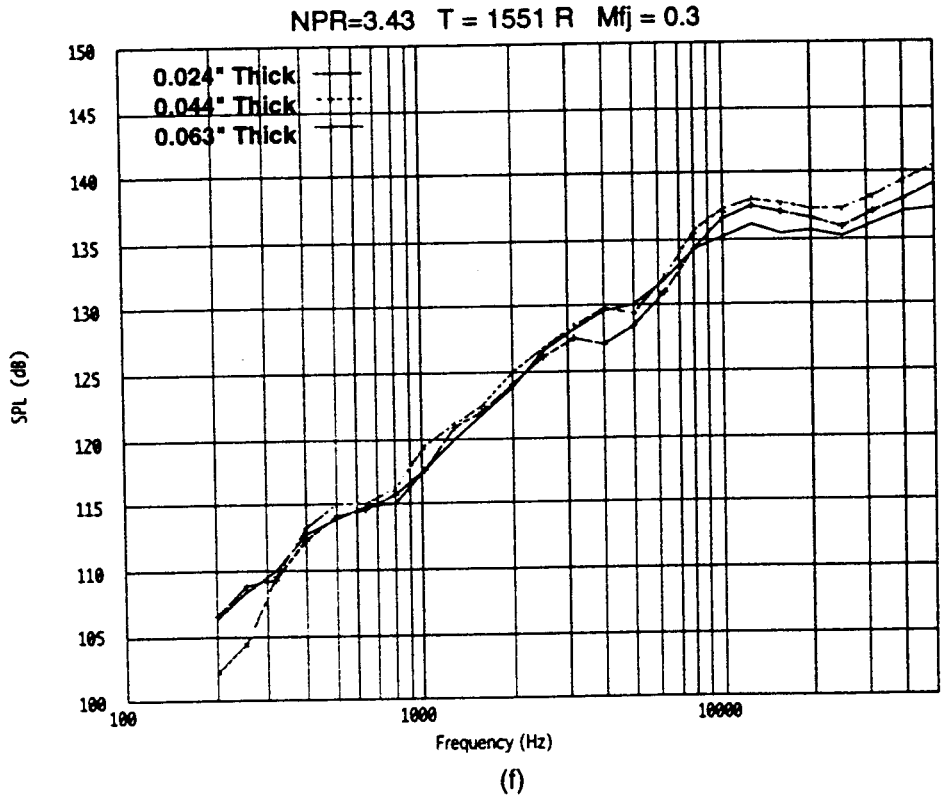

(f)

Figure 10 (continued)

Facesheet Thickness Effects
EPNL, Full Scale, Mfj=0.3

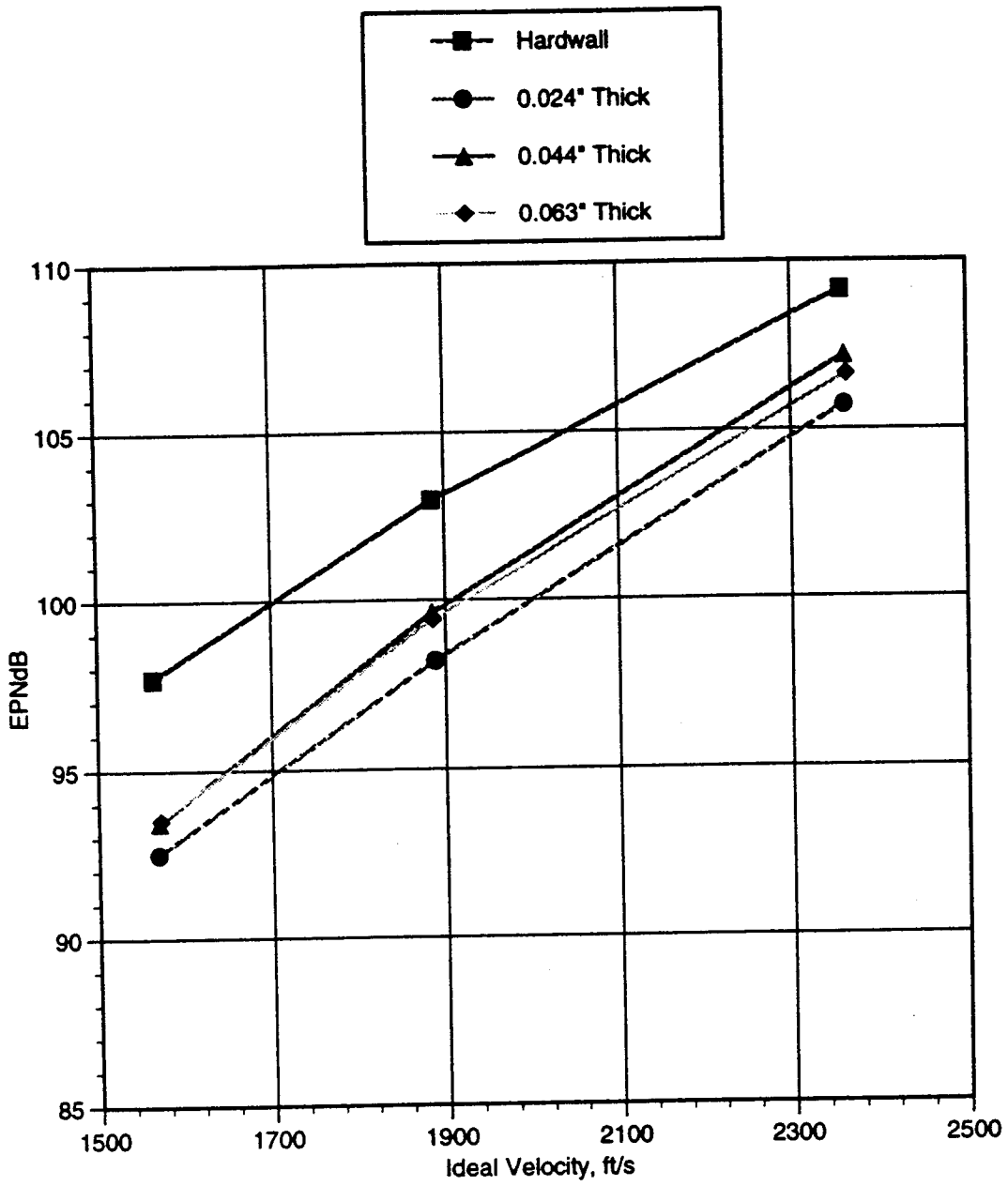

Figure 11

Honeycomb Cell Size Effects
SDOF, 10% oa, 0.04" hole dia, 0.025" thick fs, 0.375 Deep
1 Ft Radius, Lossless, Model Scale, 115°

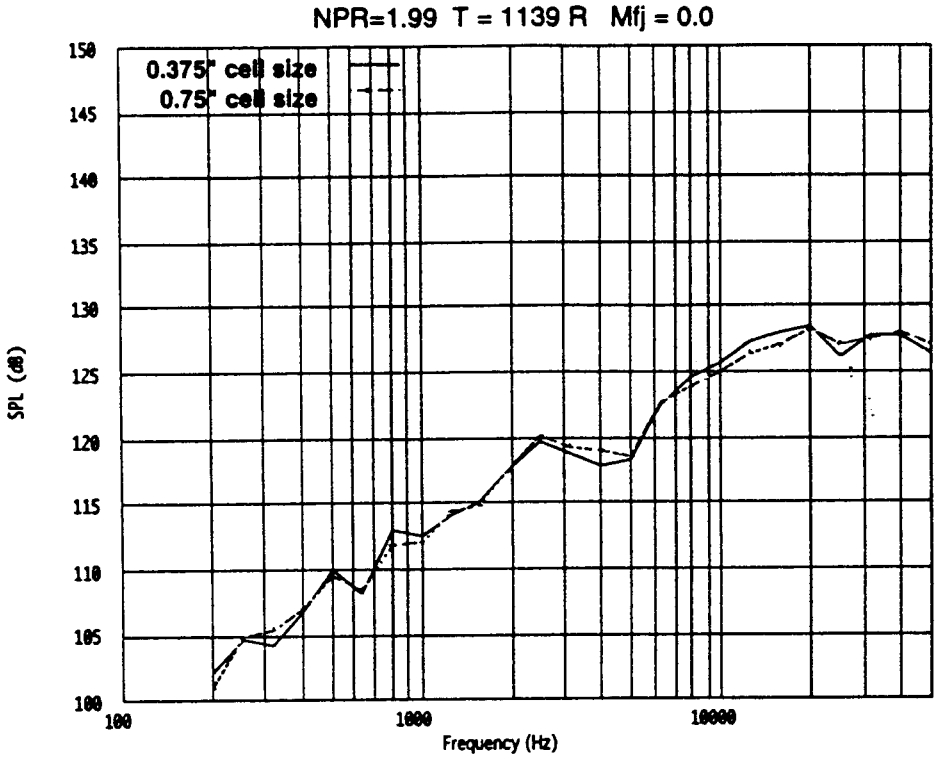

(a)

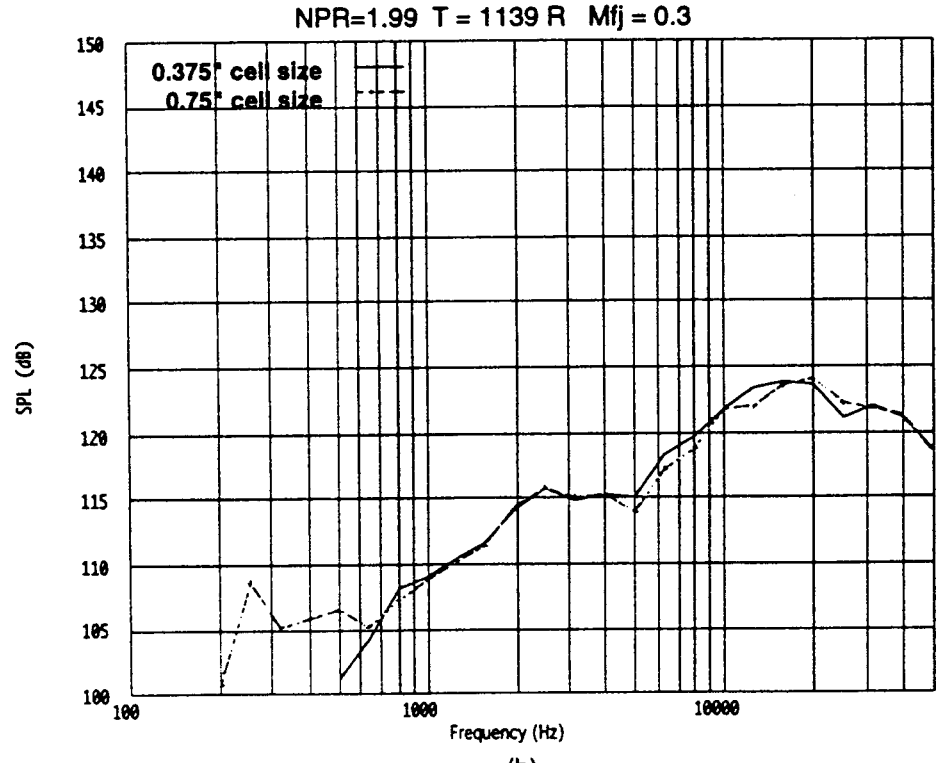

(b)

Figure 12

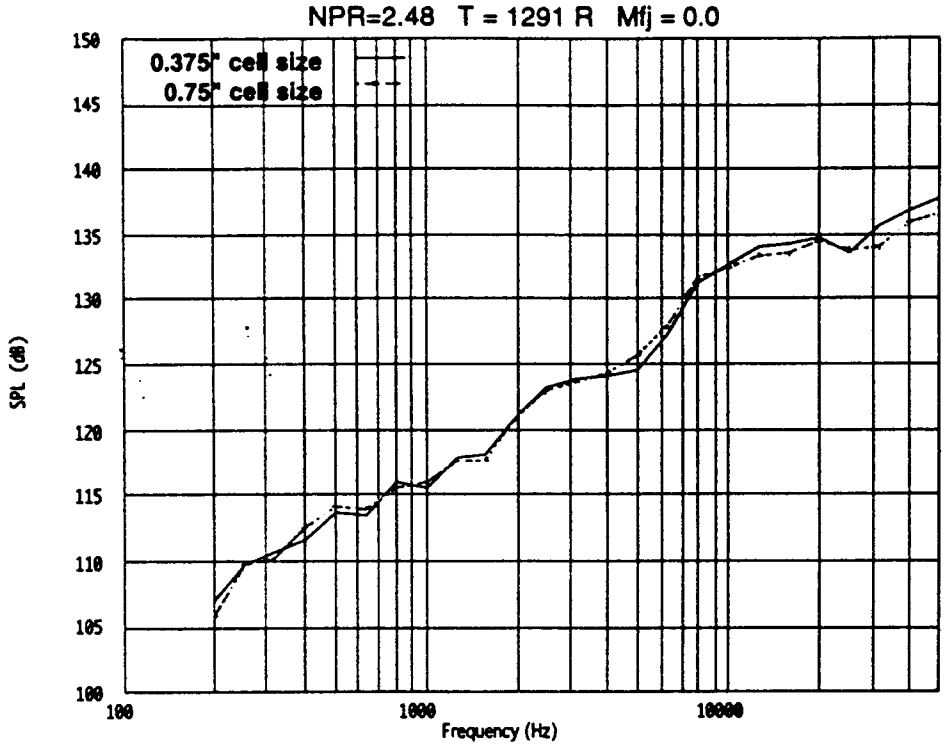

(c)

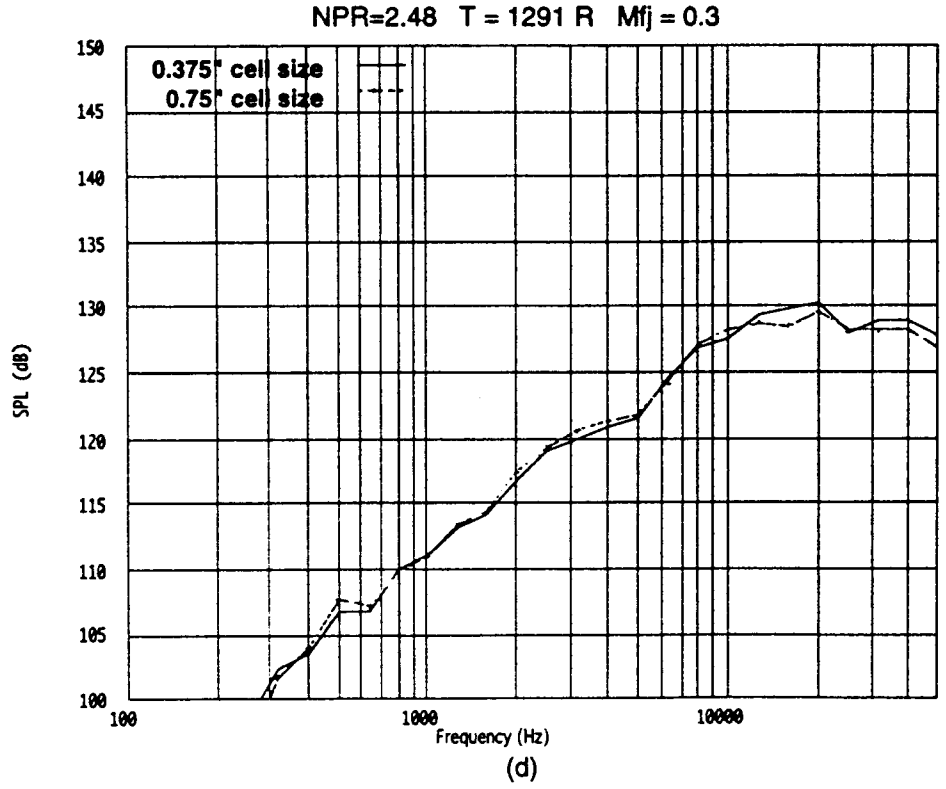

(d)

Figure 12 (continued)

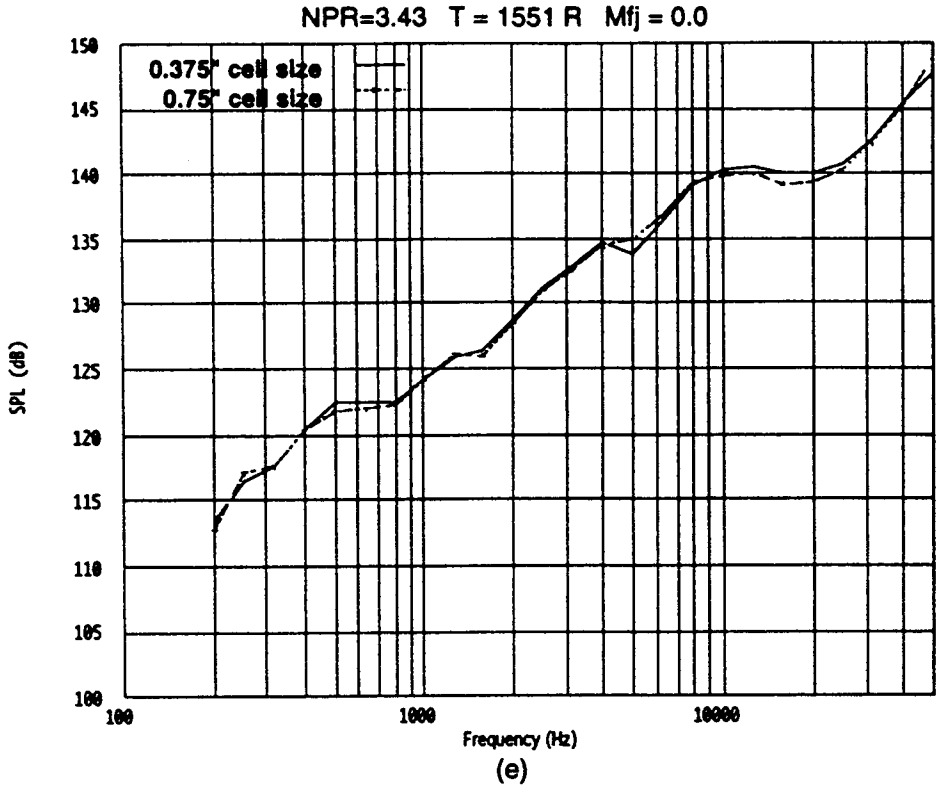

(e)

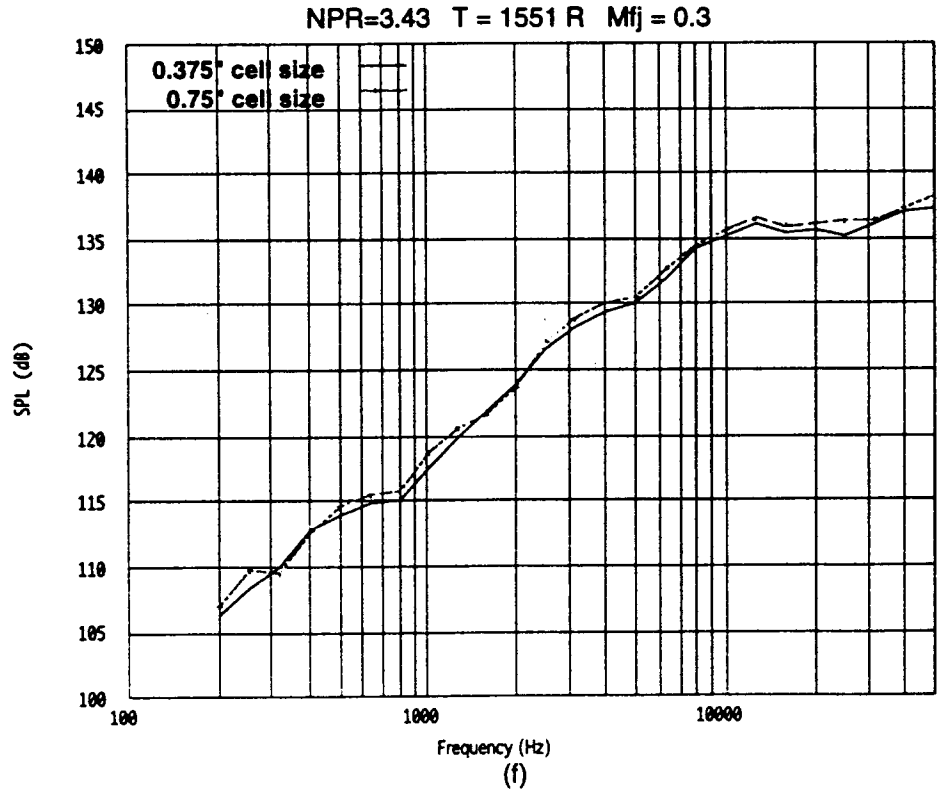

(f)

Figure 12 (continued)

Honeycomb Backing Depth Effects
SDOF, 10% oa, 0.04" hole dia, 0.025" thick fs
1 Ft Radius, Lossless, Model Scale, 115°

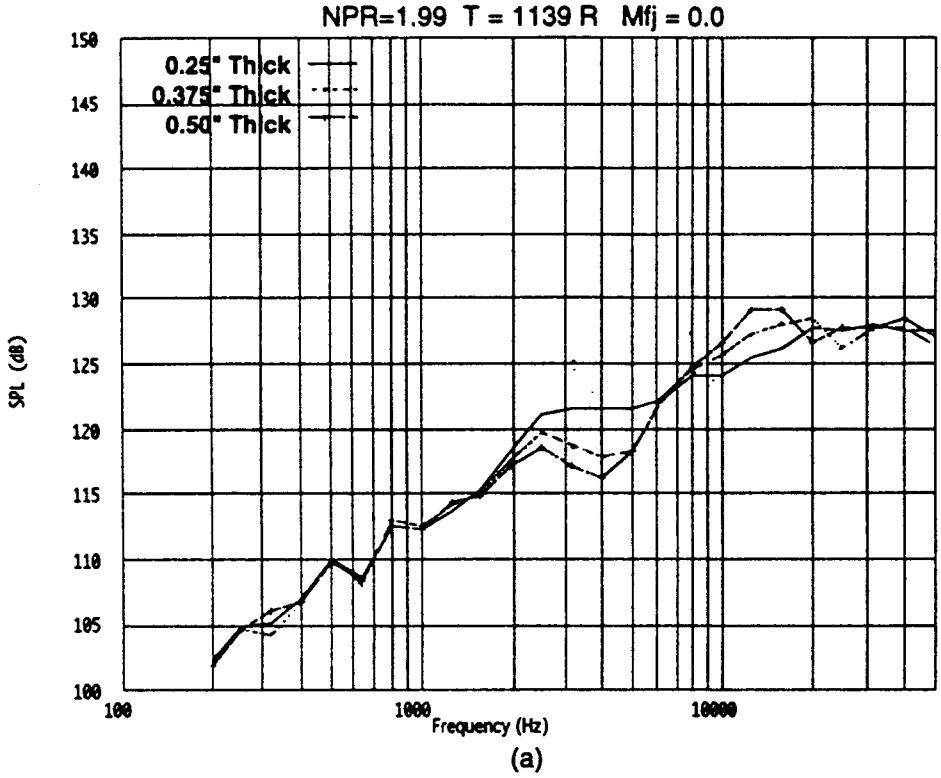

(a)

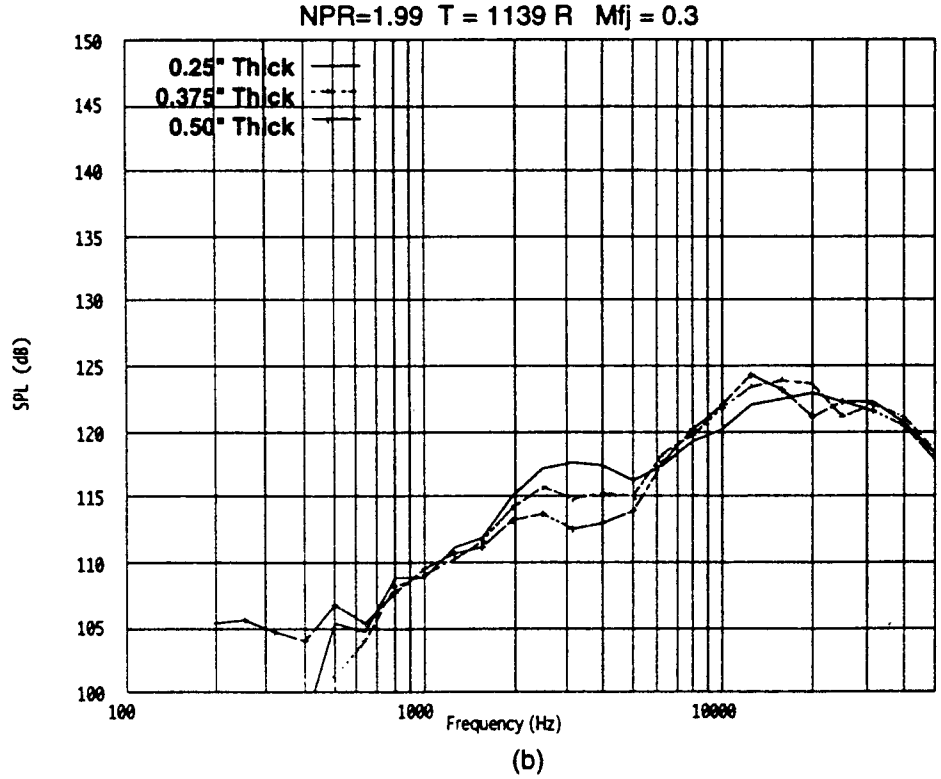

(b)

Figure 13

Honeycomb Backing Depth Effects
SDOF, 10% oa, 0.04" hole dia, 0.025" thick fs
1 Ft Radius, Lossless, Model Scale, 115°

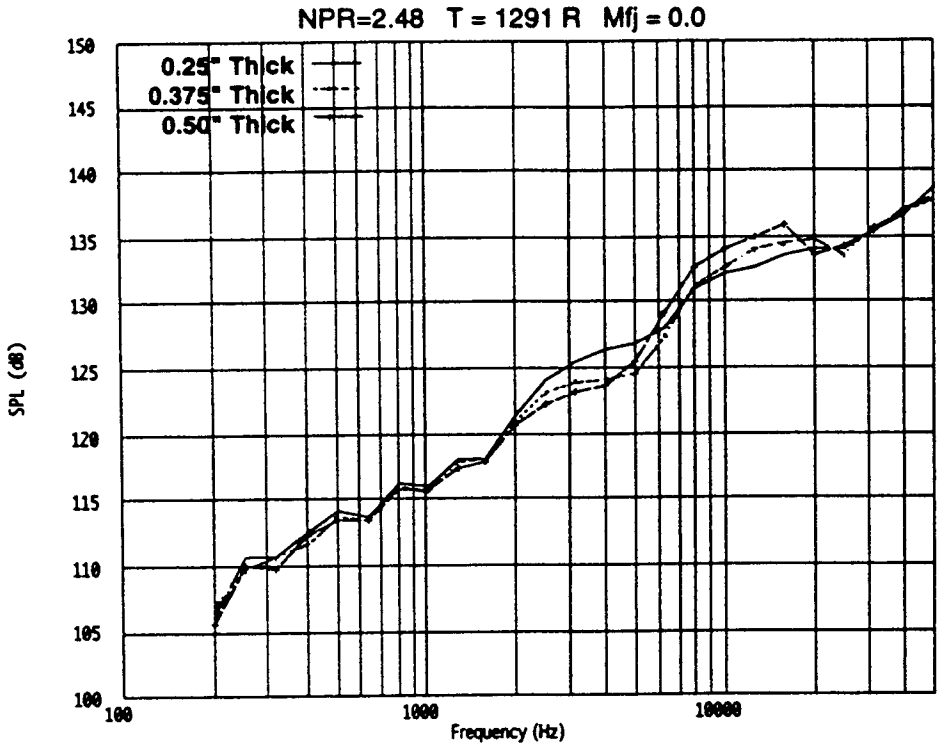

(c)

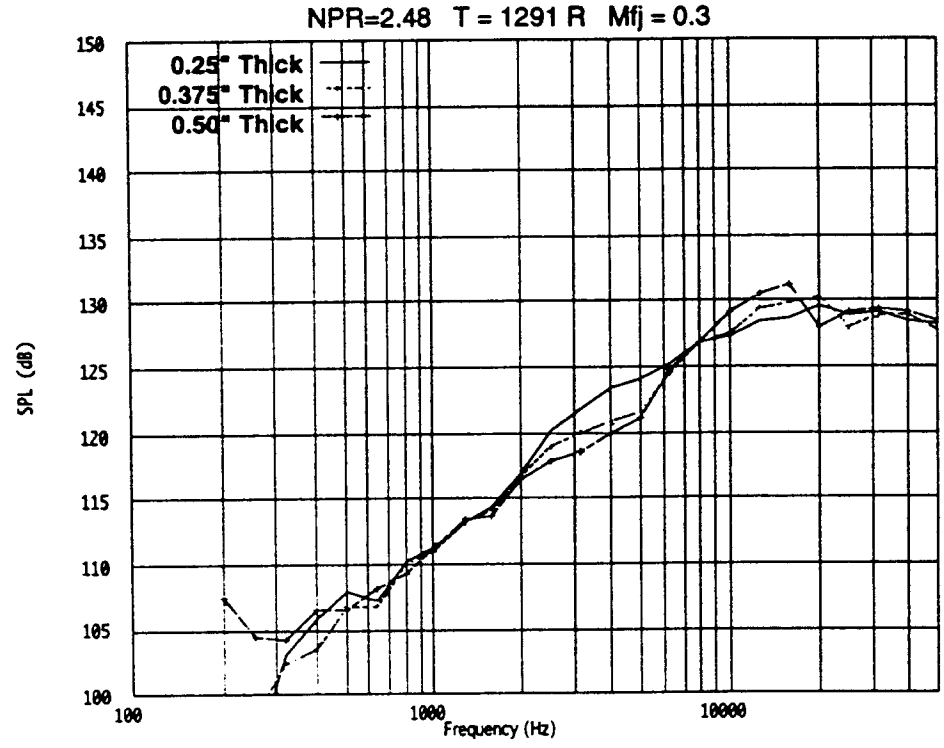

(d)

Figure 13 (continued)

Honeycomb Backing Depth Effects
SDOF, 10% oa, 0.04" hole dia, 0.025" thick fs
1 Ft Radius, Lossless, Model Scale, 115°

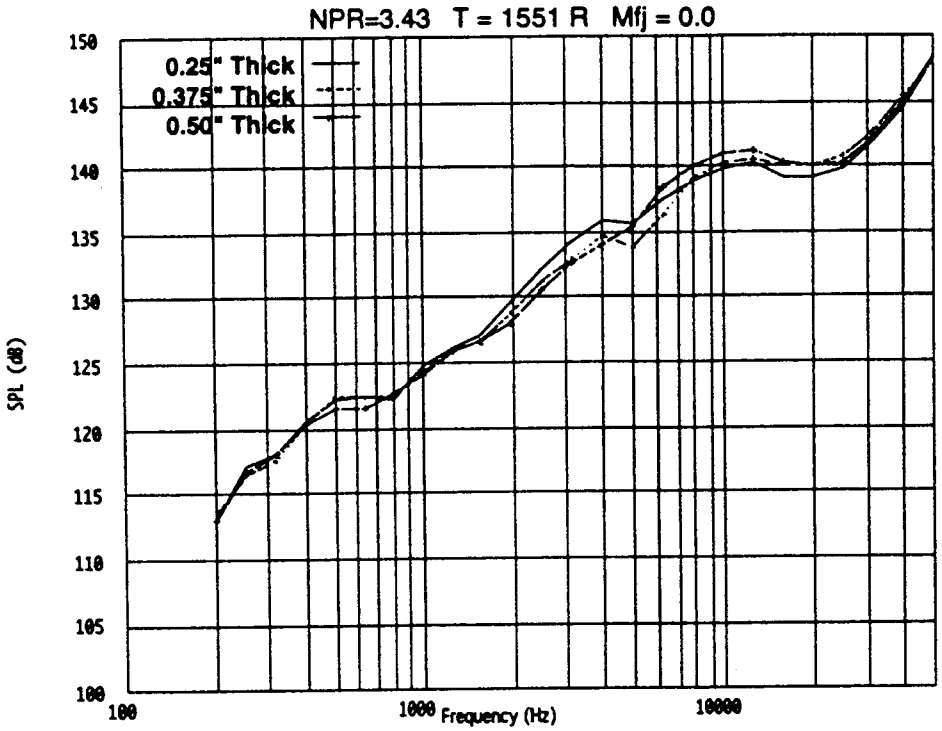

(e)

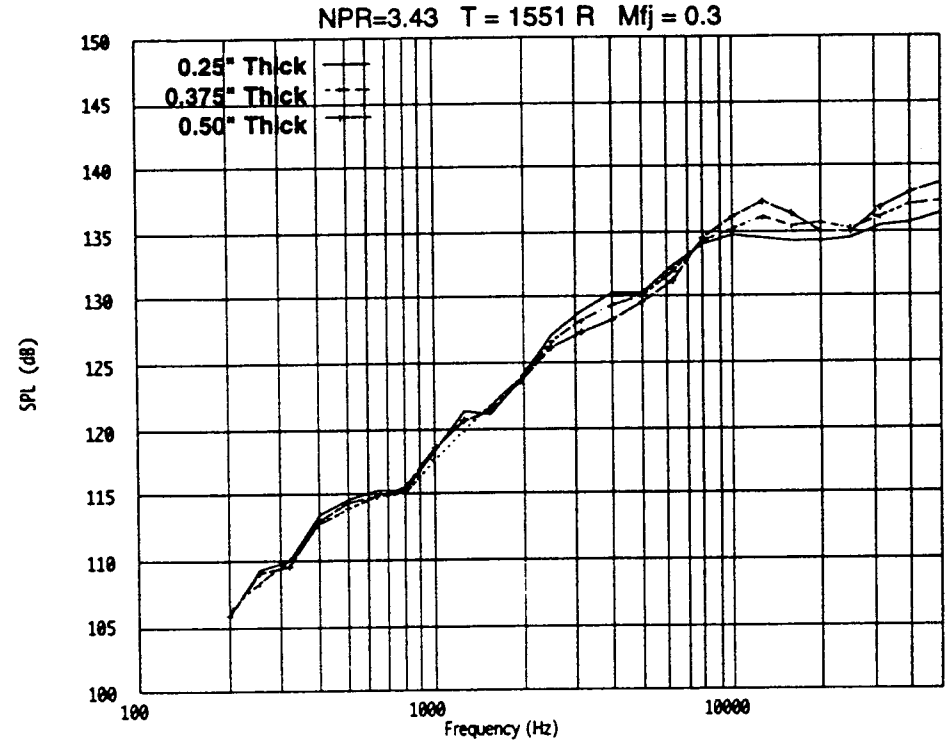

(f)

Figure 13 (continued)

Honeycomb Backing Depth Effects
EPNL, Full Scale, Mfj=0.3

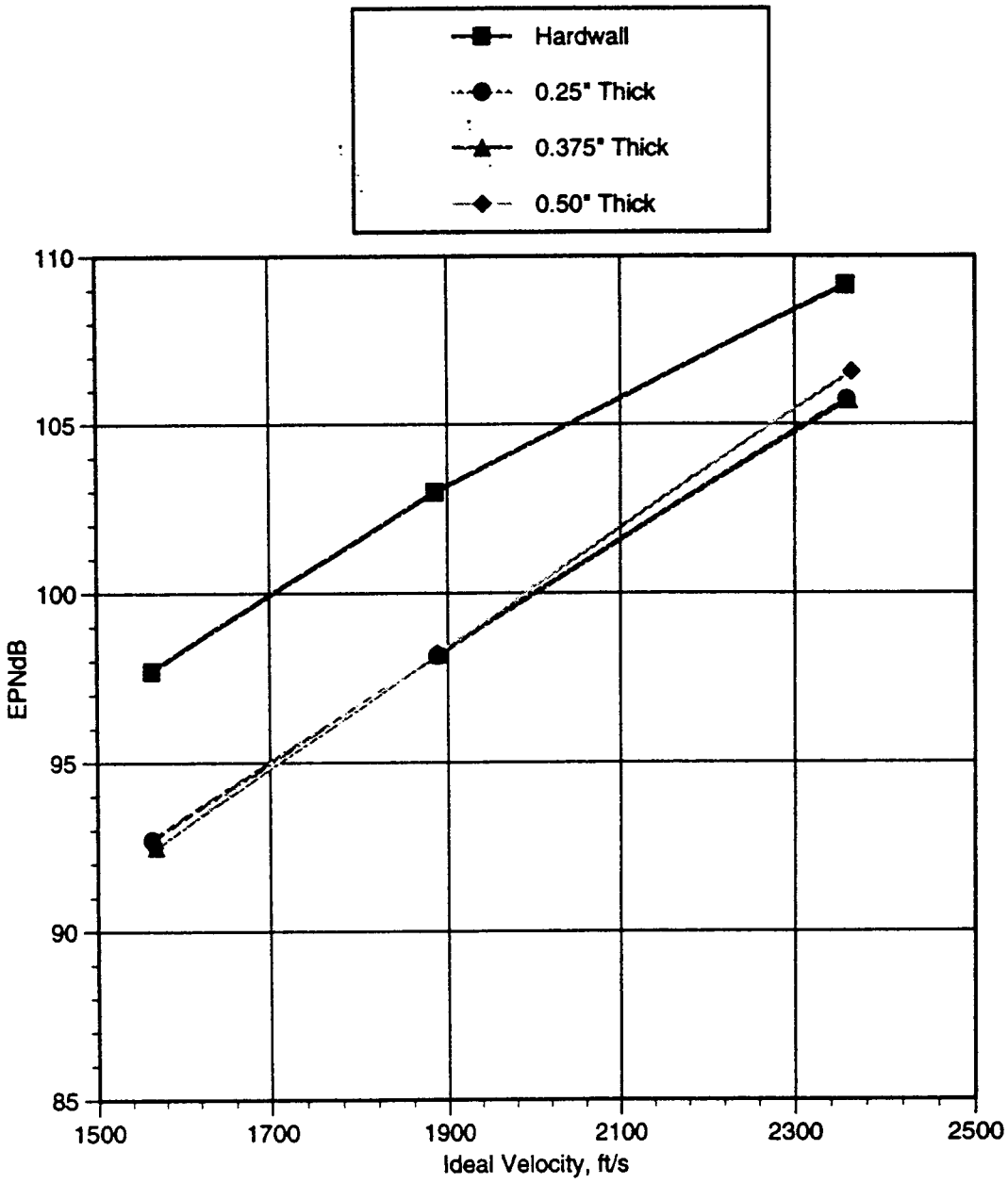

Figure 14

HTP Foam with No Facesheet
Measured Normal Impedance

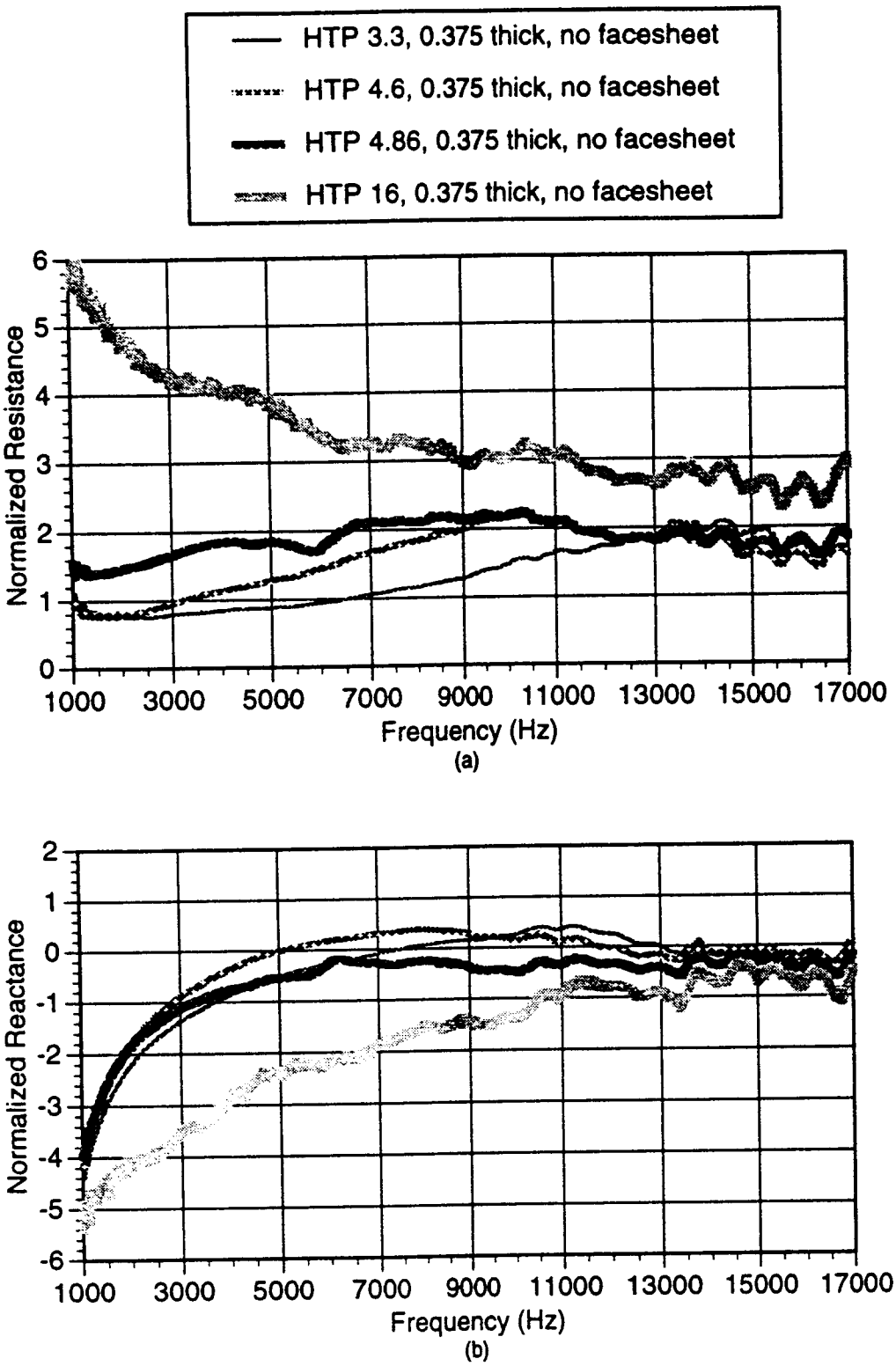

Figure 15

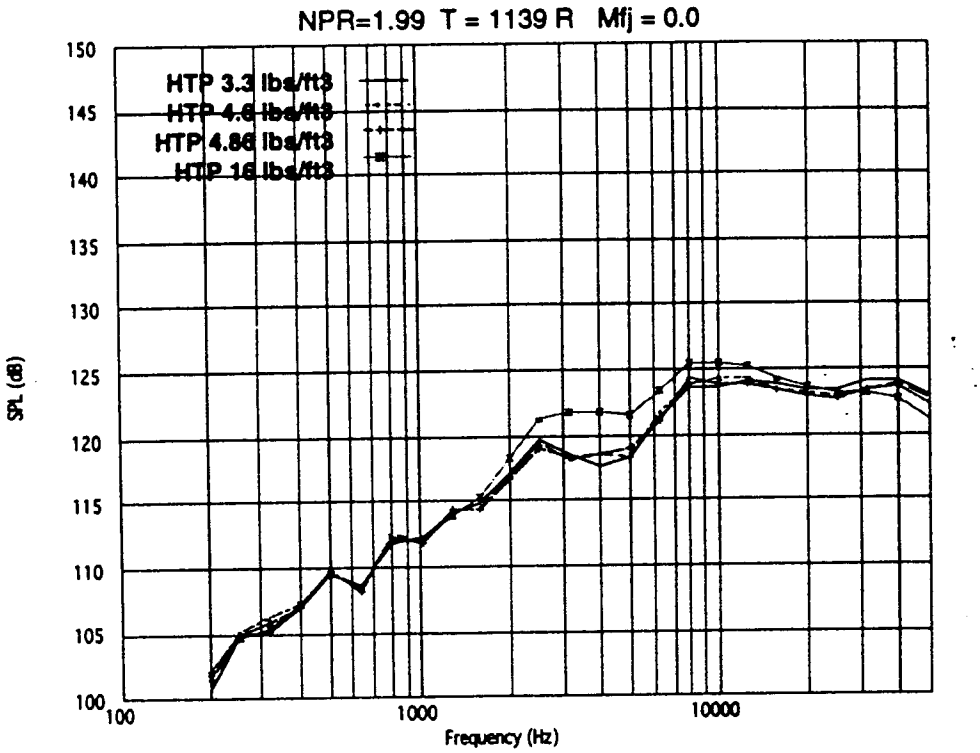
NPR=1.99 T = 1139 R Mfj = 0.0
HTP 3.3 lbs/ft3
HTP 4.6 lbs/ft3
HTP 4.86 lbs/ft3
HTP 16 lbs/ft3
SPL (dB)
150
145
140
135
130
125
120
115
110
105
100
100
1000
10000
Frequency (Hz)

(a)

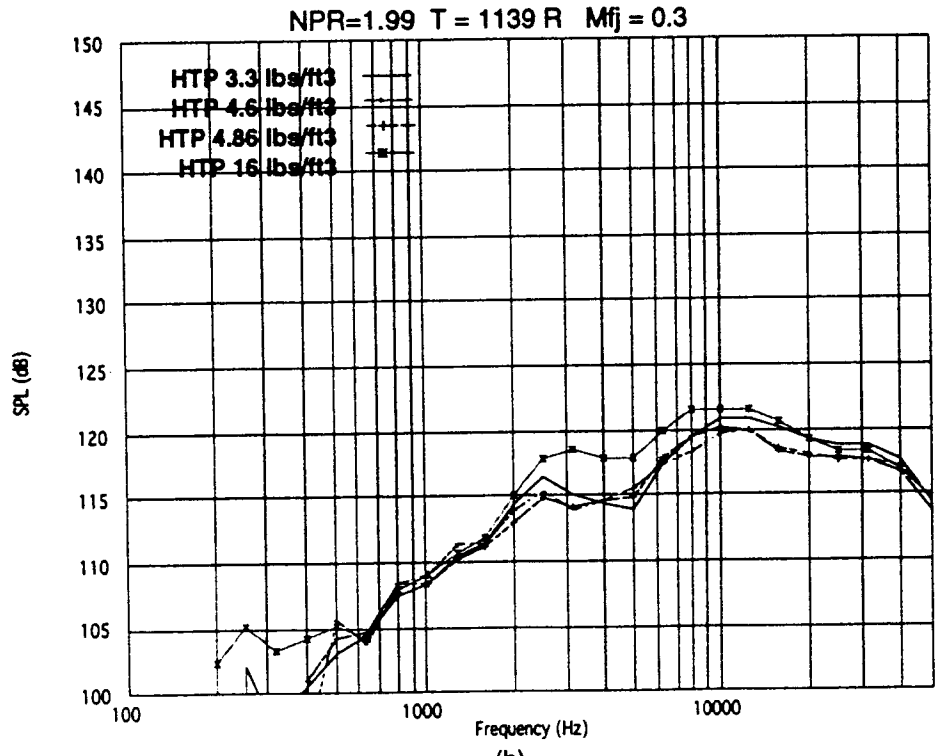
NPR=1.99 T = 1139 R Mfj = 0.3
HTP 3.3 lbs/ft3
HTP 4.6 lbs/ft3
HTP 4.86 lbs/ft3
HTP 16 lbs/ft3
SPL (dB)
150
145
140
135
130
125
120
115
110
105
100
100
1000
10000
Frequency (Hz)

(b)

Figure 16

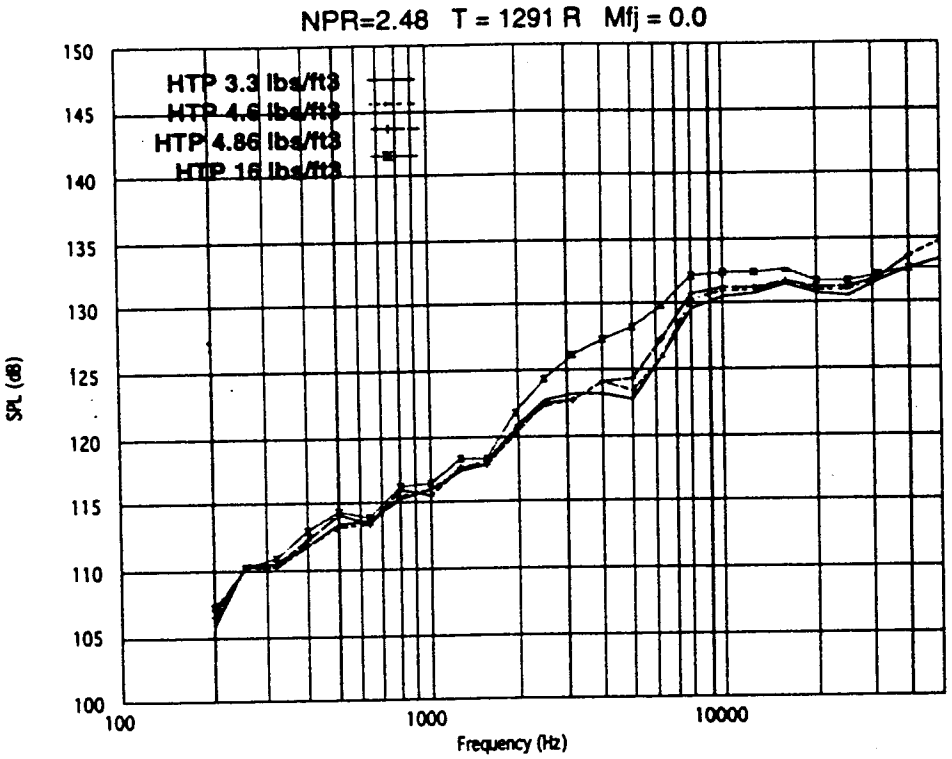

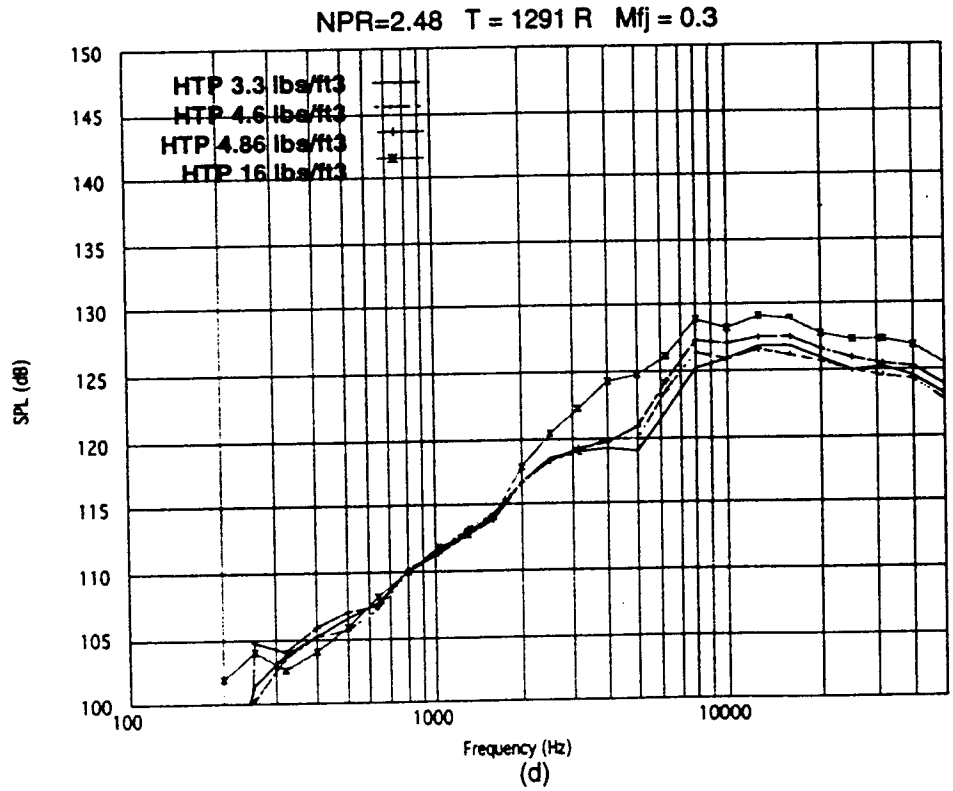

Figure 16 (continued)

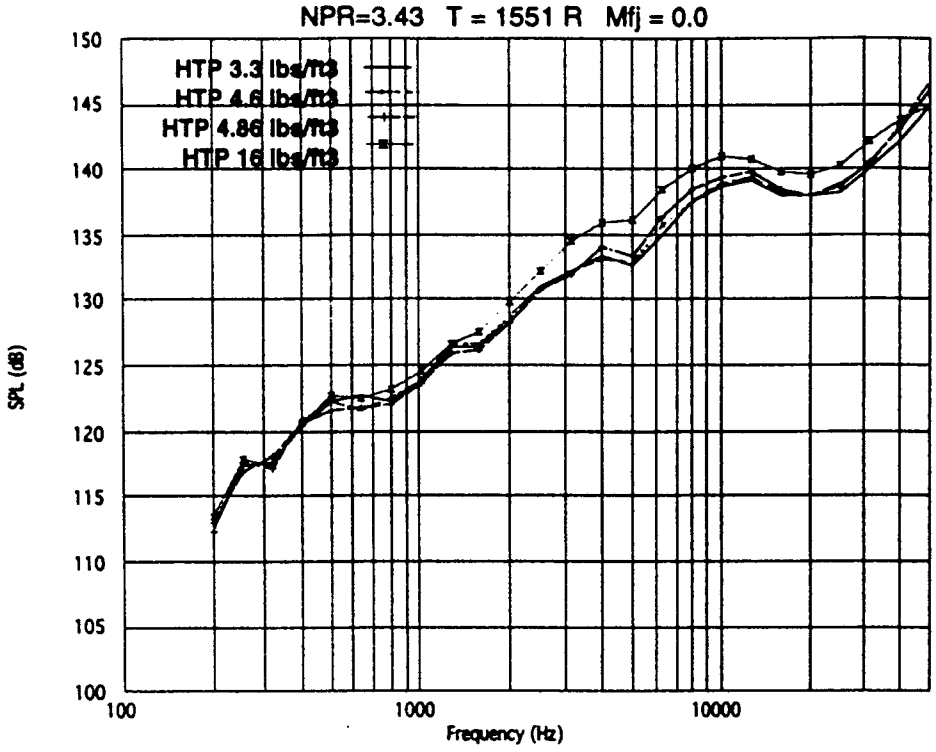

(e)

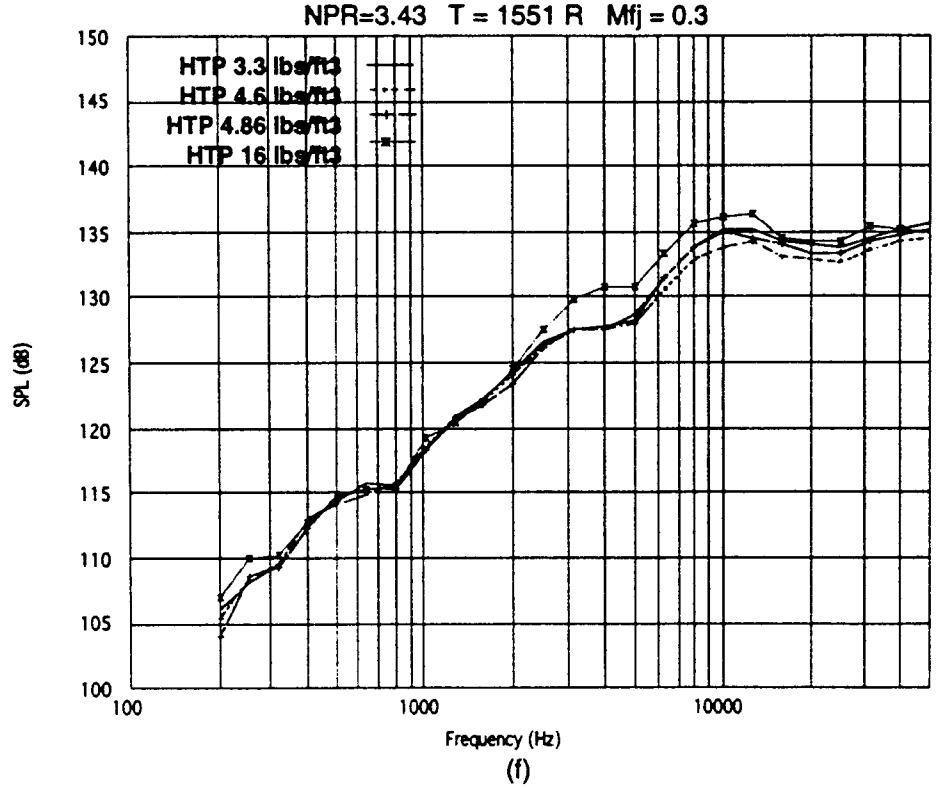

(f)

Figure 16 (continued)

HTP Materials with 37% OA Facesheet
EPNL, Full Scale, Mfj=0.3

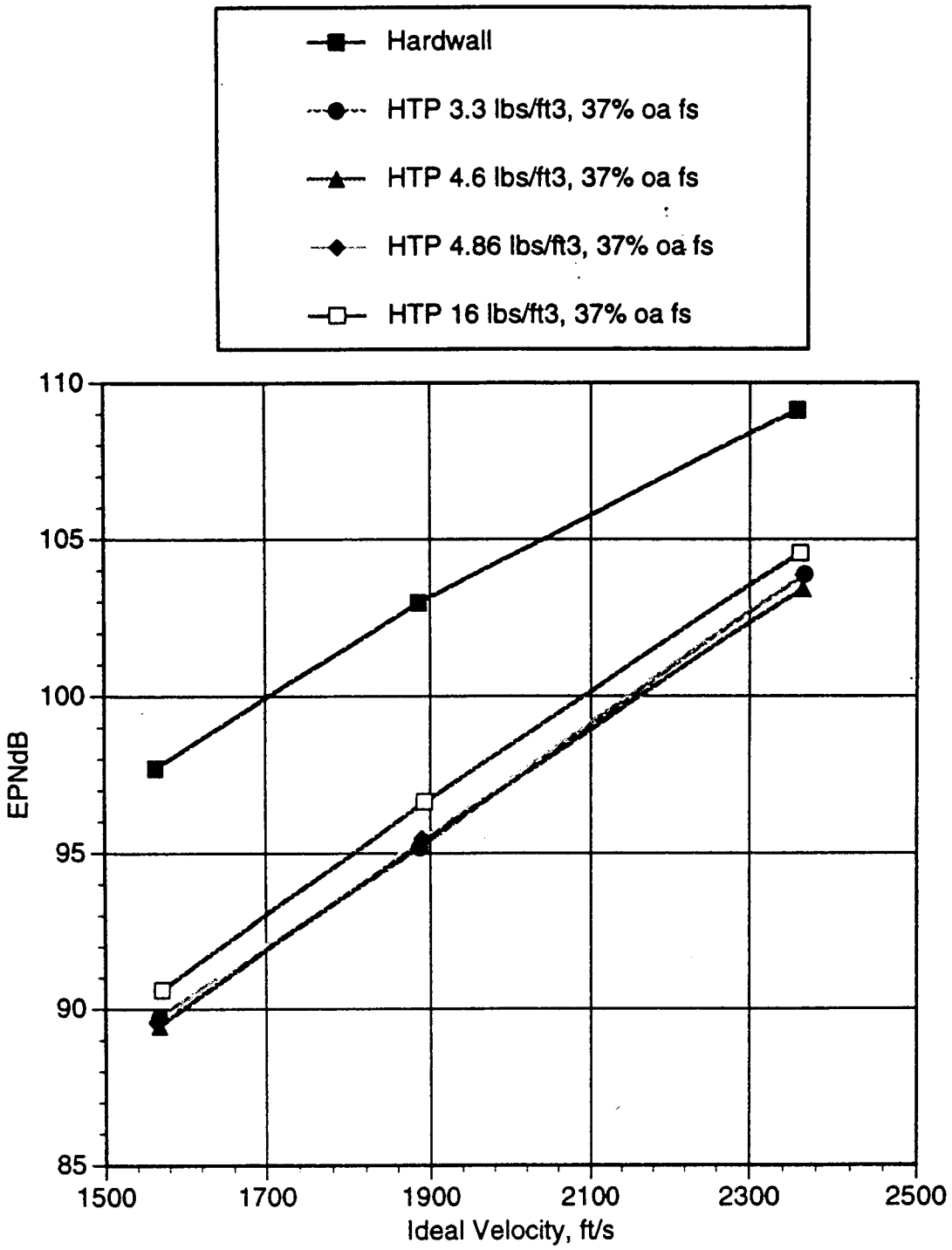

Figure 17

Silicon Carbide Foam With No Facesheet
Measured Normal Impedance

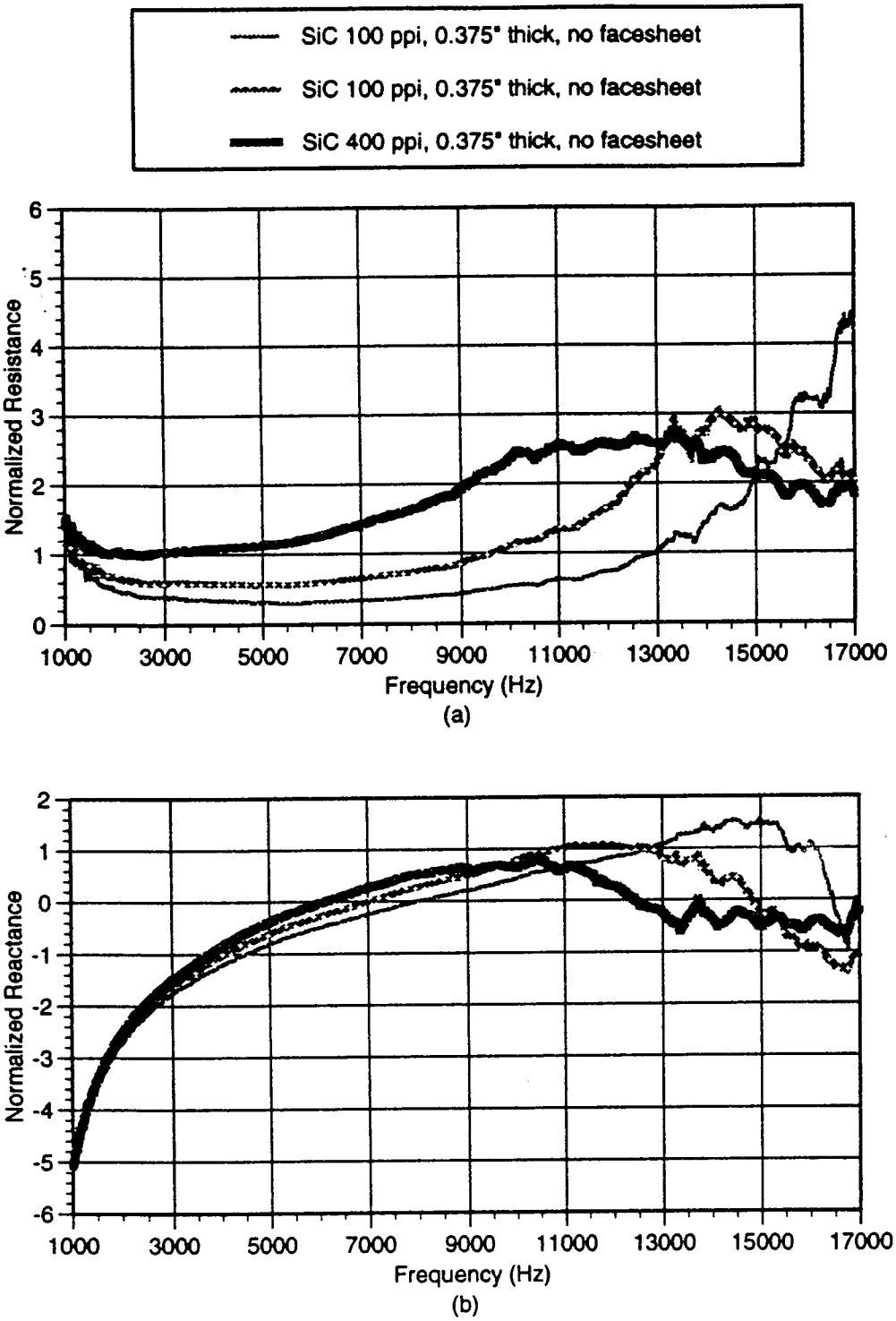

Figure 18

Silicon Carbide Foam With 37% Open Facesheet
Measured Normal Impedance

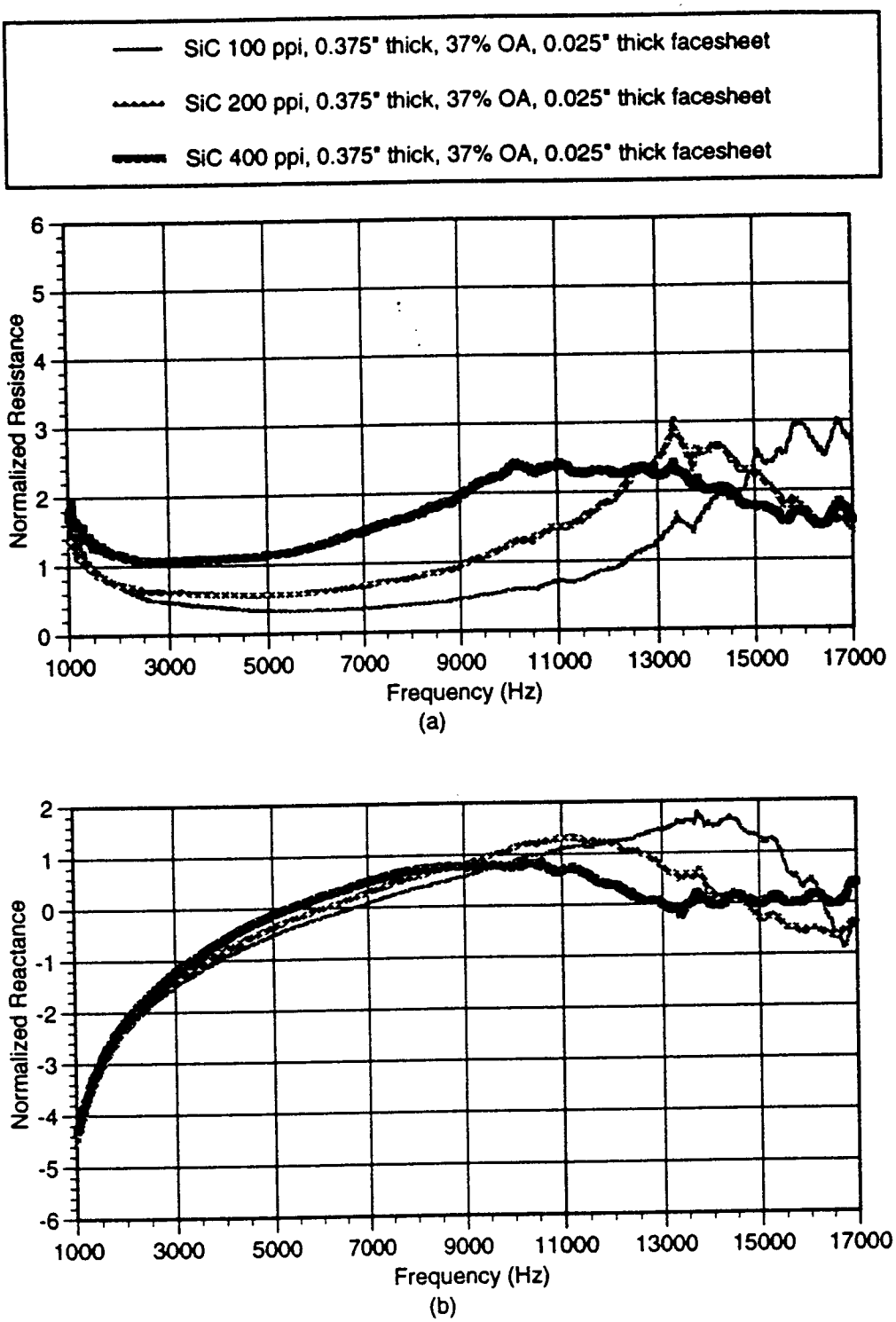

Figure 19

Silicon Carbide Foam with 37% OA Facesheet
1 Ft Radius, Lossless, Model Scale

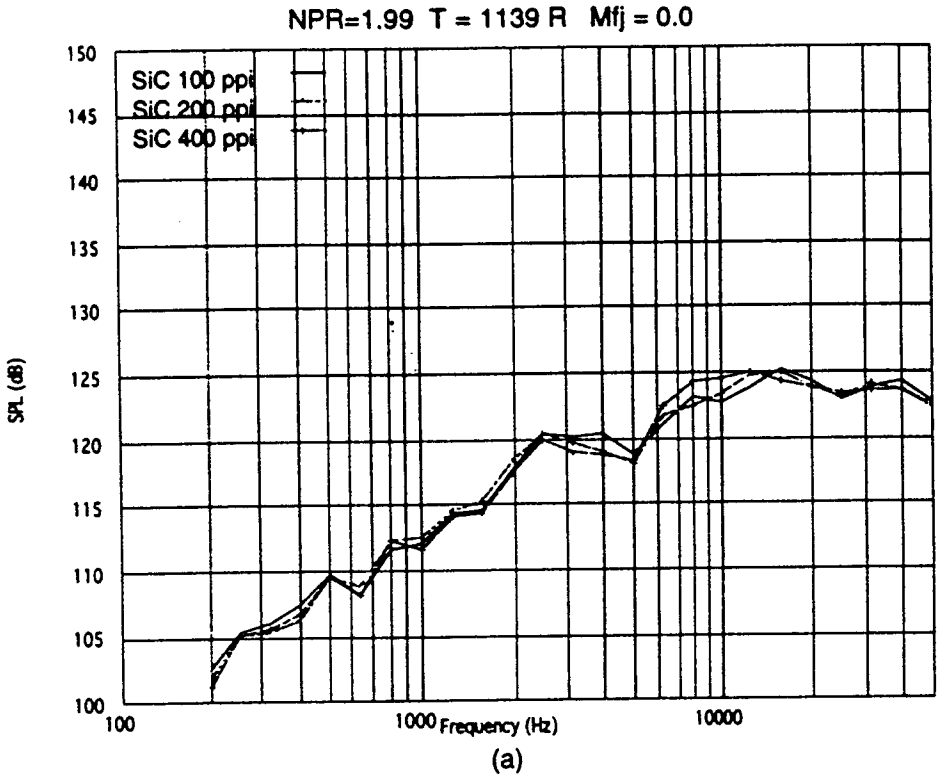

(a)

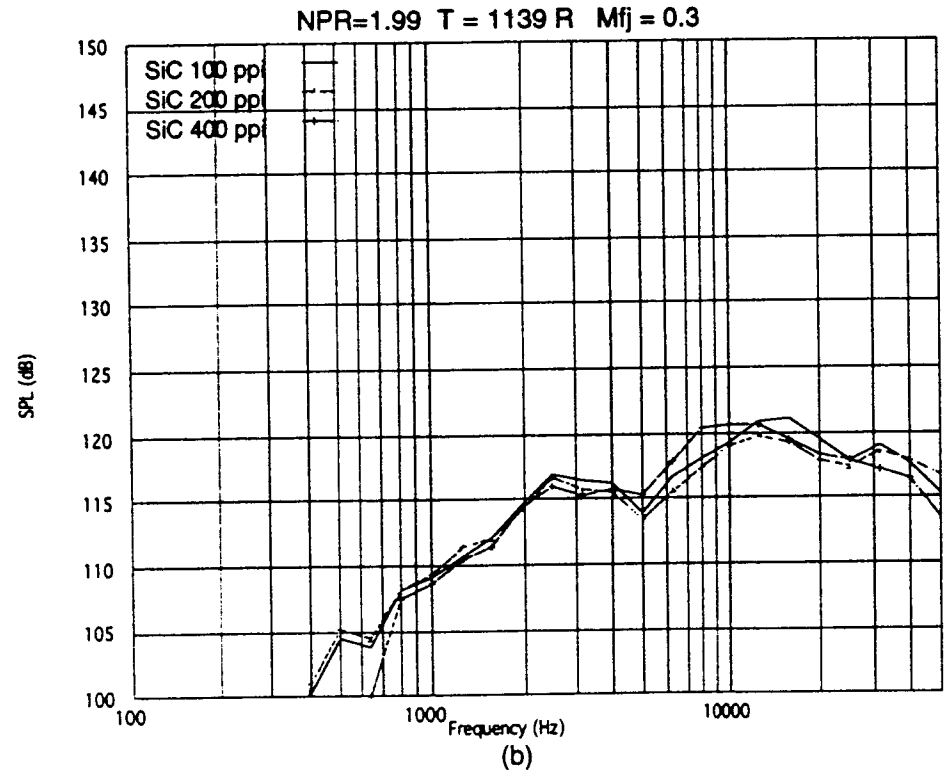

(b)

Figure 20

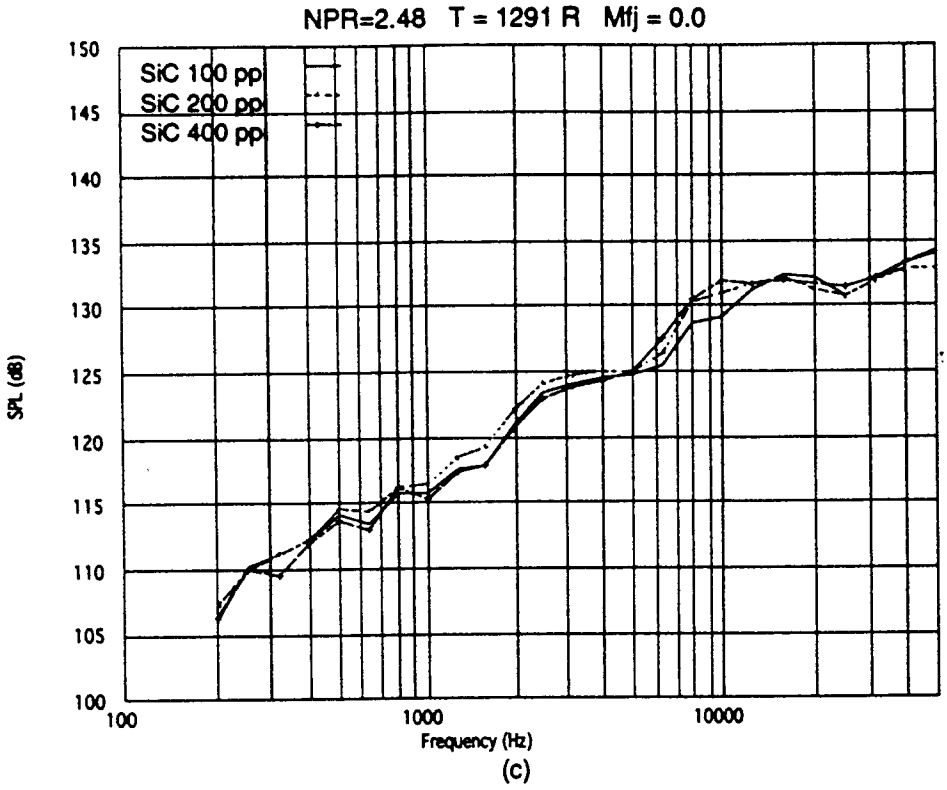

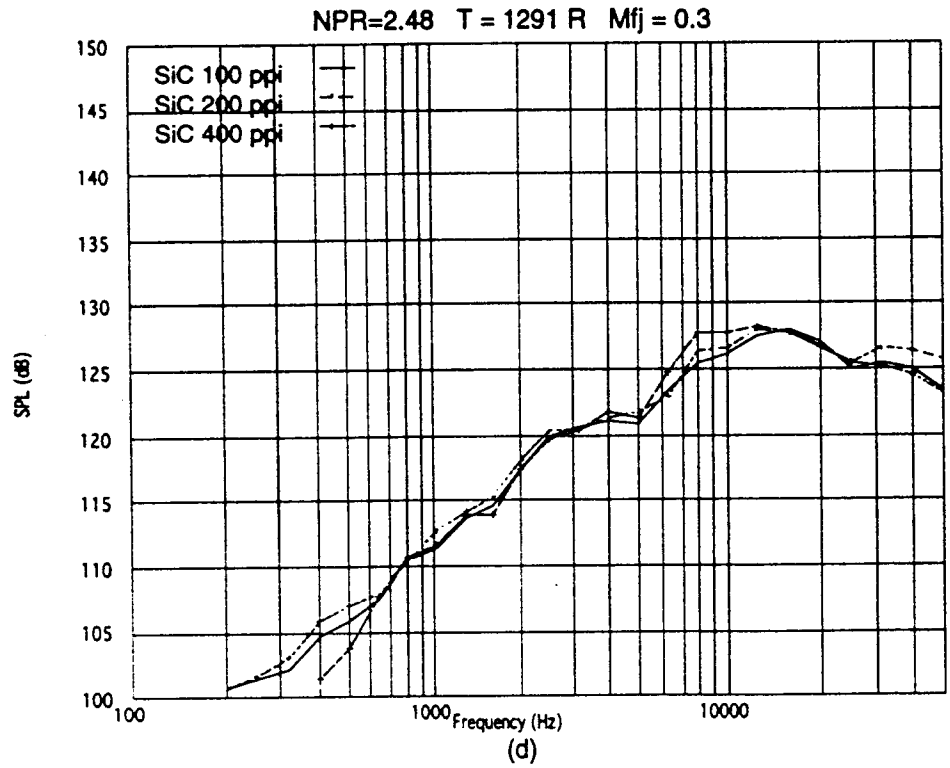

Figure 20 (continued)

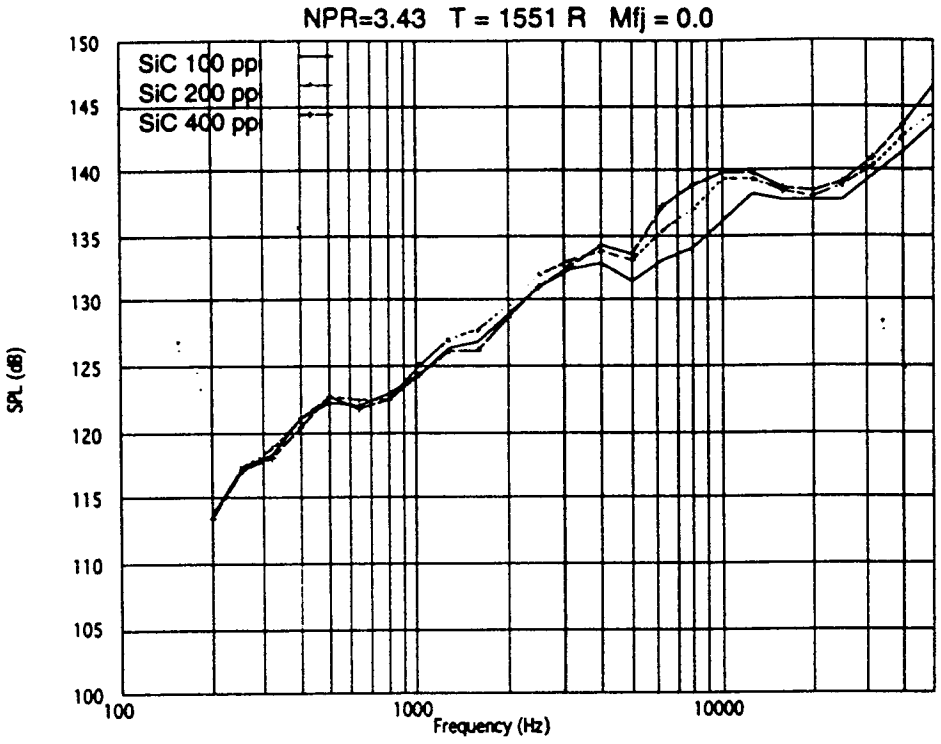

(e)

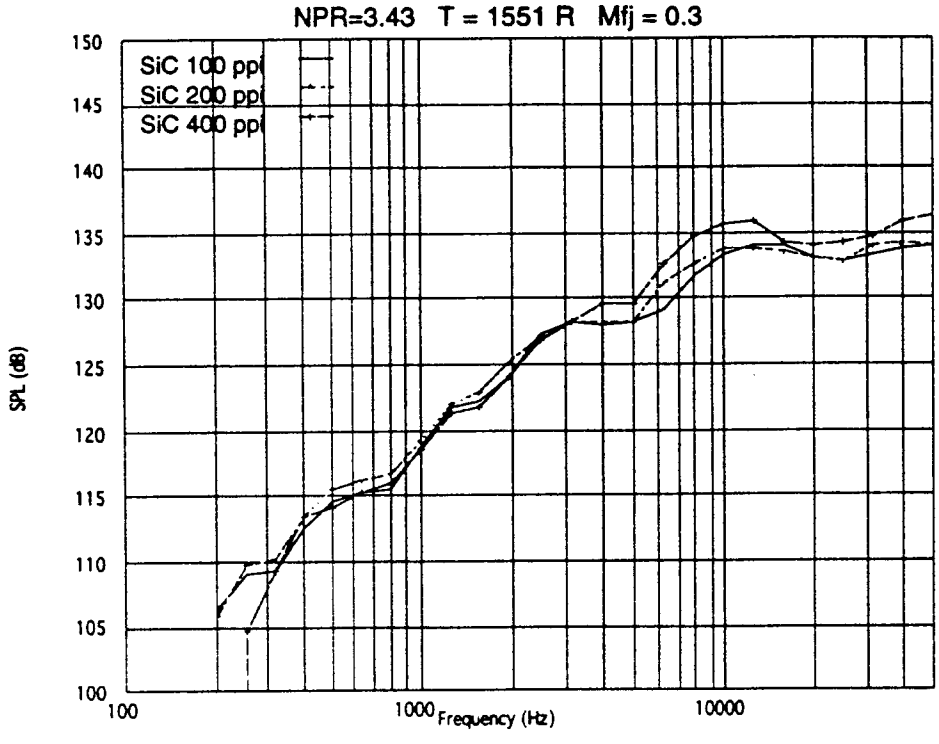

(f)

Figure 20 (continued)

Silicon Carbide Foam with 37% OA Facesheet
EPNL, Full Scale, Mfj=0.3

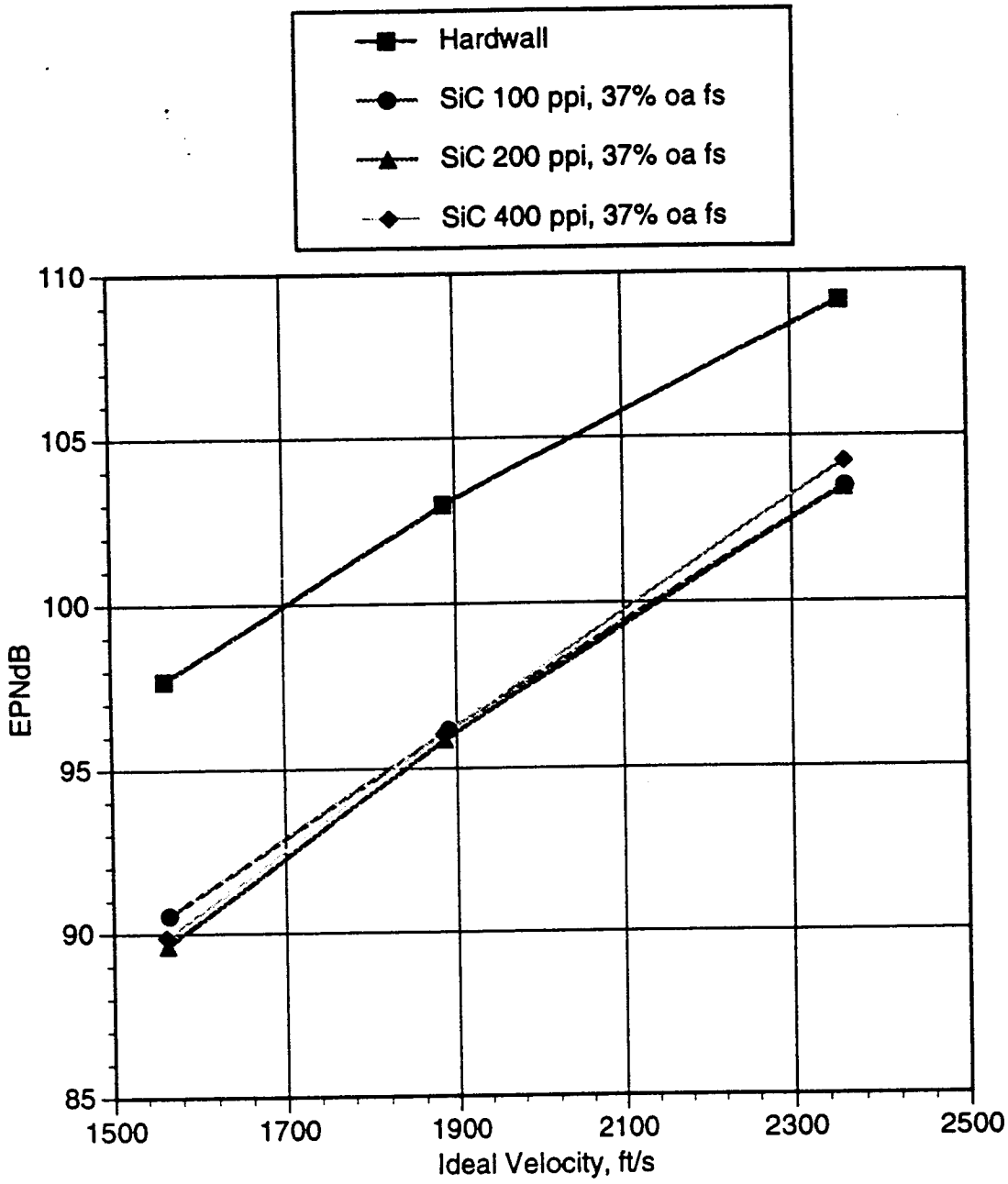

Figure 21

Bulk Facesheet Porosity Effects
Measured Normal Impedance

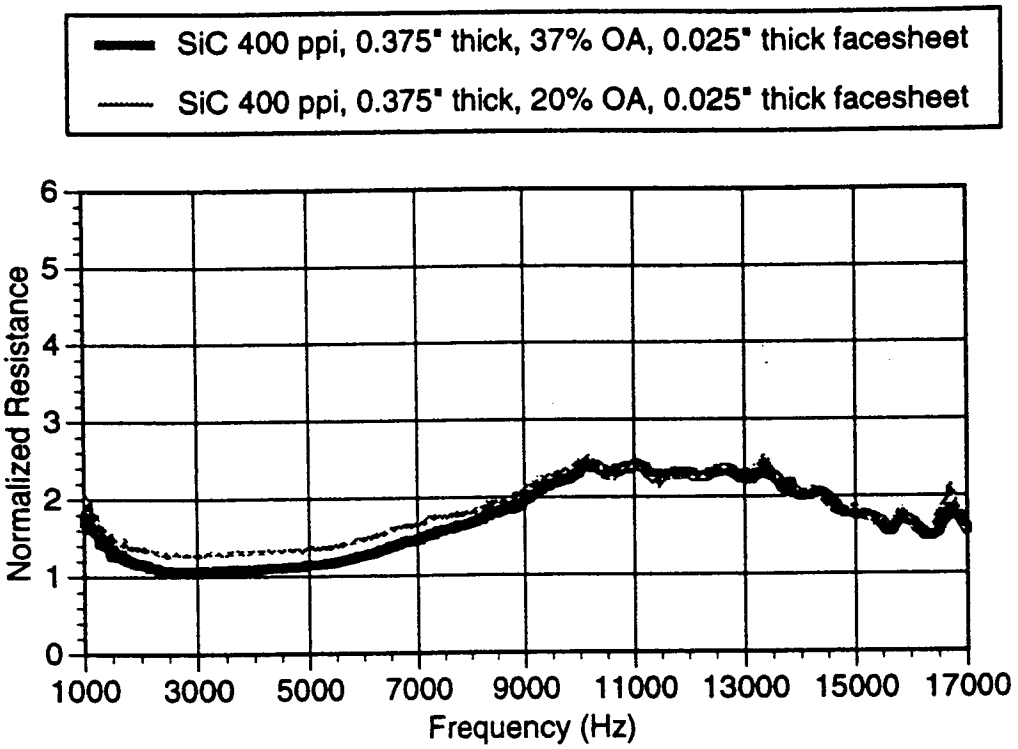

(a)

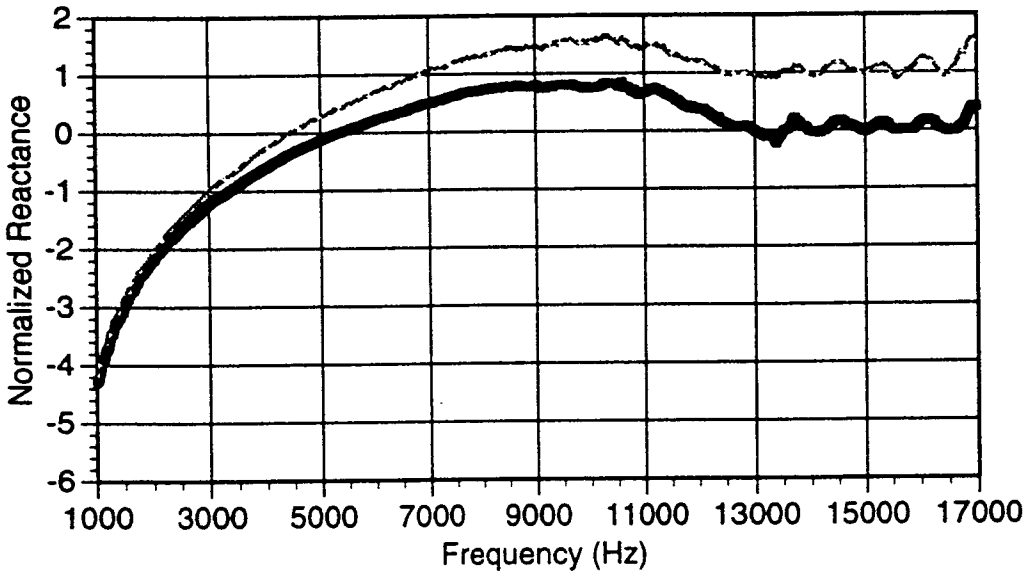

(b)

Figure 22

Facesheet Porosity Effects
Bulk, 0.375" Deep
1 Ft Radius, Lossless, Model Scale, 115°

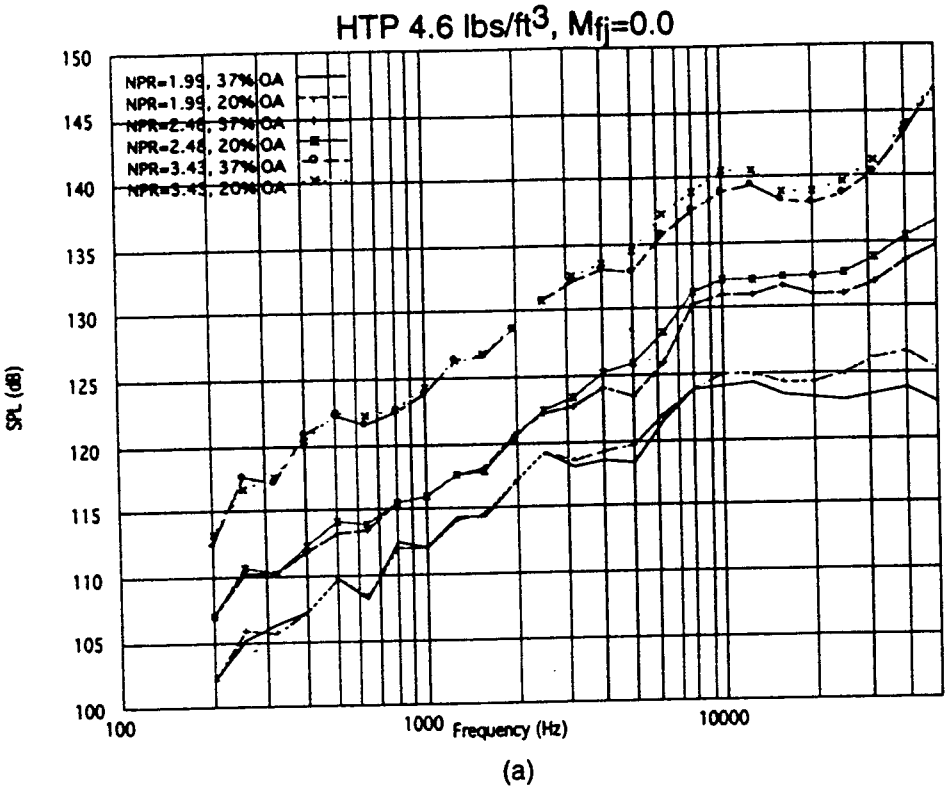

(a)

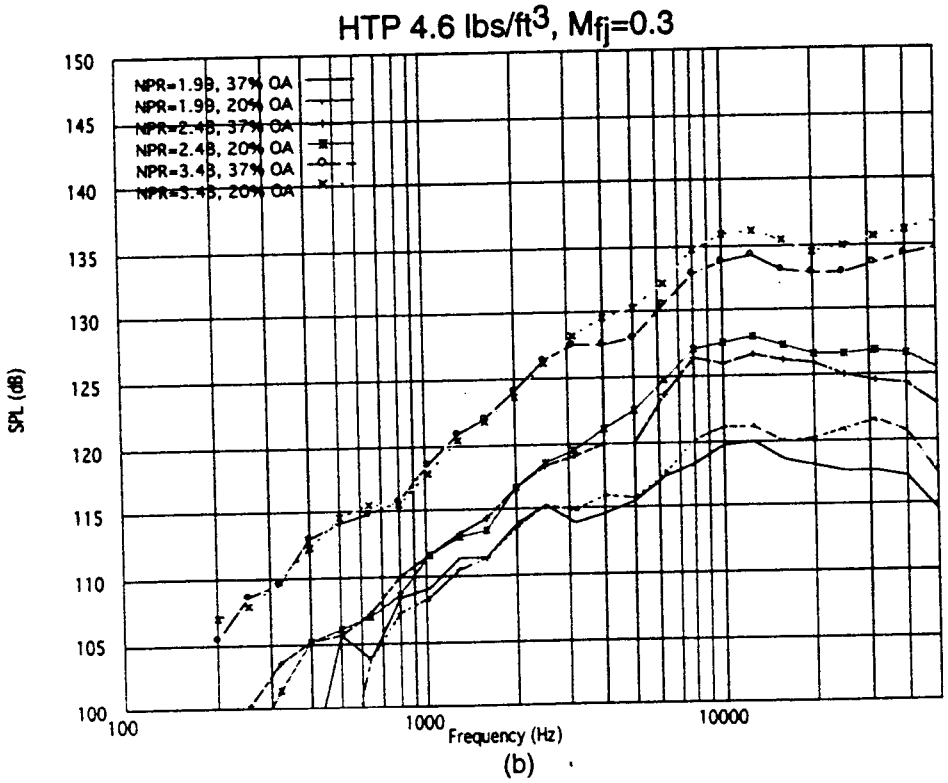

(b)

Figure 23

Facesheet Porosity Effects
Bulk, 0.375" Deep
1 Ft Radius, Lossless, Model Scale, 115°

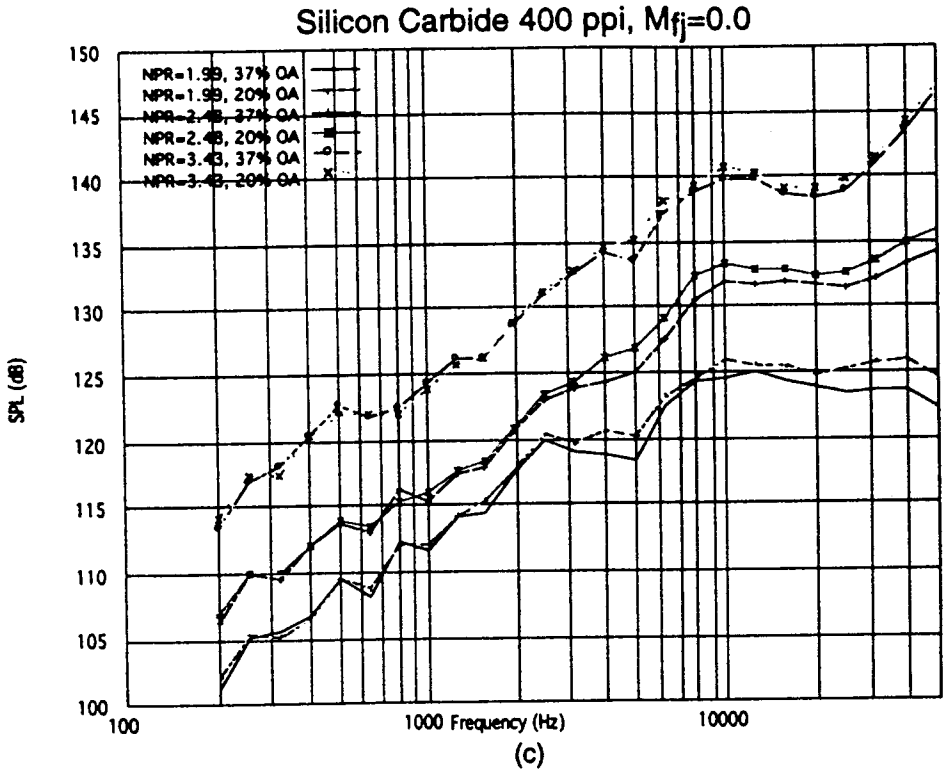

(c)

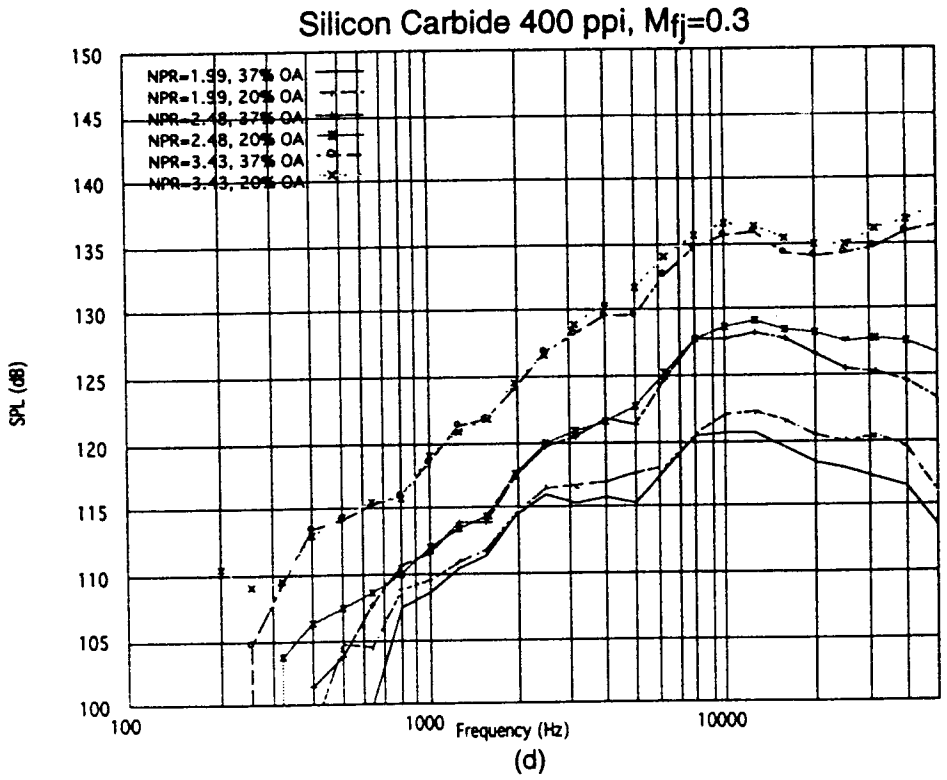

(d)

Figure 23 (continued)

Facesheet Porosity Effects
Bulk, 0.375" Deep
1 Ft Radius, Lossless, Model Scale, 115°

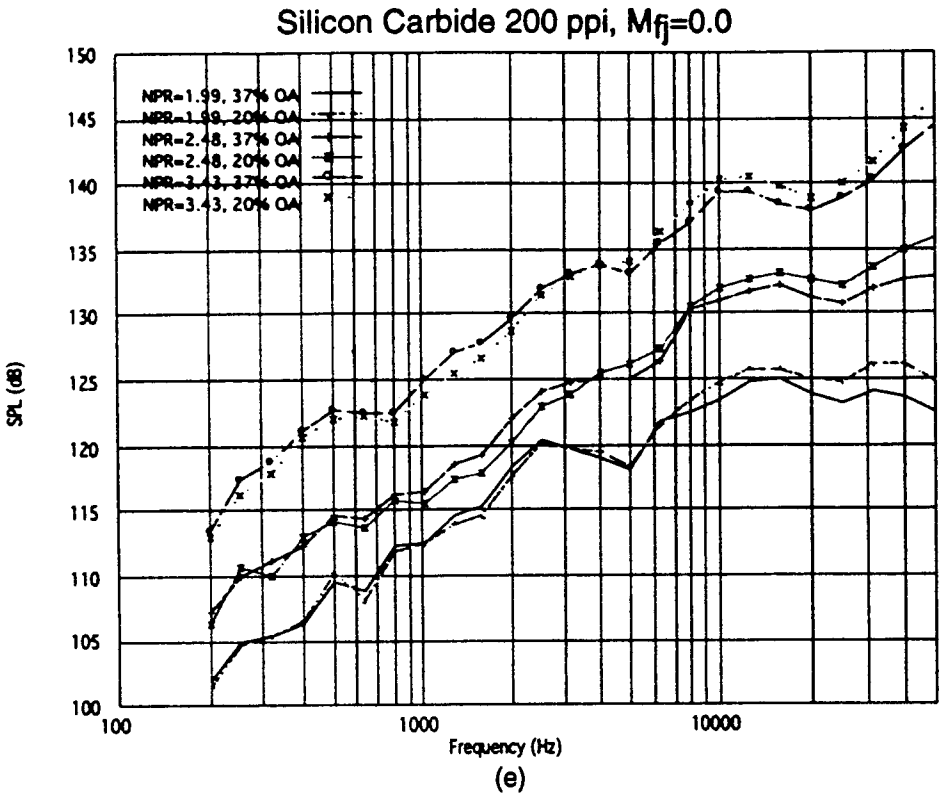

(e)

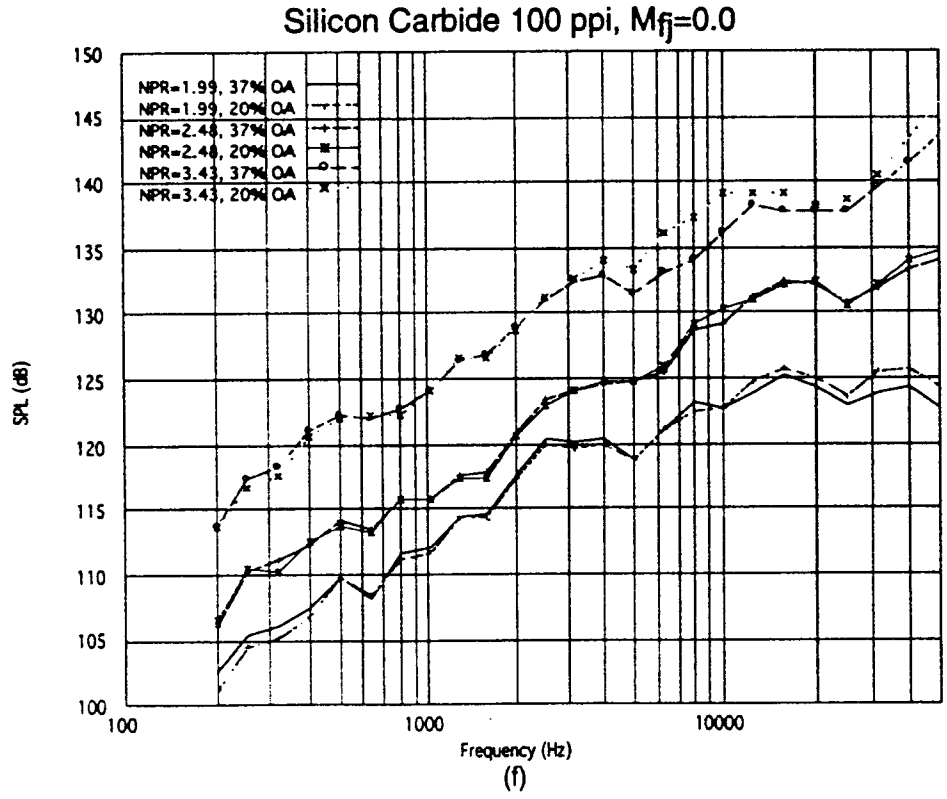

(f)

Figure 23 (continued)

Facesheet Porosity Effects
Bulk, EPNL, Full Scale, Mfj=0.3

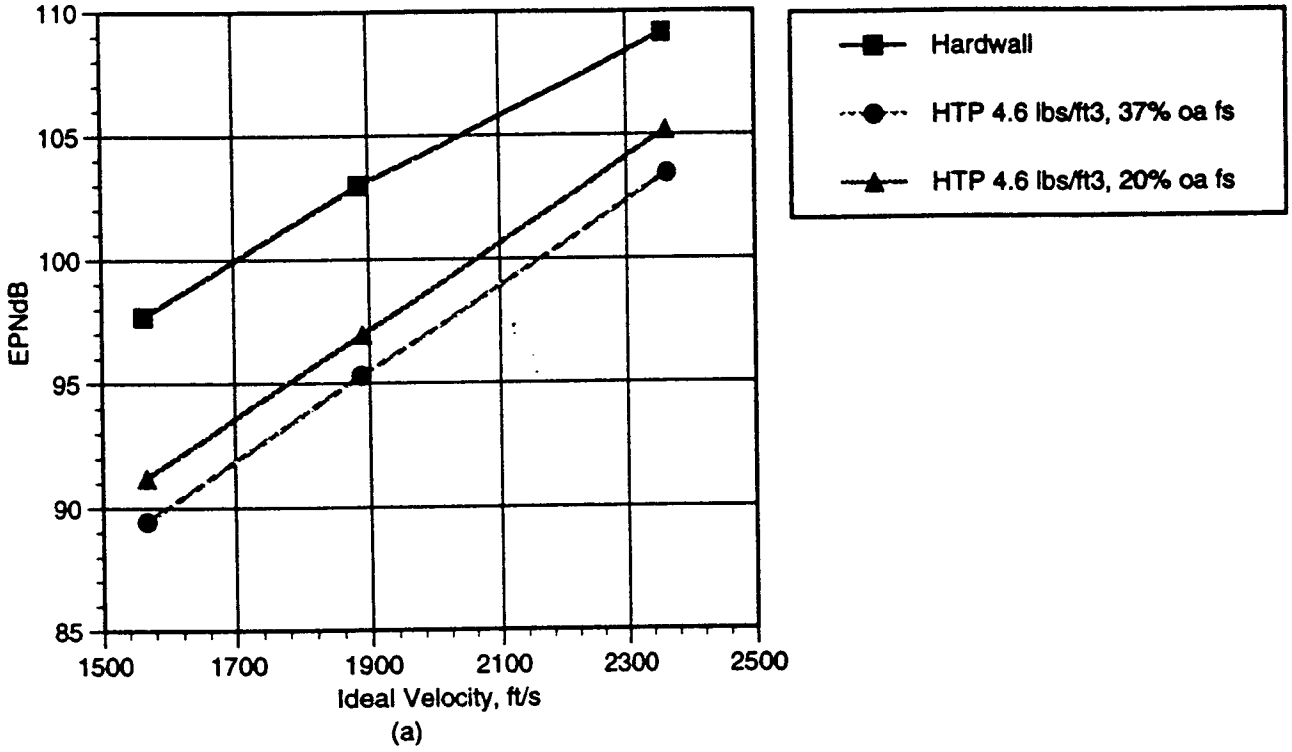

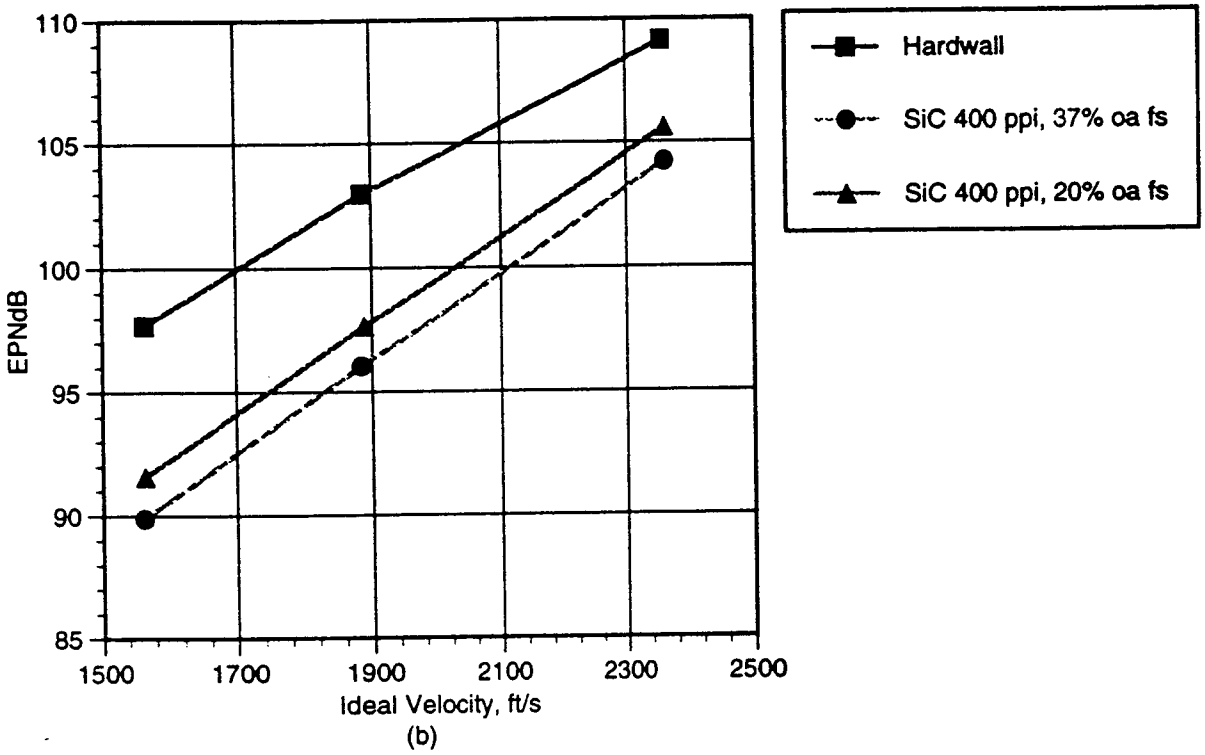

Figure 24

Bulk Facesheet Thickness Effects
Measured Normal Impedance

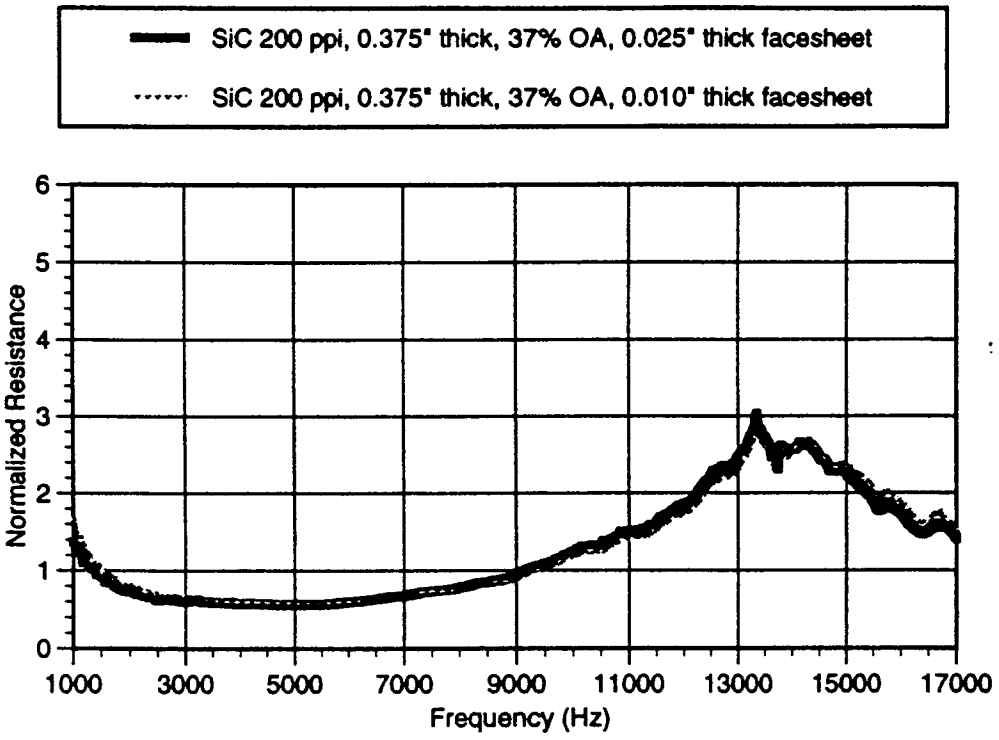

(a)

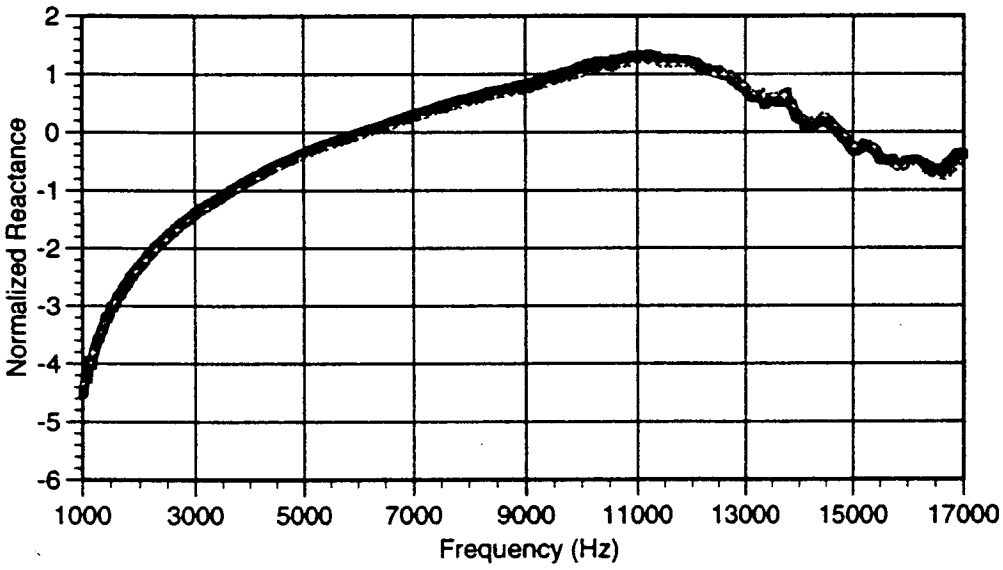

(b)

Figure 25

Facesheet Thickness Effects
Bulk, 0.375" Deep, 37% OA Facesheet
1 Ft Radius, Lossless, Model Scale, 115°

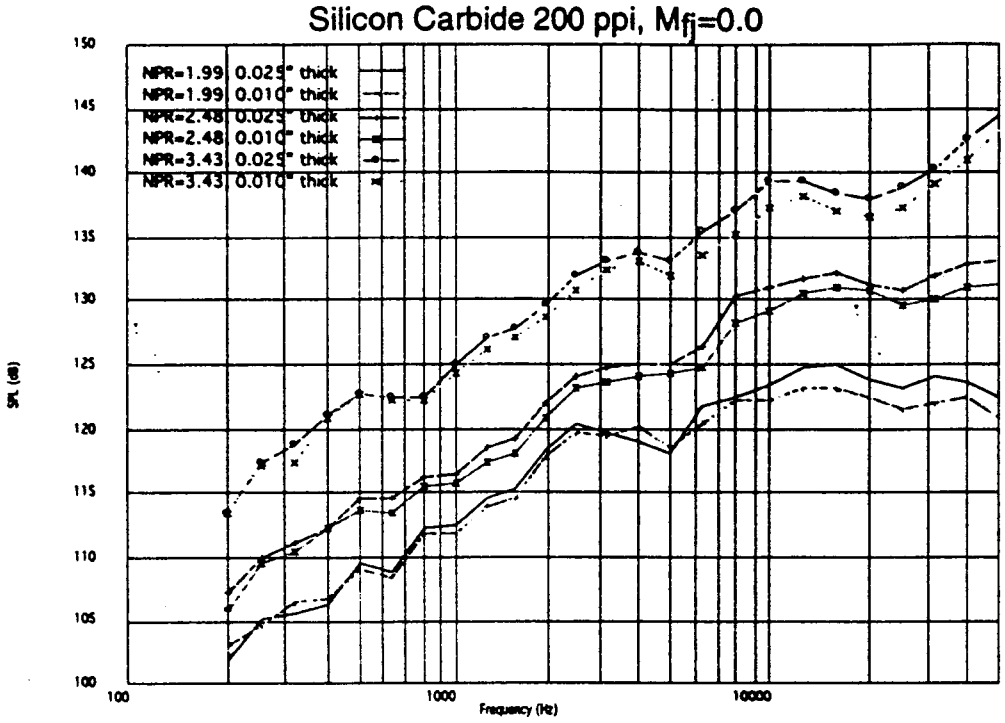

(a)

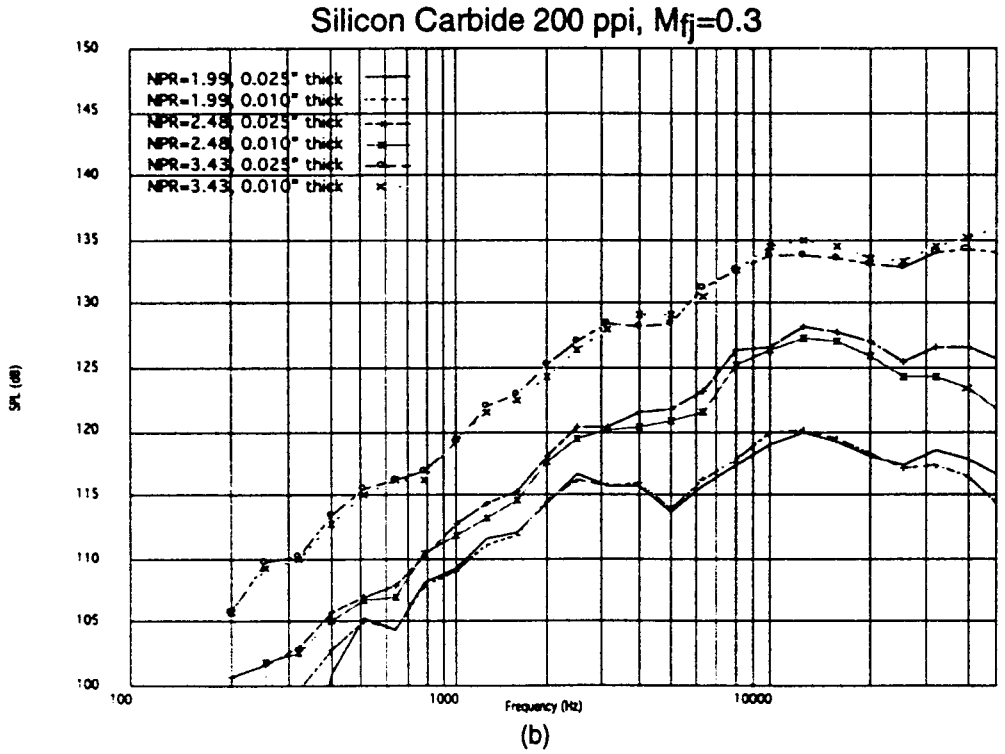

(b)

Figure 26

Facesheet Thickness Effects
Bulk, 0.375" Deep, 37% OA Facesheet
1 Ft Radius, Lossless, Model Scale, 115°

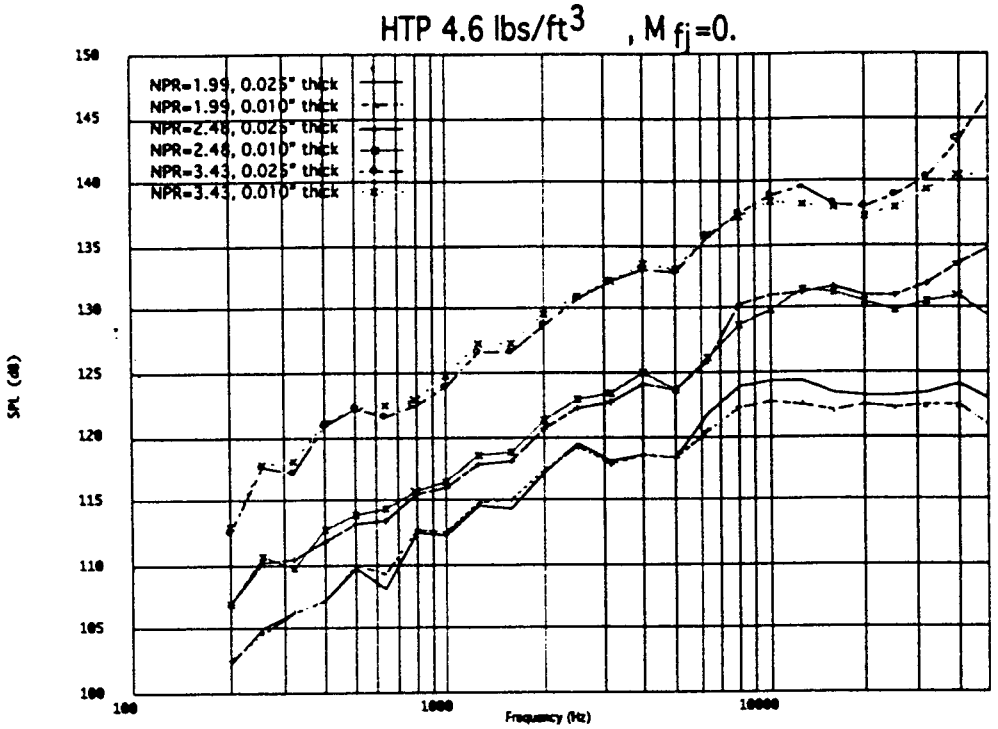

(c)

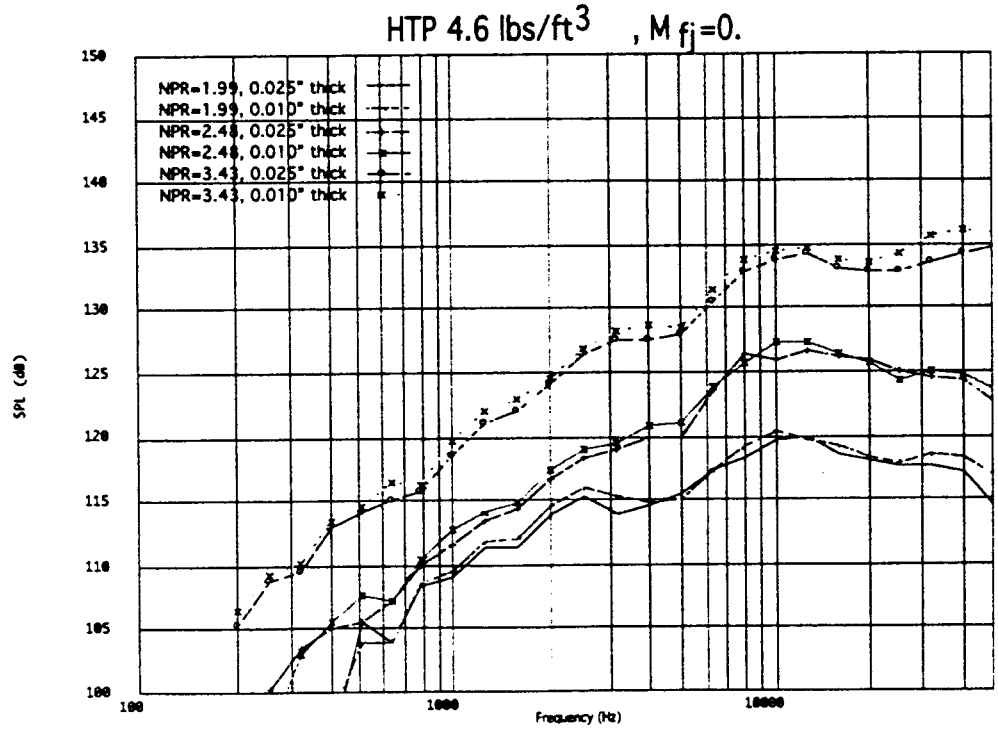

(d)

Figure 26 (continued)

Facesheet Porosity Effects
Bulk, EPNL, Full Scale, Mfj=0.3

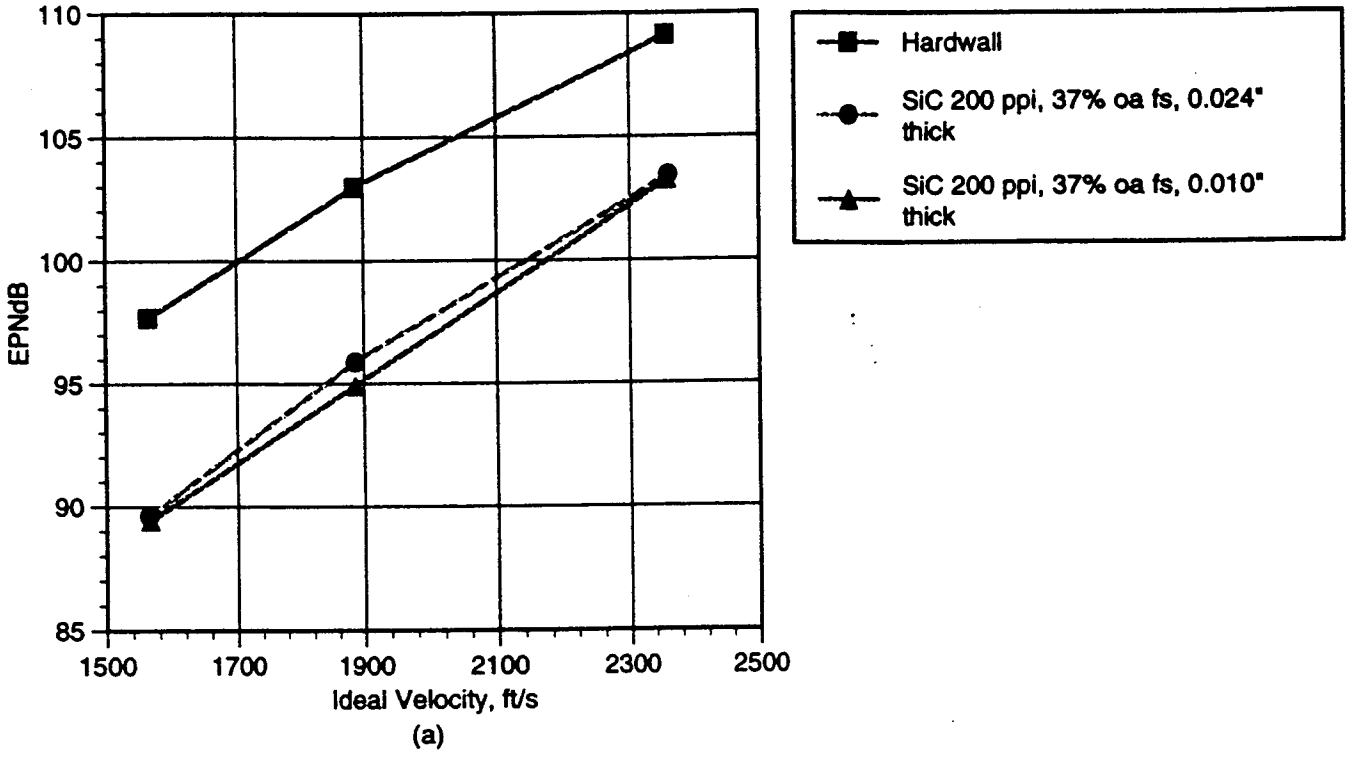

(a)

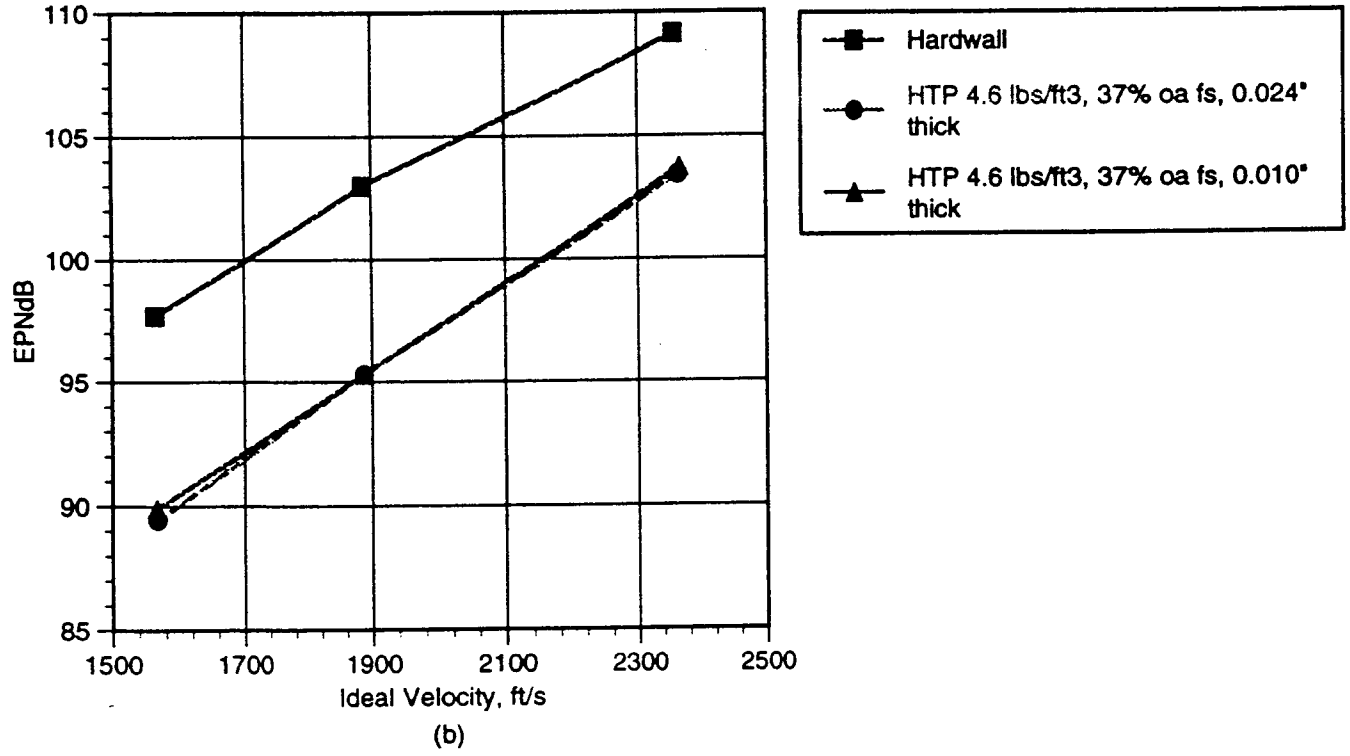

(b)

Figure 27

Bulk Liner Thickness Effects
Measured Normal Impedance

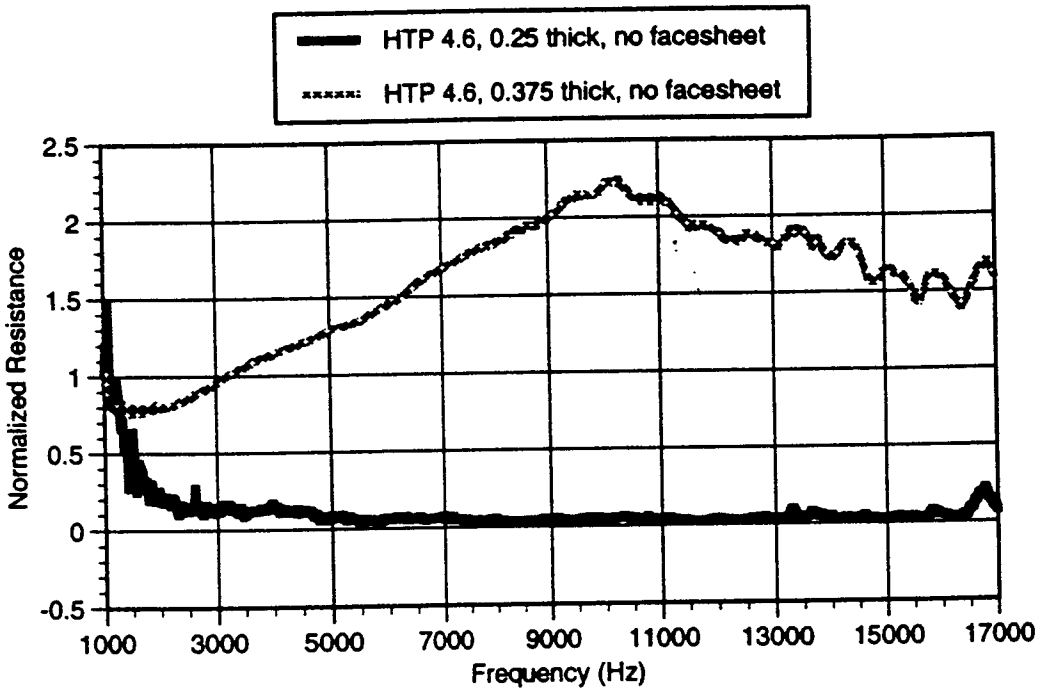

(a)

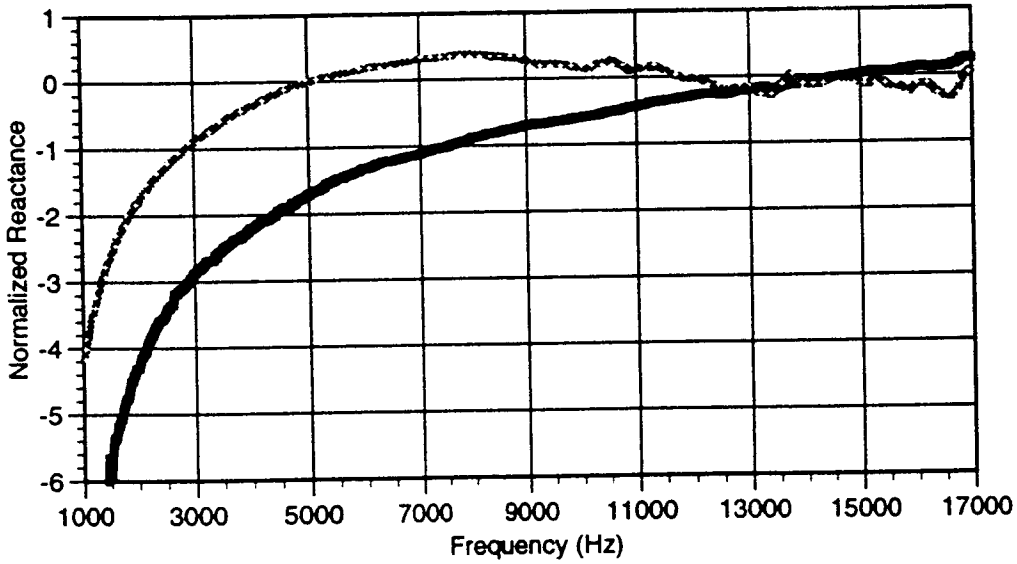

(b)

Figure 28

Bulk Liner Thickness Effects
HTP 4.6 lbs/ft3, 37% OA, 0.025" Thick Facesheet
1 Ft Radius, Lossless, Model Scale, 115°

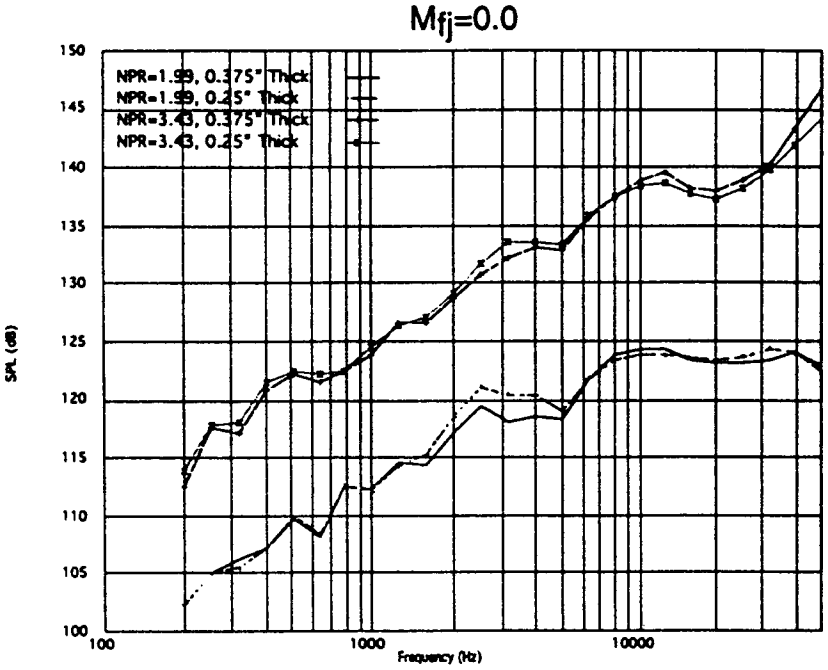

(a)

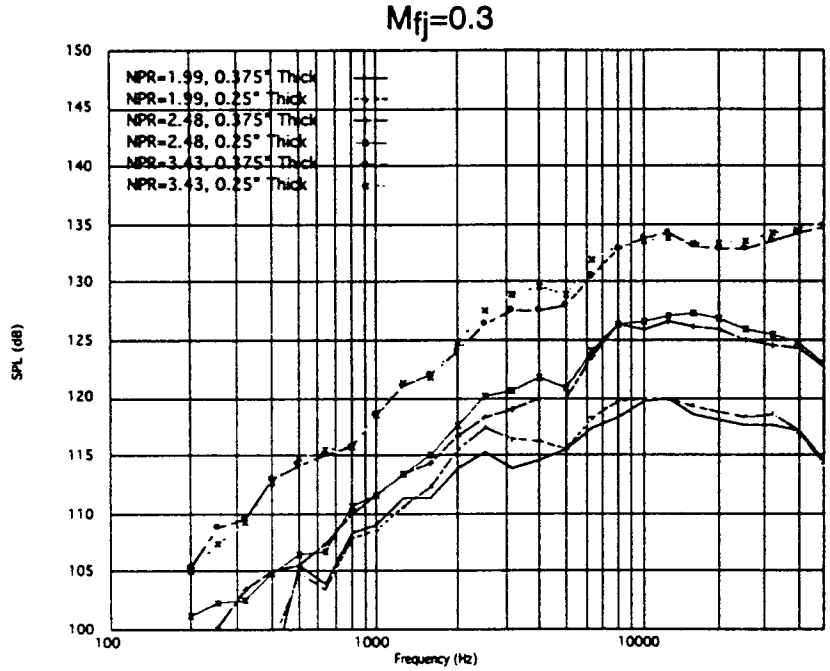

(b)

Figure 29

Bulk Liner Thickness Effects
EPNL, Full Scale, Mfj=0.3

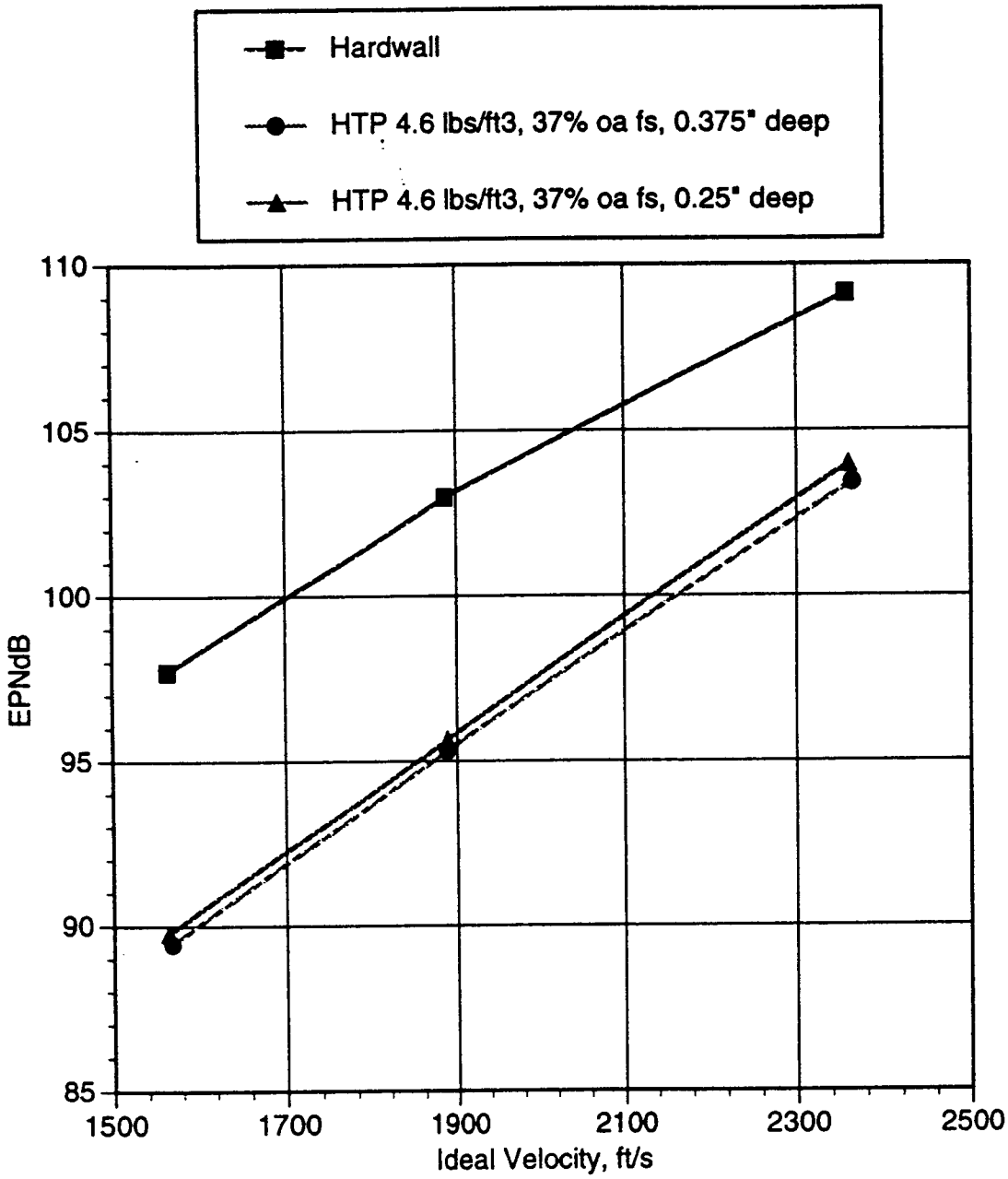

Figure 30

Locally Reacting Effects
HTP 4.6 lbs/ft3, 0.375" Deep, 37% OA Facesheet
1 Ft Radius, Lossless, Model Scale, 115°

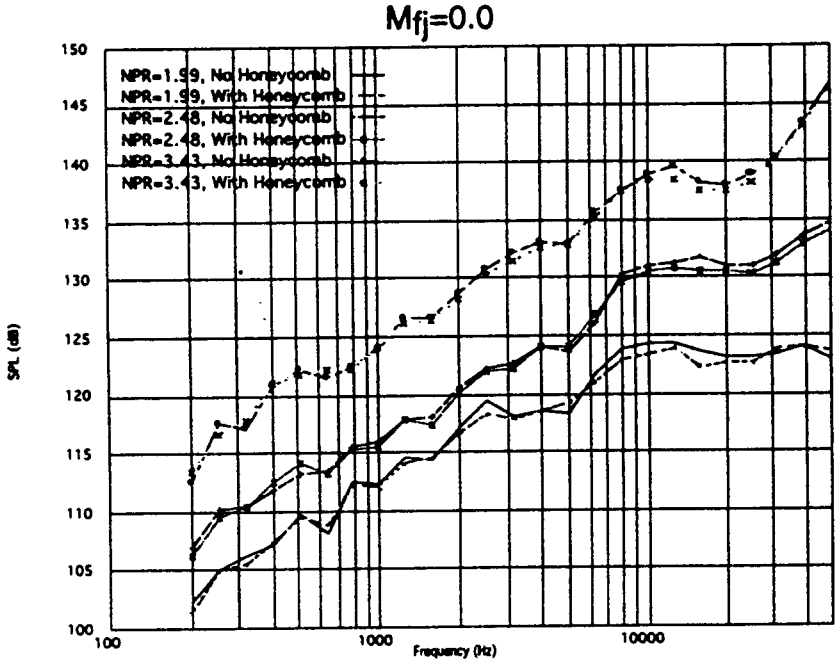

(a)

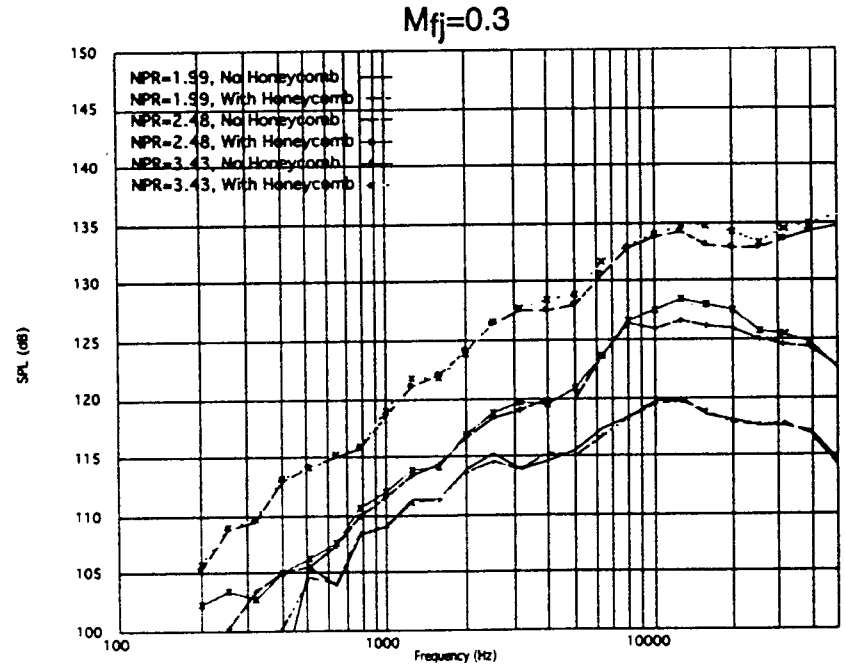

(b)

Figure 31

Velocity coefficient results from repeat configurations

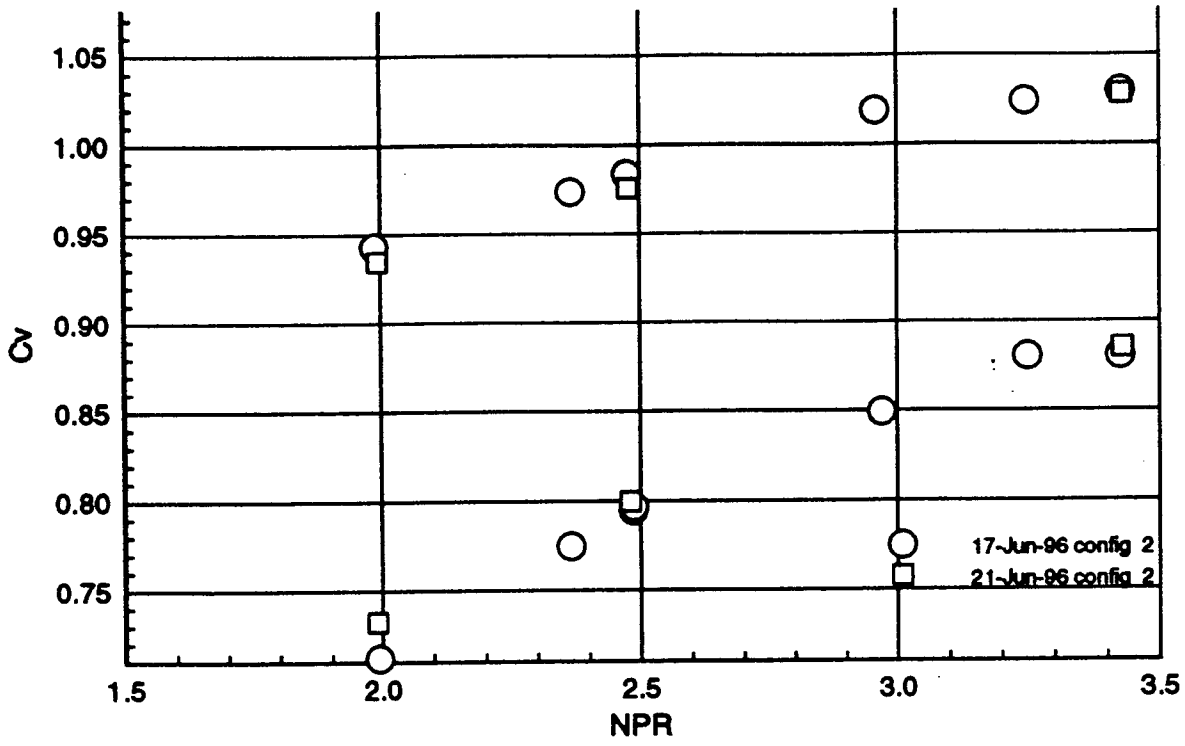

a.) for configuration 2

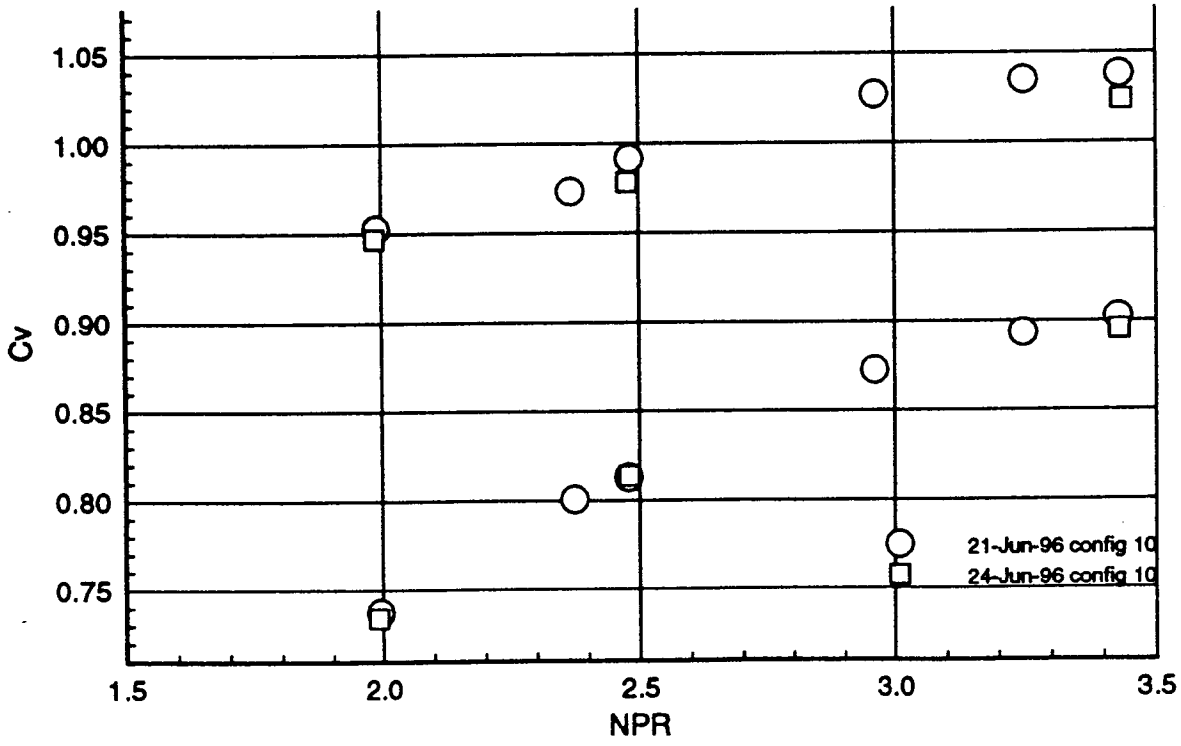

b.) for configuration 10

Figure 32

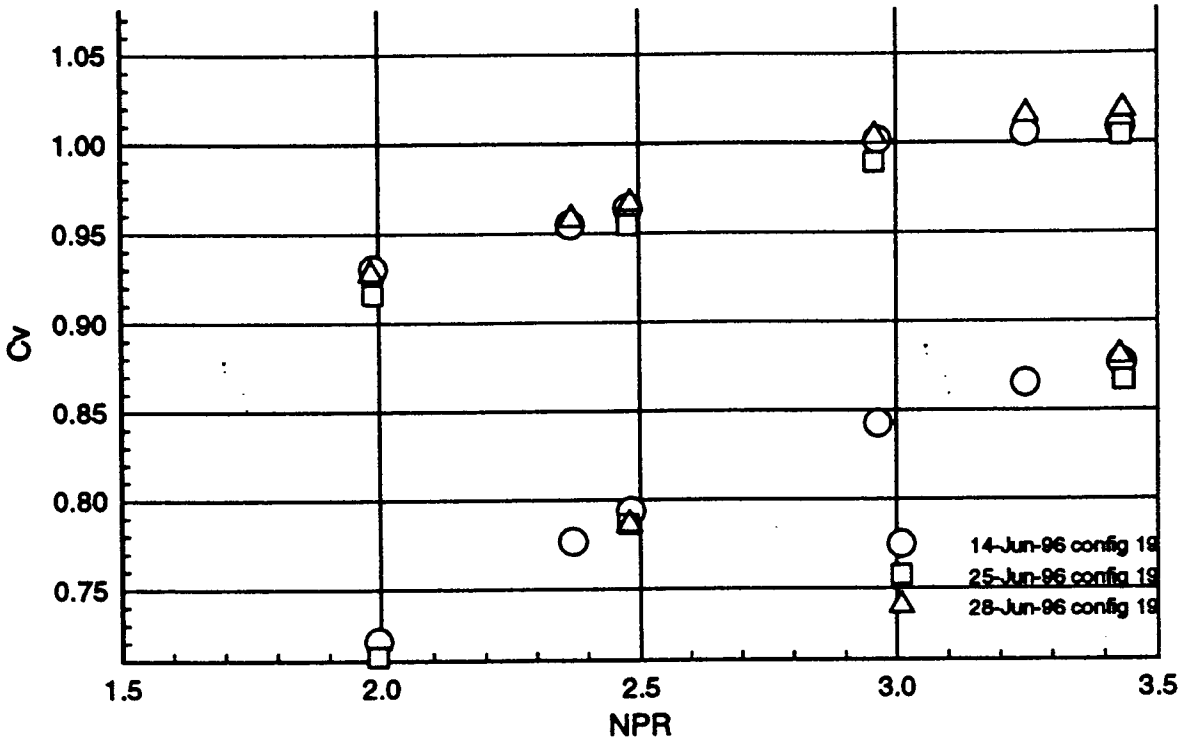

c.) for configuration 19

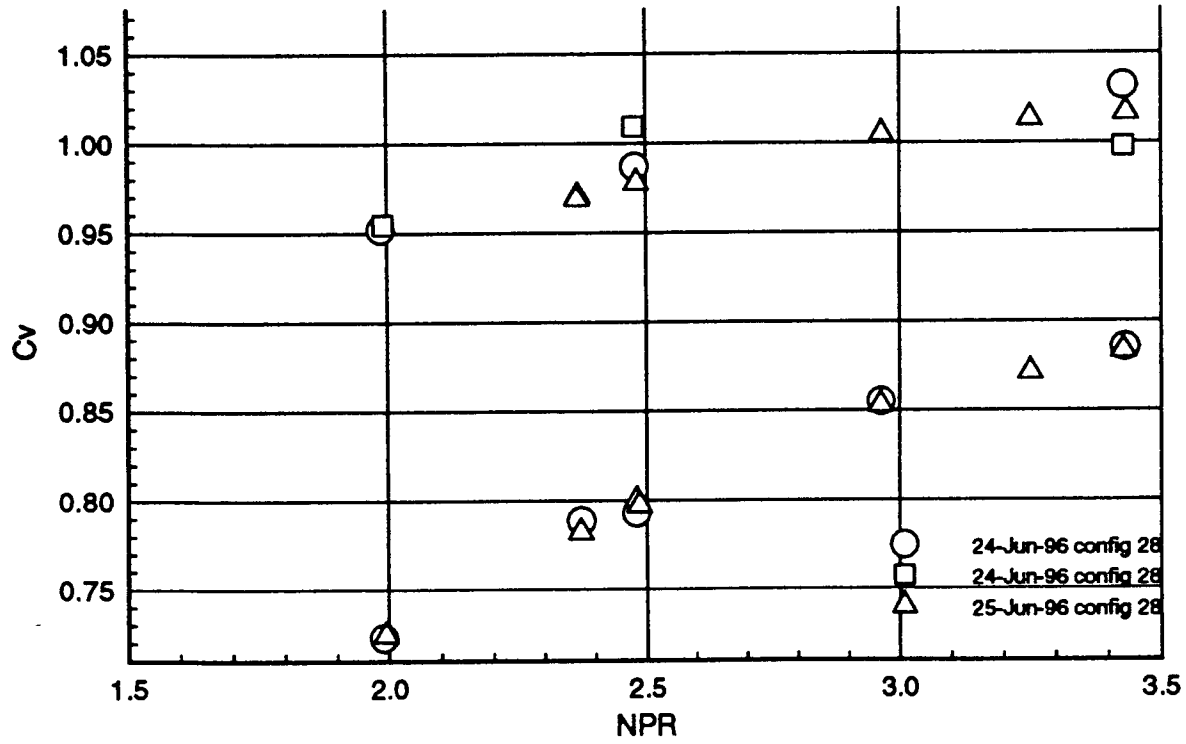

d.) for configuration 28

Figure 32, concluded

Effect of liner porosity for SDOF liners. Porosity values: config 1-7%; config 2-10%; config 3-15%

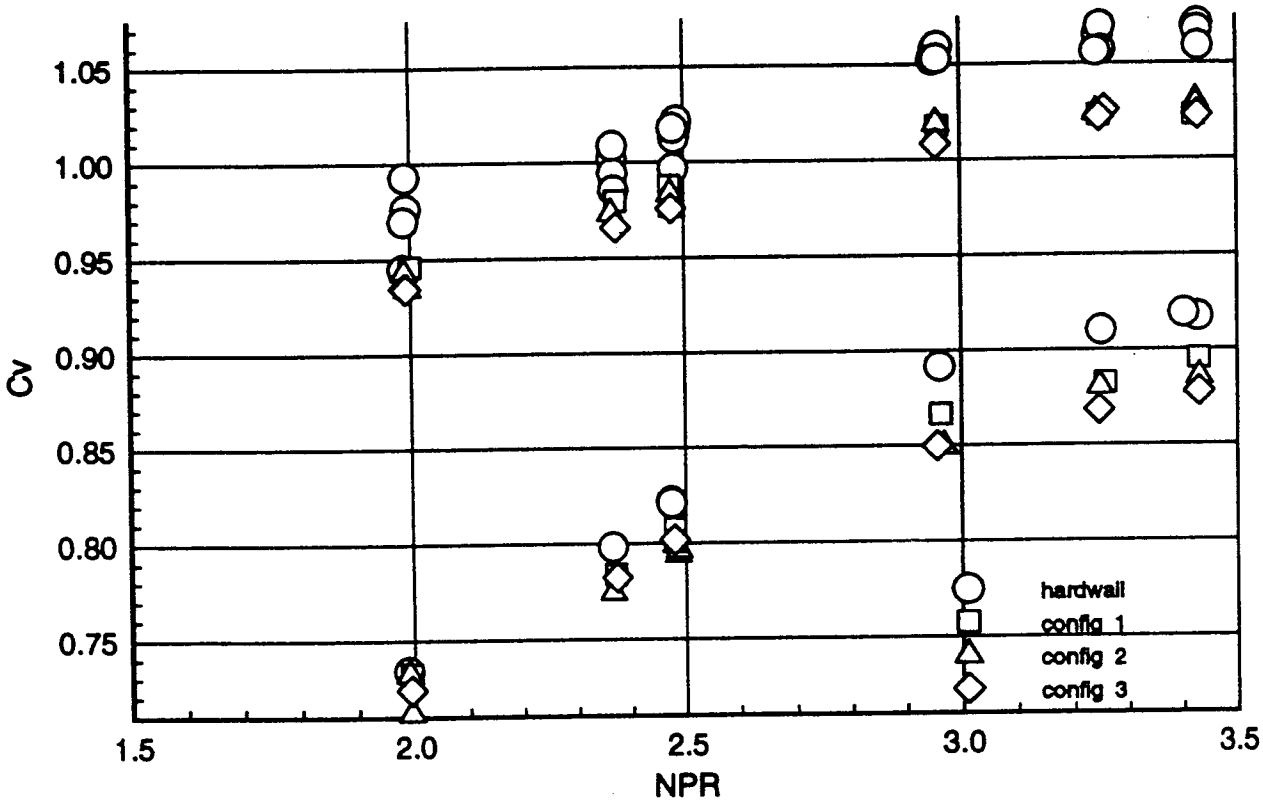

Figure 33

Effect of facesheet hole diameter for SDOF liners. Hole diameter values, in inches: config 2-0.04; config 4-0.02; config 5-0.06

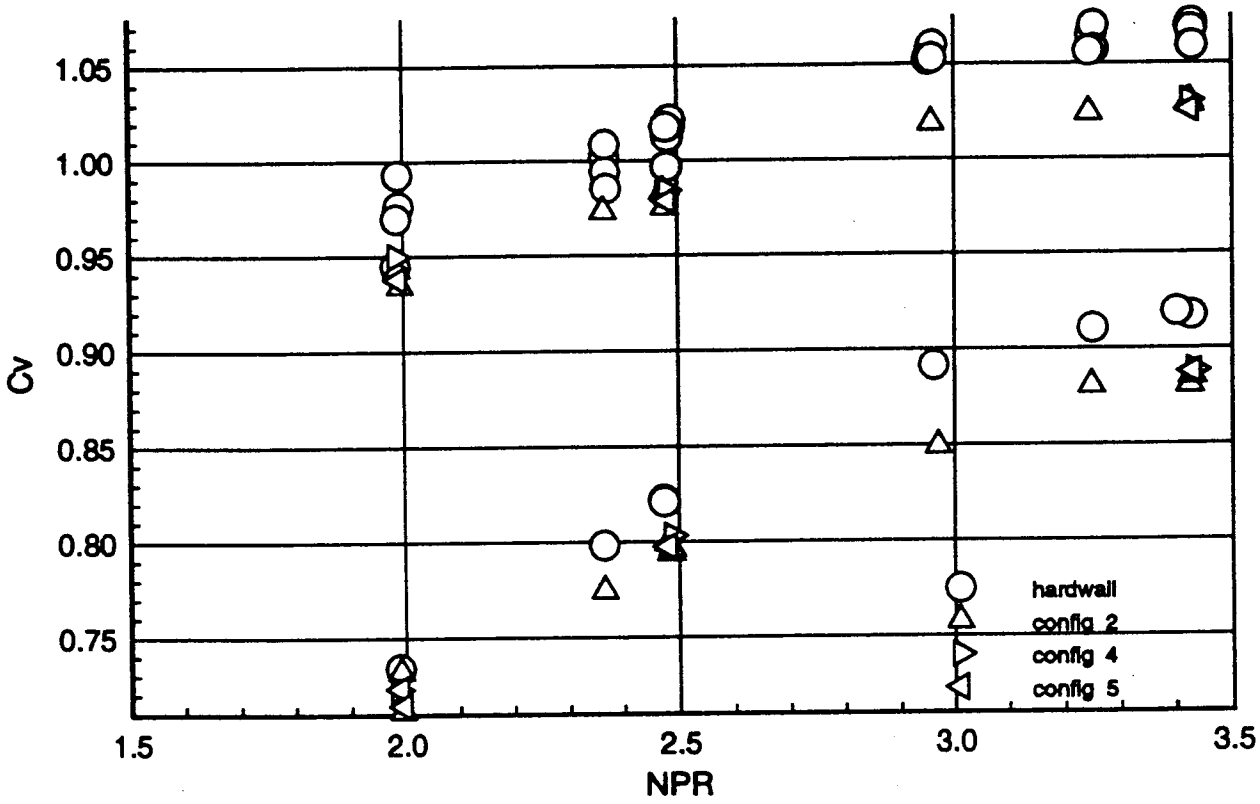

Figure 34

Effect of honeycomb cell size for SDOF liners. Honeycomb cell size values, in inches: config 2-0.375; config 6-0.75

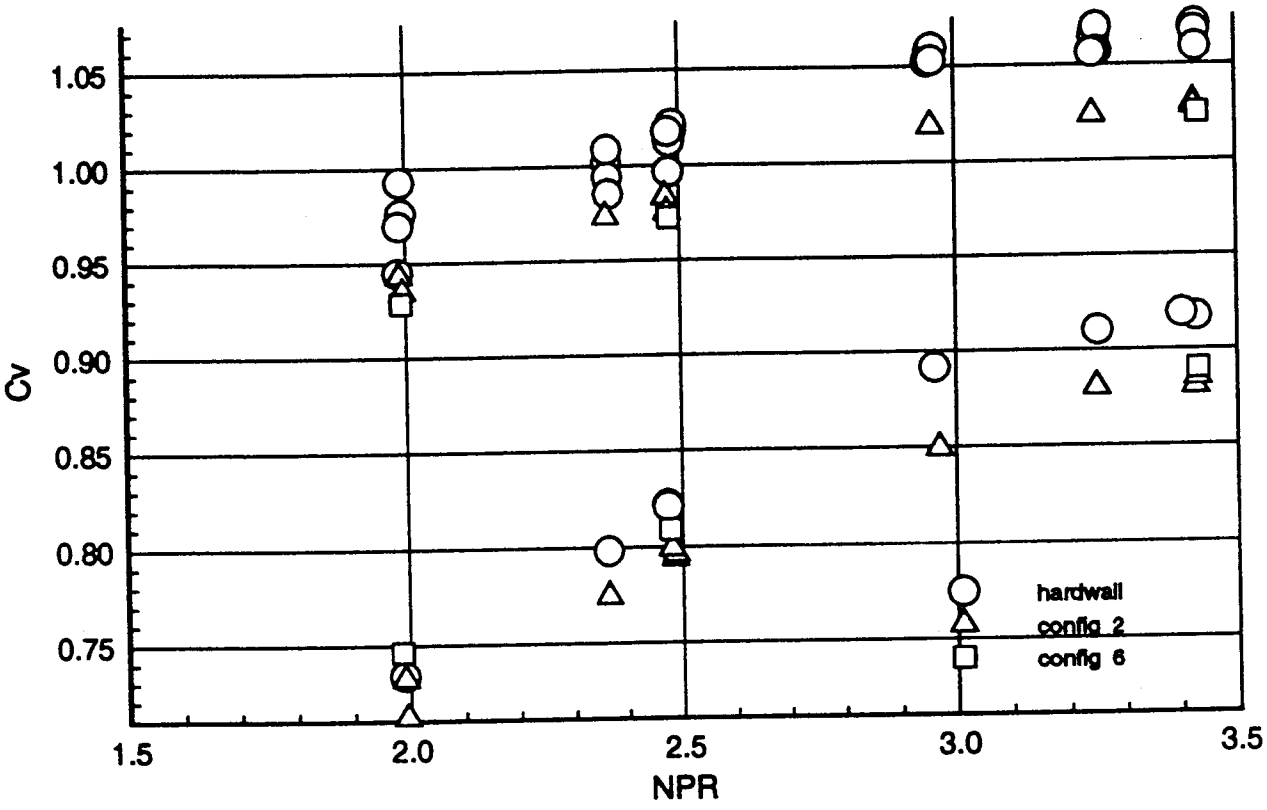

Figure 35

Effect of facesheet material thickness for SDOF liners. Material thickness values, in inches: config 2-0.025; config 7-0.044; config 8-0.063

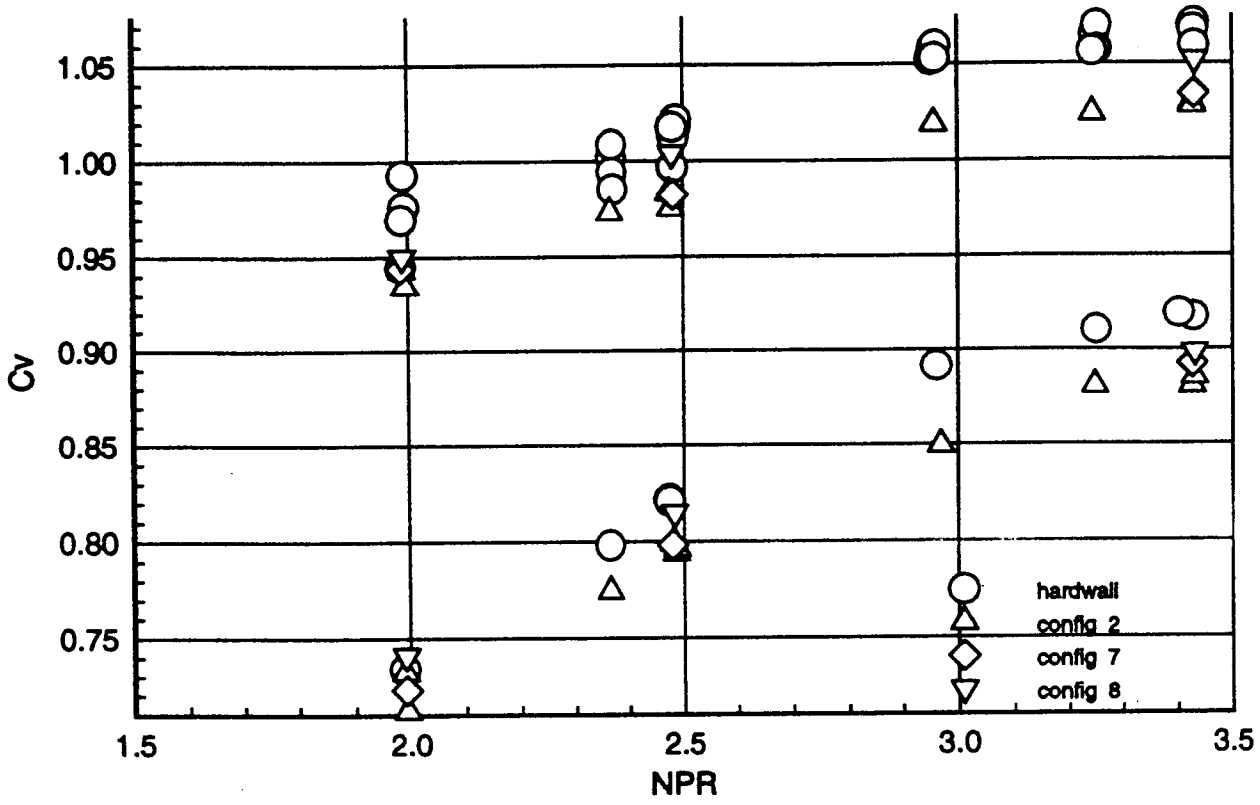

Figure 36

Effect of honeycomb depth for SDOF liners. Honeycomb depth values, in inches: config 2-0.375; config 9-0.25; config 10-0.5

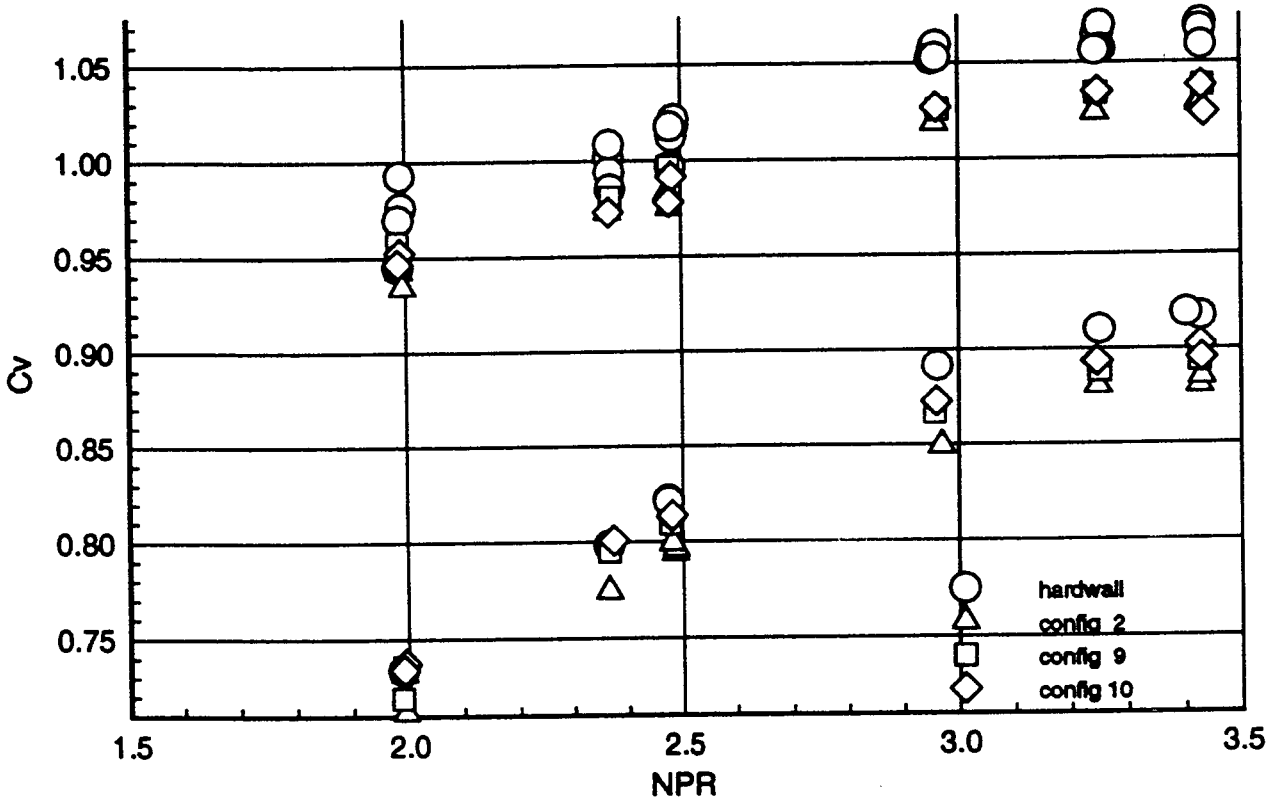

Figure 37

Effect of facesheet porosity and thickness for Ultramet SiC bulk liners

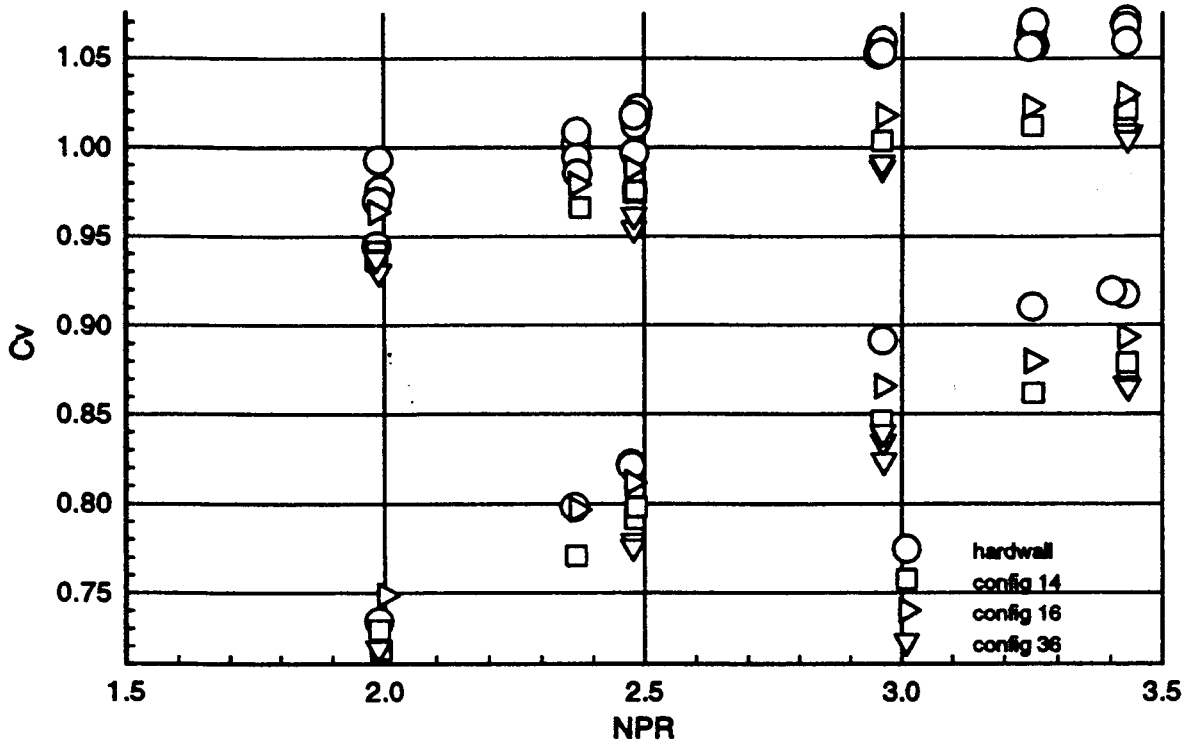

a.) for 200 ppi material. Porosity values: configs 14 and 36-37%; config 16-20%; Thicknesses: configs 14 and 16-baseline; config 36-thin

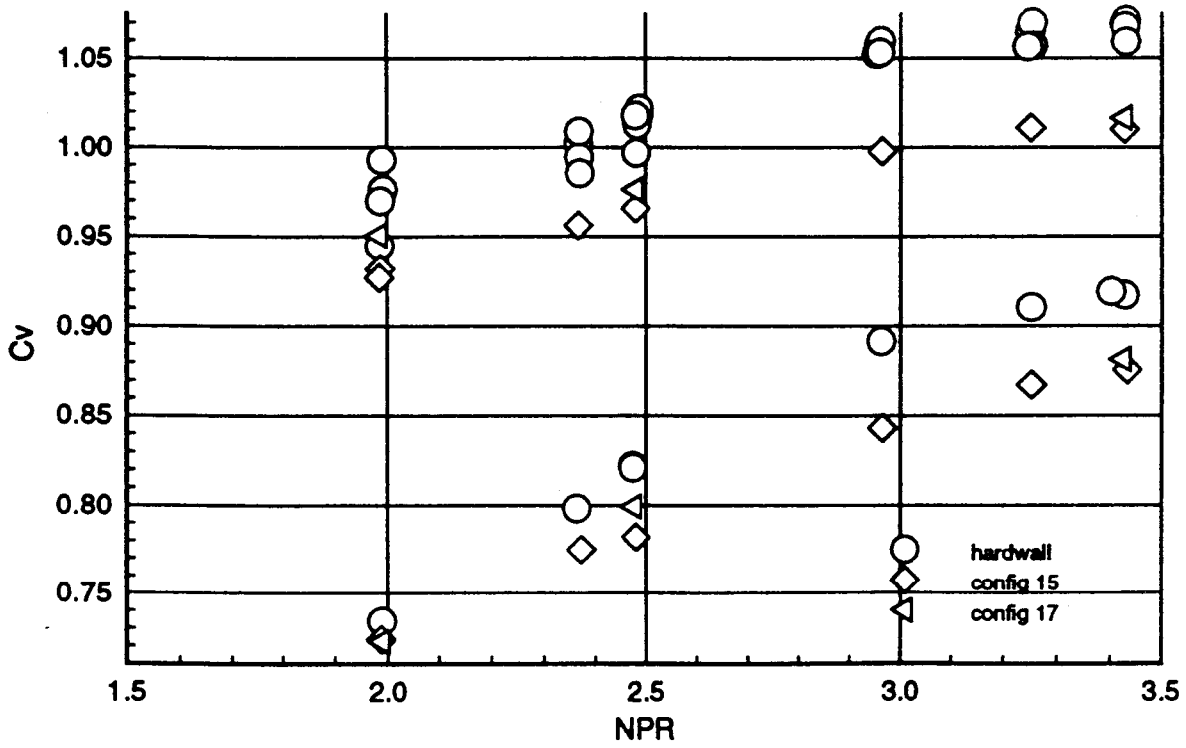

b.) for 400 ppi material. Porosity values: config 15-37%; config 17-20%

Figure 38

Effect of bulk material pores per inch for Ultramet SiC bulk liners

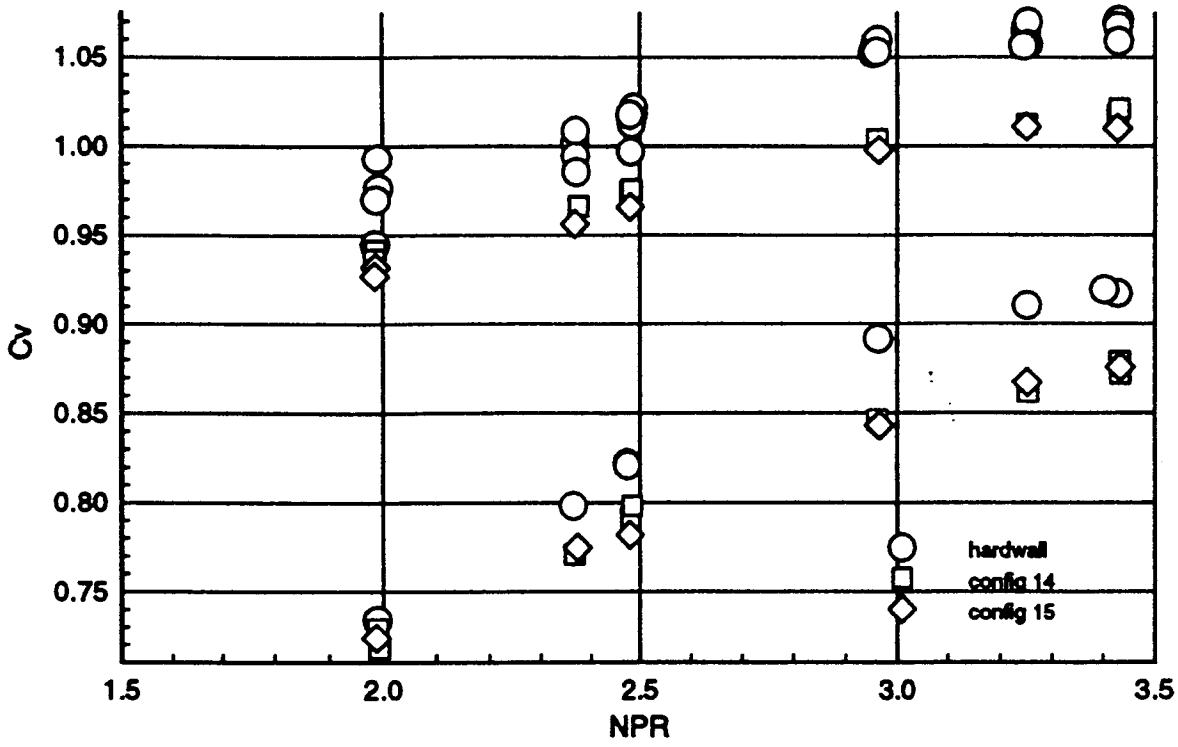

a.) for 37% porosity facesheet. Pores per inch values: config 14-200; config 15-400

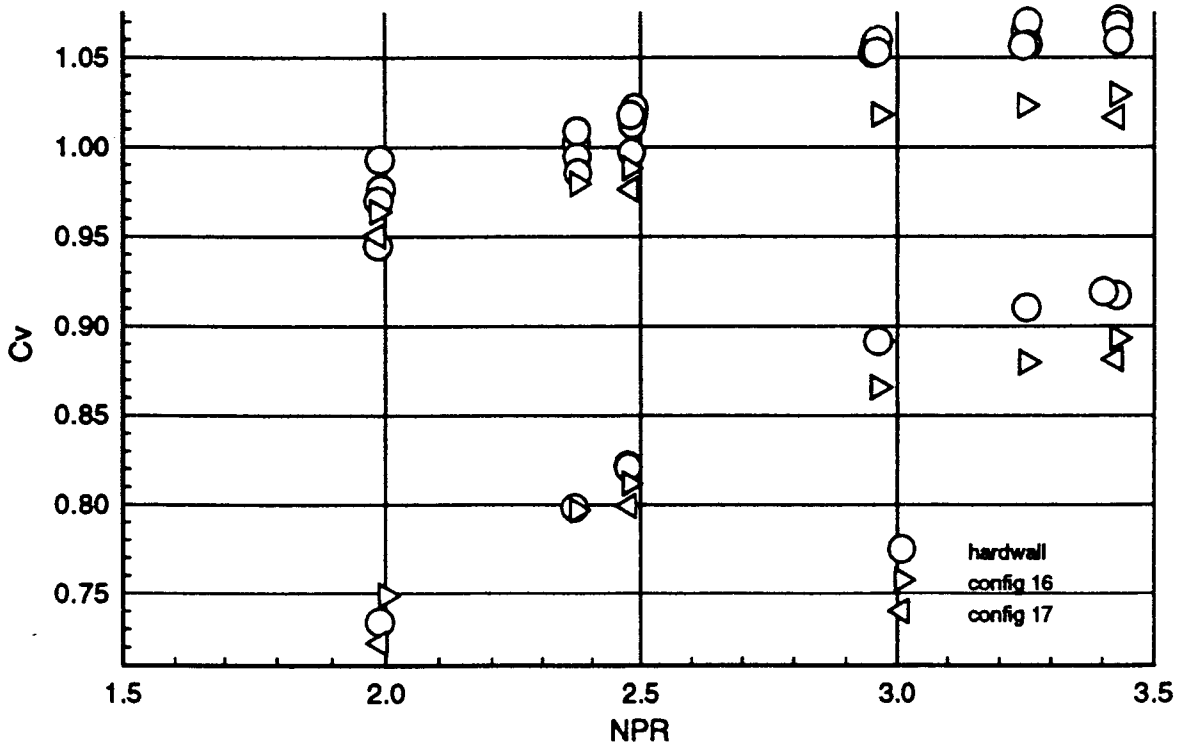

b.) for 20% porosity facesheet. Pores per inch values: config 16-200; config 17-400

Figure 39

Effect of bulk material density for Rohr/Lockheed HTP bulk liners. Density values, in lbm./cu. ft.: config 19-4.6; config 20-4.86; config 21-3.3; config 28-16

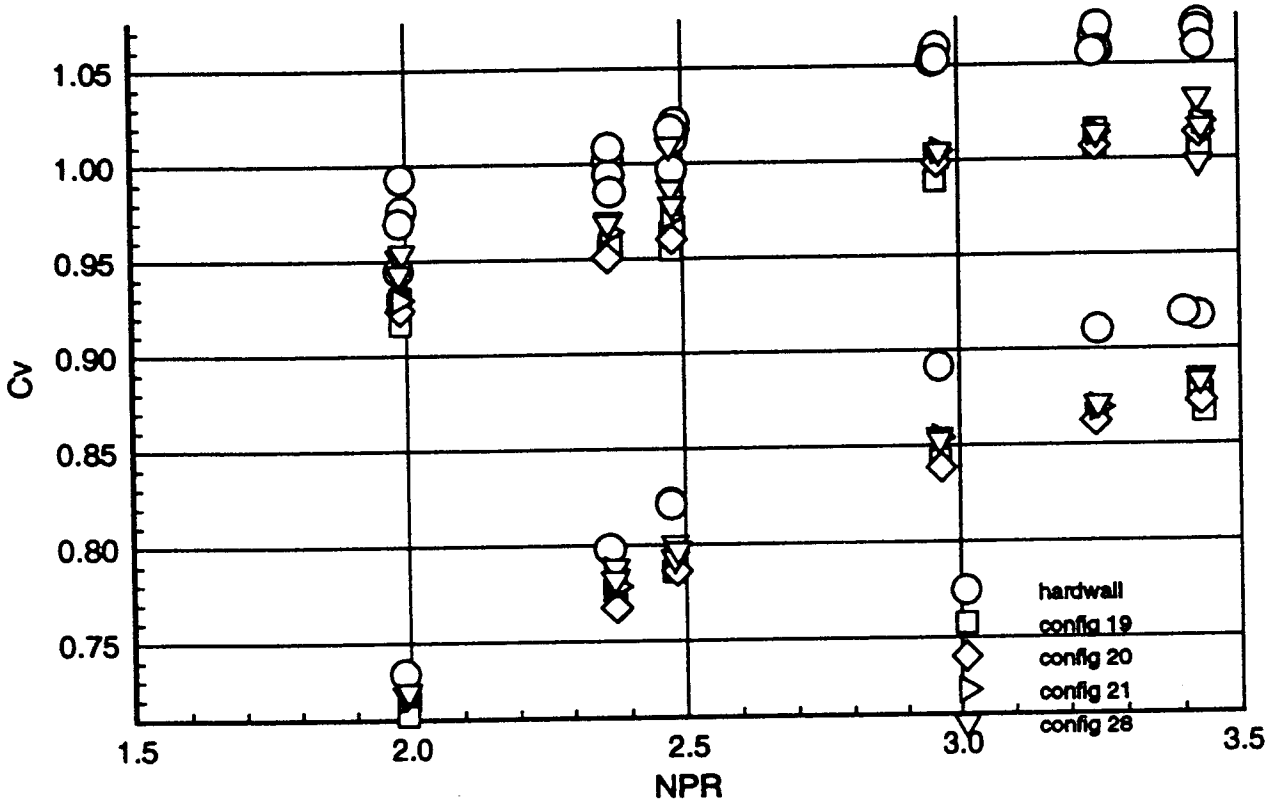

Figure 40

Effect of facesheet porosity and thickness for Rohr/Lockheed HTP 1 bulk liners. Porosity values: configs 19 and 29-37%; config 22-20%. Thicknesses: configs 19 and 22-baseline; config 29-thin

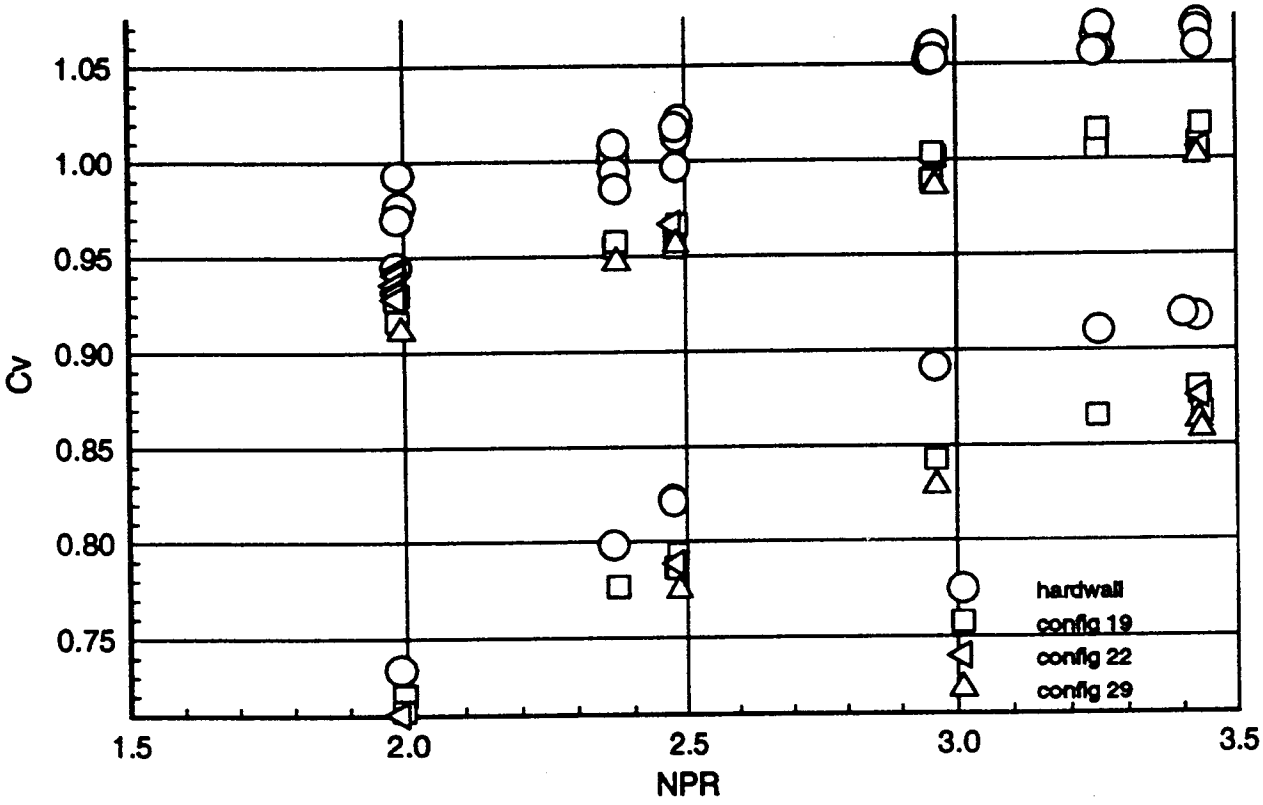

Figure 41

Effect of bulk material config and thickness for Rohr/Lockheed HTP 1 bulk liners. configs 19 and 25-bulk; config 24-0.375 in HC. Thickness values, in inches: configs 19 and 24: 0.375; config 24-0.25

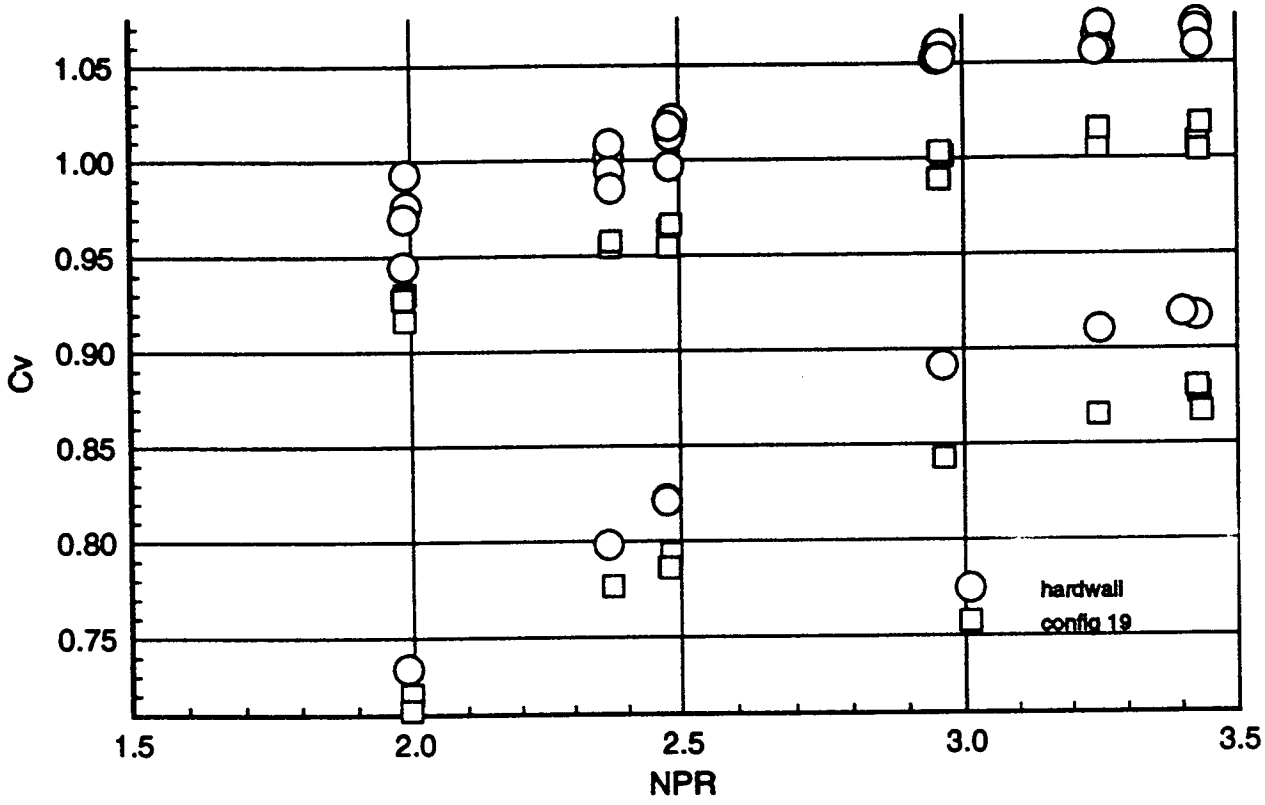

Figure 42

Effect of facesheet porosity for Americom SiC bulk material. Porosity values: config 26-37%; config 27-20%

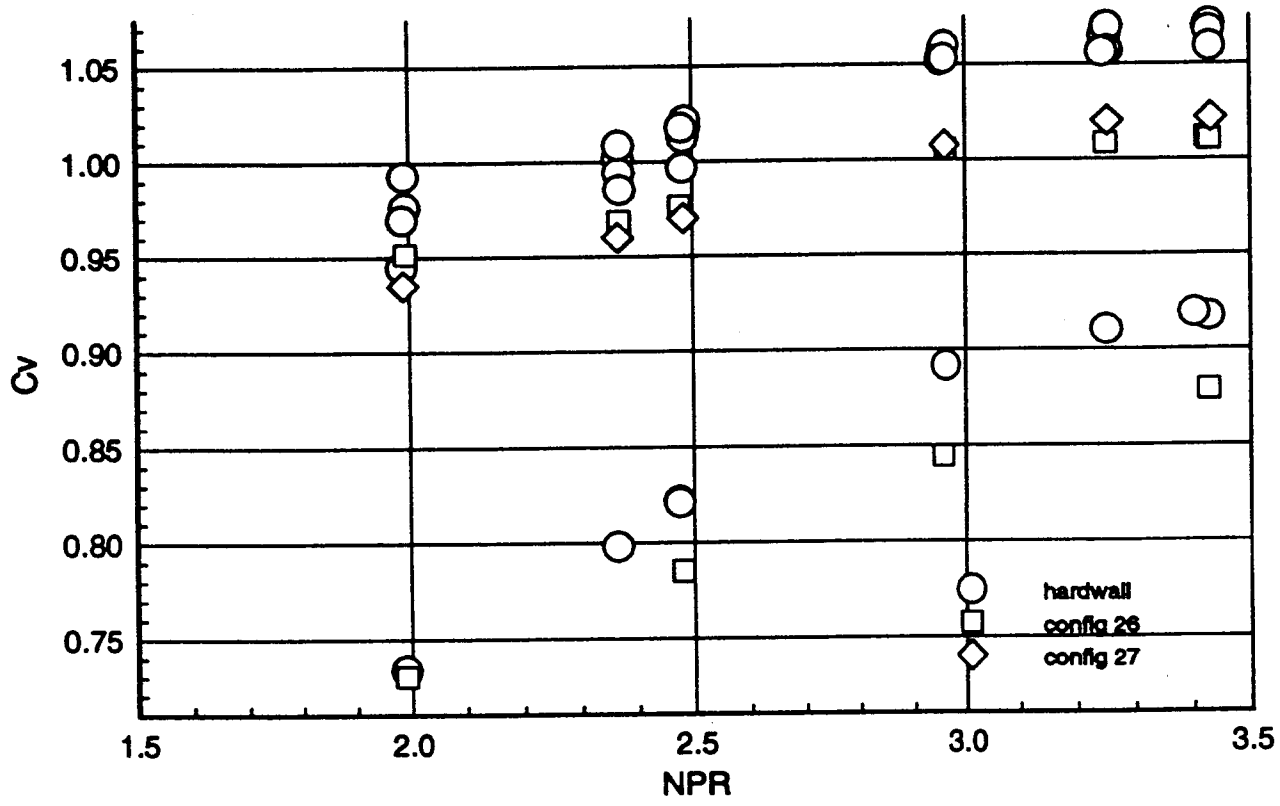

Figure 43

REPORT DOCUMENTATION PAGE

Form Approved
OMB No. 0704-0188

1. AGENCY USE ONLY (*Leave blank*)	2. REPORT DATE	3. REPORT TYPE AND DATES COVERED
	October 2004	Technical Memorandum

4. TITLE AND SUBTITLE

Results From a Parametric Acoustic Liner Experiment Using P&W GEN1 HSR Mixer/Ejector Model

5. FUNDING NUMBERS

WBS–22–714–09–46

6. AUTHOR(S)

Kathleen C. Boyd and John D. Wolter

7. PERFORMING ORGANIZATION NAME(S) AND ADDRESS(ES)

National Aeronautics and Space Administration
John H. Glenn Research Center at Lewis Field
Cleveland, Ohio 44135–3191

8. PERFORMING ORGANIZATION REPORT NUMBER

E–14736

9. SPONSORING/MONITORING AGENCY NAME(S) AND ADDRESS(ES)

National Aeronautics and Space Administration
Washington, DC 20546–0001

10. SPONSORING/MONITORING AGENCY REPORT NUMBER

NASA TM—2004-213289

11. SUPPLEMENTARY NOTES

This research was originally published internally as HSR054 in August 1997. Responsible person, Diane Chapman, organization code 2100, 216–433–2309.

12a. DISTRIBUTION/AVAILABILITY STATEMENT

Unclassified - Unlimited
Subject Category: 07 Distribution: Nonstandard

Available electronically at http://gltrs.grc.nasa.gov

This publication is available from the NASA Center for AeroSpace Information, 301–621–0390.

12b. DISTRIBUTION CODE

13. ABSTRACT ***(Maximum 200 words)***

This report documents the results of an acoustic liner test performed using a Gen 1 HSR mixer/ejector model installed on the Jet Exit Rig in the Nozzle Acoustic Test Rig in the Aeroacoustic Propulsion Laboratory or NASA Glenn Research Center. Acoustic liner effectiveness and single-component thrust performance results are discussed. Results from 26 different types of single-degree-of-freedom and bulk material liners are compared with each other and against a hardwall baseline. Design parameters involving all aspects of the facesheet, the backing cavity, and the type of bulk material were varied in order to study the effects of these design features on the acoustic impedance, acoustic effectiveness and on nozzle thrust performance. Overall, the bulk absorber liners are more effective at reducing the jet noise than the single-degree-of-freedom liners. Many of the design parameters had little effect on acoustic effectiveness, such as facesheeet hole diameter and honeycomb cell size. A relatively large variation in the impedance of the bulk absorber in a bulk liner is required to have a significant impact on the noise reduction. The thrust results exhibit a number of consistent trends, supporting the validity of this new addition to the facility. In general, the thrust results indicate that thrust performance benefits from increased facesheet thickness and decreased facesheet porosity.

14. SUBJECT TERMS	15. NUMBER OF PAGES
Acoustics; Linings; Aerodynamic drag	81
	16. PRICE CODE

17. SECURITY CLASSIFICATION OF REPORT	18. SECURITY CLASSIFICATION OF THIS PAGE	19. SECURITY CLASSIFICATION OF ABSTRACT	20. LIMITATION OF ABSTRACT
Unclassified	Unclassified	Unclassified	